Vulnerability Function Framework for Consequence-based Engineering

MAE Center Project DS-4 Report

by

Y. K. Wen
B. R. Ellingwood
J. Bracci

April 28, 2004

Vulnerability Function Framework for Consequence-based Engineering

Vulnerability Function Framework for Consequence-based Engineering

1.0 Introduction - Vulnerability Functions

Consequence-based engineering is a new paradigm for seismic risk reduction across regions or interconnected systems (Abrams, 2002). In CBE, the risk to a distributed infrastructure systems is quantified, evaluated and managed through an assessment and selective intervention process aimed at selected components of that system. This process enables the benefits of alternate seismic risk mitigation strategies to be assessed in terms of their impact on the performance of the built environment during a spectrum of earthquake hazards and on the affected population. It is clear that components and systems that are dominant contributors to risk should receive the focus of attention in the assessment process underlying CBE. These dominant contributors can be identified through the formalism of a probabilistic safety assessment, or PSA.

A PSA is a structured framework for evaluating uncertainty, performance and reliability of an engineered system, and accordingly must play a central role in CBE. It is distinguished from traditional deterministic approaches to safety assurance by its focus on why and how the system might fail and by its explicit treatment of uncertainties, both in the phenomena and in the analytical tools used to model them. A PSA provides a basis for decision-making in the presence of uncertainty that can be scrutinized by the stakeholders of the project, audited independently by a building official or other regulatory authority, and updated periodically as circumstances warrant. The move toward quantitative risk assessment began in the nuclear industry in the mid-1970''s, and has accelerated in recent years as the benefits of quantitative risk analysis have become apparent in many fields (Ellingwood, 1999).

One begins the PSA process by identifying limit states (LS), or conditions in which the system ceases to perform its intended functions in some way. In a (narrow) structural engineering sense, such limit states for specific structural components and systems may be either strength or deformation-related (as discussed subsequently). In a broader socioeconomic context, the LS may be related to repair costs (e.g., expressed as a percentage of replacement value) that are in excess of a desired amount, opportunity losses, or morbidity/mortality. Limit state identification requires a thorough understanding of the behavior of the safety-related systems within the plant and the role of structural components and systems in ensuring acceptable behavior of such systems. With the limit states identified, the limit state probability can be expressed as,

$$P[LS] = \Sigma P[LS|D = d] P[D = d] \qquad (1.0.1)$$

in which D is a random variable (or random vector) describing the intensity of the demand on the system, and P[LS|D = d] is the conditional limit state probability, given that D = d, and the summation is taken over all possible values of D. The probability P[D = d] defines the hazard (in earthquake engineering, the seismic hazard is defined by the complementary cumulative distribution function, P[D > d]), which can be determined for a specific site from the U.S. Geological Survey website (www.usgs.gov/). The variable d is denoted the "control" or "interface" variable. The conditional probability, P[LS|D = d]

= $F_R(x)$, is the fragility. The fragility of a component or system defines the conditional probability of its attaining a performance limit state, which may range from loss of function to incipient collapse, given the occurrence of a particular operational or environmental demand. Eq (1.0.1) shows that assessment of structural fragility is a key ingredient of any PSA. Furthermore, fragility provides a probabilistic measure of safety margin with respect to design-basis or other events specified by a stakeholder. Such a margin can be used to evaluate system weaknesses or deficiencies identified during an inspection or condition assessment and can provide a means to assess if the observed weaknesses or deficiencies might be expected to have a significant impact on system risk. The concept of a vulnerability (or vulnerability function) is integrally related to PSA and fragility assessment. Modeling and engineering analysis provide a measure of response to a prescribed demand. For example, structural analysis of a building for an ensemble of ground motions, characterized by a median spectral acceleration, yields a corresponding set of deformations. Those deformations are uncertain, due to uncertainties in the ground motion as well as the dynamic properties describing the structure and the structural modeling process itself. In turn, those deformations give rise to various states of damage and potential economic loss to structural and nonstructural components and systems. Those losses also are uncertain, due to uncertainties in the deformations, resulting damage, and the economic models used to model costs associated with different damage states. The general concept of vulnerability, as used in this project, is as a term to describe the susceptibility of a system to serious consequences (expressed in monetary terms or other appropriate metrics).

If the term LS in Eq. (1.0.1) is interpreted broadly as a structural state or a damage or economic state, then the mathematical descriptions of the PSA are similar. This concept will be illustrated in Section 4 of this report.

1.1 Fragility Curve (FC)

As noted above, fragility (or vulnerability) can be described in terms of the conditional probability of a system reaching a prescribed limit state (LS) for a given system demand $D = d$, $P(LS \mid D = d)$.

Limit states related to structural behavior range from unserviceability to various degrees of damage including incipient collapse. Demands can be in the form of maximum force, displacement caused by earthquake ground motions, or more generally a prescribed intensity measure of the ground motion, over a given period of time. Expressed in this general manner, the fragility (or vulnerability) is a function of the system capacity against each limit state as well as the uncertainty in the capacity. The capacity controls the central location of the FC and the uncertainty in the capacity controls the shape (or dispersion) of the FC (see Figure 1.1.1). For a deterministic system with no capacity uncertainty, the FC is a step function. Strictly speaking, FC is primarily a property of the system dependent on the limit state but depends very little on the system site seismic environment (an exception to this occurs when the facility is sited in proximity to the causative source of the ground motion, giving rise to so-called “near-field” effects). In other words, identical systems located in regions of different seismicity will have the

same FC if the demand is structural response or force. The FC will not be the same but similar for different sites if the demand is a prescribed excitation intensity measure such as spectral acceleration since spectral acceleration for higher modes would be different for different locations.

A fragility analysis is an essential ingredient of the fully coupled risk analysis embodied in Eq.(1.0.1). It also can be used to determine probabilistic safety margins against specific identified events for decision purposes. Identification of probabilistic safety margins is central to modern engineered facility risk management. Although providing a less informative measure of safety than that obtained from the fully coupled risk analysis in Eq. (1.0.1), risk-informed decision-making based on the results of fragility assessment has several advantages:

(1) The probabilistic system analysis is effectively uncoupled from the hazard analysis. Thus, while knowledge of the hazard is useful in identifying appropriate events for risk assessment purposes (e.g., a 2,475yr mean recurrence interval earthquake), such knowledge is not essential. Absent credible data on such events, one might simply inquire as to the fragility were the design-basis event to be exceeded by some arbitrary margin, say 50 percent.

(2) The need to interpret and defend very small limit state probabilities (on the order of 10^{-5}/yr or less) is avoided. There are limited data to support probabilities of this level, and such estimates are highly dependent on the probabilistic models selected. At the current state-of-the-art, (conditional) fragilities are more robust than unconditional limit state probabilities.

(3) A properly conducted fragility analysis is less complex, less costly, and involves fewer disciplines than a fully coupled risk analysis. Accordingly, there is less likelihood of miscommunication among members of the risk analysis team and the results are more easily understood by a non-specialist stakeholder or decision-maker.

Fragility modeling of reinforced concrete, steel and masonry structural systems typical of construction in the Eastern United States is illustrated in Section 4 of this report.

1.2 Limit State (LS) Probability and Displacement Demand Curve (DDC)

To tie the vulnerability of a given system to the seismicity of the region, the seismic hazard needs to be included in the consideration. The vulnerability needs to be described in terms of probability of a set of given limit states being reached of a system at a given location over a given period of time (0, t). Alternatively, the vulnerability can be stated in terms of occurrence rates of the prescribed limit states. In other words, a system of given capacity may be more vulnerable to earthquakes if it is located in a region of high seismicity than in a region of moderate or low seismicity. Knowing the fragility curve, the limit state (LS) probability over the time period (0, t) can be evaluated (cf Eq. (1.0.1))

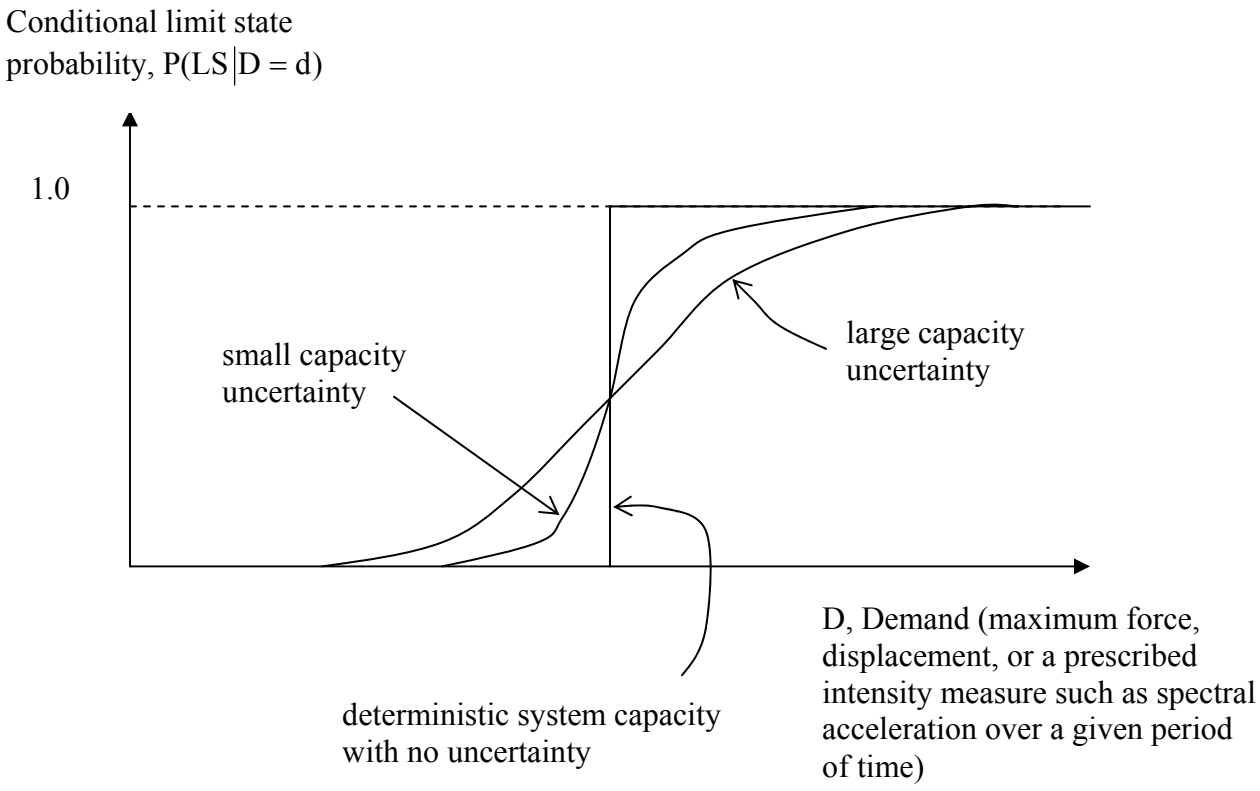

Figure 1.1.1. Characteristic of a Fragility Curve

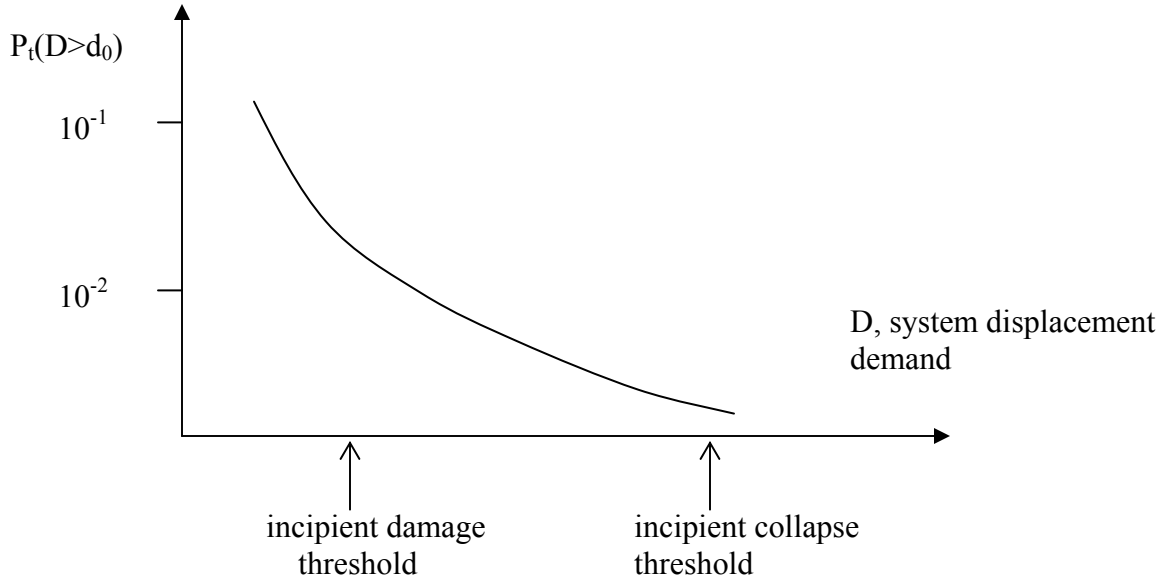

Figure 1.1.2. System Displacement Demand Curve (DDC)

$$P_t(LS) = \int_0^\infty P(LS|D = d) f_D(d) dd \quad (1.2.1)$$

in which $f_D(d)$ = the probability density function of the demand during (0, t), depending on the regional seismicity and ground excitation. In other words, through Eq. 1.2.1 the fragility curve and the probabilistic demand curve are combined. If the demand is in the form of a prescribed earthquake intensity measure such as maximum annual or 50- year spectral acceleration, $f_D(d)$ can be obtained from seismic hazard analysis. Further more if the limit state can be described by the system response variable X exceeding a deterministic threshold x_0 (or the fragility is described by the step function in Fig. 1.1.1) and the demand variable is a selected excitation intensity measure such as the annual maximum spectral acceleration S_a, the limit state probability is then

$$P_t(X \geq x_0) = \int_0^\infty P(X \geq x_0 | S_a = s) f_{S_a}(s) ds \quad (1.2.2)$$

Different values of threshold x_0 refer to different limit states. A typical plot of the probabilistic performance curve in terms of response threshold is shown in Fig. 1.1.2. In this case, the probabilistic performance curve is often referred to as the displacement demand curve (DDC).

Because of the uncertainty in capacity, the limit state threshold in general is a random variable. The limit state probability can be evaluated from the probabilistic demand curve and the probability distribution of the capacity C. In other words, Eq. 1.2.2 can be rewritten as

$$P_t(LS) = \int_0^\infty P_t(X \geq C) f_C(c) dc \quad (1.2.3)$$

in which $f_C(c)$ is the density function of the capacity.

2. Methods for Determination of Vulnerability Functions

Depending on the problem and information available, different methods can be used to evaluate the vulnerability of a system in terms of either FC or DDC.

2.1 FC and DDC Analysis via an Excitation Intensity Measure

To evaluate the vulnerability of systems under future earthquakes, the uncertainty in each element of the chain of events (Figure 2.1.1) from the seismic source to the structural response and their propagation needs to be accounted for. A convenient approach, which has been used by the profession, is to select a scalar intensity measure of the excitation that can be correlated well with the system response. Peak ground acceleration, velocity and displacement have been used in the past but generally have poor correlation with structural response. Recent studies such as Luco and Cornell (2001) has shown that

measures including some of the structural properties such as those in terms of spectral accelerations with 5% damping of the first two modes elastic and inelastic response give

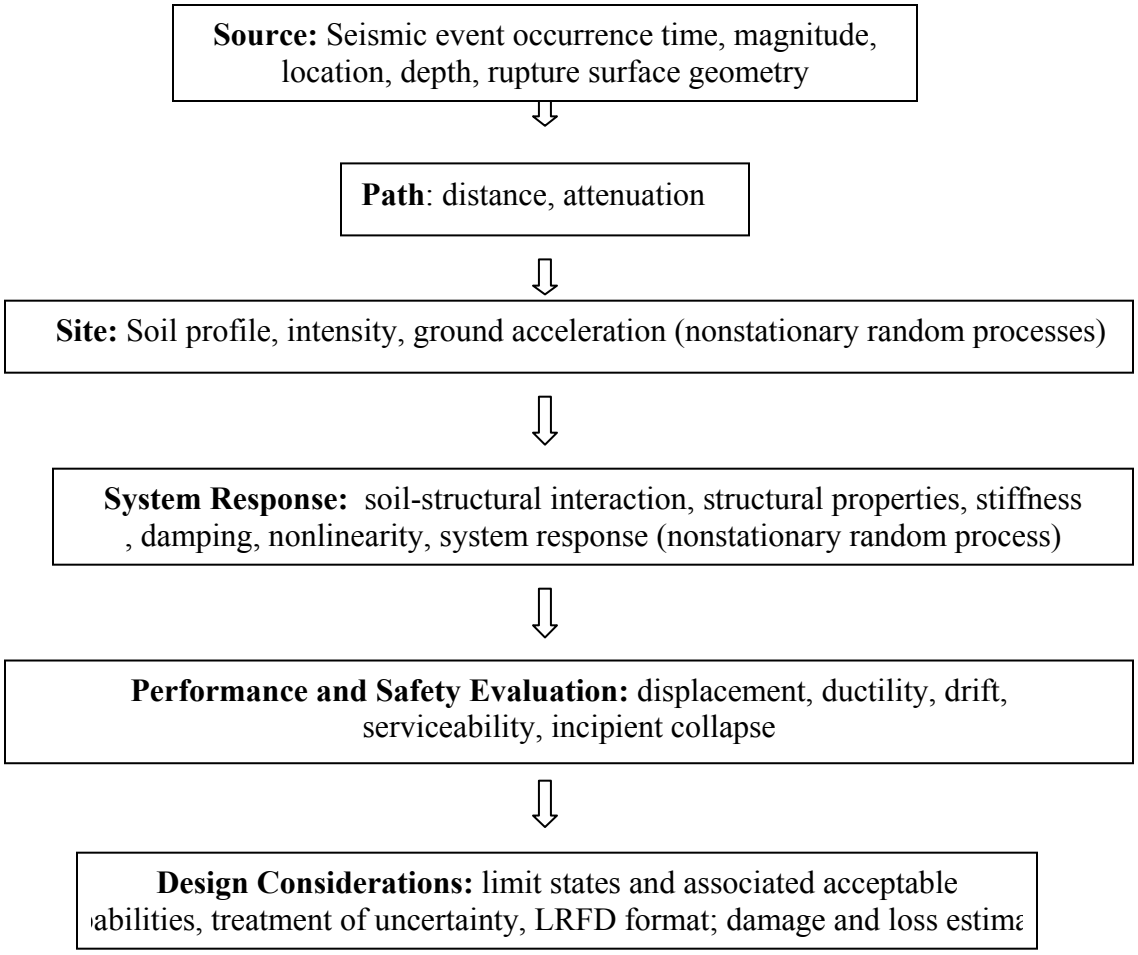

Figure 2.1.1 Probabilistic Performance Evaluation and Design for Earthquakes

much better results. The linear elastic spectral acceleration is especially convenient since the probability of these parameters can be readily evaluated from the USGS National Earthquake Hazard Maps (2002) (www.usgs.gov). Once an intensity measure is selected, the next step is to establish the relation between system response and the intensity measure.

2.1.1 FC Analysis of a Linear Elastic System

If the system stays within the linear range, the relationship can be constructed via a linear structural dynamic analysis using method of modal superposition. Since the relationship so established is analytical, only additional uncertainty is due to those in the structural modeling and response analysis method. A functional relationship between structural response demand D and intensity measure S can be then described by

$$D = N\, g\,(S) \tag{2.1.1}$$

in which g is the results of the dynamic and modal analysis and N is (random) correction factor for the uncertainty in the method of modeling and dynamic analysis. Note that for a MDOF system and when more than one mode is considered, g may be a function of spectral accelerations of more than one mode. The relationship between these spectral accelerations depends on the excitation and separation of the modes. The uniform hazard acceleration response spectra can be used for this purpose. For a given value of S of the fundamental mode corresponding to a hazard level, the spectral acceleration corresponding to other modes are determined from the uniform hazard spectrum. From Eq. 1.2.3 one can evaluate FC for given S and PPC by incorporating the seismic hazard information of S as given in Eqs 1.0.1 to 1.2.3. For a given S = s, the only uncertainty is due to the modeling error and the mean and standard deviation of X are

$$\mu_{D|S=s} \approx \mu_N g(s) \tag{2.1.2}$$

$$\sigma_{D|S=s} \approx \sigma_N g(s) \tag{2.1.3}$$

in which μ_N is the bias factor and σ_N is the uncertainty in the modeling and dynamic analysis. With an appropriate chosen distribution for N, the FC is simply the probability of D exceeding the capacity of the system, C, corresponding to the given limit state which can be readily obtained as long the capacity (if deterministic) or its distribution (if probabilistic) is known. The probabilistic performance function can be then evaluated according to Eq. 1.2.2 or Eq.1.2.3.

2.1.2 FC of a Nonlinear Inelastic System

Under severe seismic excitation, the system generally goes into the nonlinear inelastic range. The relationship between D and S cannot be handled by modal analysis. Time history response analyses under ground excitation with a given intensity measure are required. To cover a wide range of D, ground motions from low to high intensity reflecting the seismicity of the region are needed. In areas where a large number of past records are available such as the western United States, these ground motion records can be screened and scaled for this purpose as was done in the SAC Steel Project [Somerville et al, 1997]. A proper intensity measure such as spectral acceleration may be used for the scaling such that a collection of wide range of intensity can be obtained. These ground motions can be used for excitation in time history structural response analyses. A

regression analysis of the responses related to the limit state of interest as a function of the excitation intensity measure is then performed. In view of the nonlinear nature of the problem and large scatter of the response due to record-to-record variation, a nonlinear regression analysis of the power-law form (Luco and Cornell, 2001) may be used since it is simple and flexible,

$$D = aS^b \tag{2.1.4}$$

A logarithmic transform of the above reduces it to a linear form

$$\ln D = \ln a + b \ln S \tag{2.1.5}$$

and a simple linear regression analysis can be then perform to determine the constants a and b which allow one to determine the conditional expectation of D given S, $\mu_{D|S=s}$ and also the conditional coefficient of variation of D given S, $\delta_{D|S=s}$. Note that while the power law form allows straightforward linear regression analysis, other nonlinear equations may be used if they better fit the D/S relationship. A proper distribution function (generally lognormal is a good fit) is then selected for D and based on which the FC curve can be determined. For example, if the limit state capacity is given by a deterministic response limit, d, and there are no other sources of uncertainty, the FC is given by

$$FC = P(D \geq d \,|\, S = s) = 1 - \Phi\left(\frac{\ln d - \lambda}{\beta}\right) \tag{2.1.6}$$

in which $\lambda = \ln(\mu_{D|S=s}) - \frac{1}{2}\varsigma^2$

$$\beta = \sqrt{\ln(1 + \delta_{D|S=s}{}^2)}$$

Normally, there are other sources of uncertainty; they need to be incorporated into the above formulation. The accounting and traction of uncertainty will be shown in later sections.

2.1.3 DDC Analysis Using an Excitation Intensity Measure

To obtain the unconditional limit state probability or the probabilistic performance curve, the seismic hazard analysis of the intensity measure is included and combined with the FC as shown in Eqs.1.2.2 and 1.2.3. The integration in general can be carried out numerically. It has been shown (Cornell et al 2002) that if the result of the seismic hazard analysis as given above can be approximately described by a power law

$$H_t(a) = k_0 a^{-k} \tag{2.1.7}$$

and the above lognormal distribution assumption for the demand given excitation is valid, Eq. 1.2.2 can be evaluated in a closed form

$$P_t(D > d) = H_t(a^d) \exp[\frac{1}{2}\frac{k^2}{b^2}\beta^2_{D|S_a=a}] \quad (2.1.8)$$

in which a^d is the spectral acceleration level corresponding to the demand d according to Eq. 2.1.6. Eq. 2.1.6 and 2.1.8 therefore describe the vulnerability of the system in terms of FC and DDC of the system if it exceeds a deterministic threshold corresponding to a limit state. Although the spectral acceleration has been used in most studies as the excitation intensity measure, other scalars can be considered, such as the combination of spectral accelerations at the first two modes for better correlation when higher mode effects are included. Similarly, a combination of first mode elastic and inelastic spectral accelerations can be used for better correlation for inelastic systems. In general, such improvements are achieved at the expense of more analytical and computational effort. The optimal intensity measure may also depend on the type of system investigated. What is good for steel buildings may not as good for masonry buildings.

The success of above procedure relies on the good predictive power of the excitation intensity measure S and the power-law regression equation of the structural response. This may not always be true when the system is complex and the response behavior is highly nonlinear and inelastic, such as with brittle connection failures observed for Pre-Northridge construction. For example, the higher mode effects, near-source effects, and detailed structural response behavior often cannot be predicted satisfactorily with any simple intensity measure, since in reality the structure response is a function of the whole ground excitation time history. Any scalar intensity measure would fall short in predicting accurately the detailed structural response behavior. Under such circumstances, the evaluation of the probabilistic structural demand can be evaluated directly using uniform hazard ground motions.

2.1.4 DDC Analysis Using Uniform Hazard Ground Motions

When uniform hazard ground motions are available for time history response analysis, such as in the ensembles corresponding to a given probability of exceedance level, one can take advantage of these motions to arrive at the DDC curve. For example, in the SAC Project records were selected and scaled to match the uniform response spectra for a wide range of natural period and corresponding to 50%, 10% and 2% in 50 years exceedance probabilities at the site (Somerville et al, 1997). In areas where such records are not available, such as in the eastern United States, synthetic ground motions corresponding to uniform hazard response spectra can be generated for this purpose (Wen and Wu, 2001). These ground motions represent future excitations due to events of various magnitudes, distances, and attenuation but all match the response spectra of given probability for a wide period range (Fig. 2.1.2). Since the matching was done at the median of the response spectra, the median of the structural response under the suite of the uniform hazard ground motion is a steady measure of the displacement demand corresponding to the probability of the ground motions. Wen and Wu (2001) have shown that the median response obtained for both linear and nonlinear inelastic systems from the suite of ten uniform hazard ground motions has a small coefficient of variation (< 10%) and matches closely the response corresponding to the hazard level based on simulation

using large (9000) samples. The DDC curve as shown in Fig. 1.1.2 can be then obtained by fitting a distribution (lognormal is generally a good model) through these three probability levels. This is a more direct procedure without having to identify a proper intensity measure and perform the regression analysis. Fig. 2.1.3 shows an example of such procedure for a steel building before and after retrofit in Carbondale Illinois.

2.1.5 Demand on Spatially Extended Systems

The treatment of demand uncertainty as mentioned in the foregoing is suitable for structures or systems that do not occupy a large area and can be approximated as a point system. For spatially extended systems such as long bridges, building stock and facilities in a community or a city, taken in the entirety, and transportation networks, additional considerations on the seismic demand are needed. The demand on the systems obviously depends on the spatial correlation of the seismic excitation. An independence assumption here could lead to serious underestimate of the uncertainty of the demand. The demands from the earthquake ground motion are positively correlated spatially and highly variable; this positive correlation causes the variation in the aggregated (basically summed) random damages and losses to increase significantly.

Under the assumption that the excitation can be modeled by a stationary random process, the spatial correlation of random seismic waves at two different points during a given event can be described by a coherence function. The coherence function describes the correlation or dependence between two random processes, somewhat like the correlation coefficient between two random variables. It is a function of the separation of two points, apparent wave propagation velocity, and frequency. It can be determined from array records of past earthquakes. It allows one to model the correlation of excitations at any two points of the system and hence response of a spatially extended system via a random vibration analysis or simulation (e.g. Samaras et al 1983). As seismic excitation frequency content and intensity clearly vary with time, a stationary process treatment is obviously an approximation. Another correlation that needs to be carefully considered is the event-dependent intensity correlation. In other words, during a large event, the excitation intensity would be high for an extended area, even though the excitations may not be highly correlated in time when the separation is large. Similarly, during a small event, the intensity would be low for an extended area. This correlation would play a significant role in total demand uncertainty.

To include these correlations of demand on spatially extended systems, an event-based or scenario-type approach seems to be most suitable. The demand on the system can be described in terms of events of given magnitudes and distances. The deterministic scenario earthquake approach such as the worst-case scenario has been commonly used in the past. Such an event of course has extremely small probability of occurrence. It does not give a true picture of the future seismic demand on the system and provides little information for long-term planning based on cost versus benefit. For example, it may be the moderate and frequent events that cause the most damage/ cost to the systems.

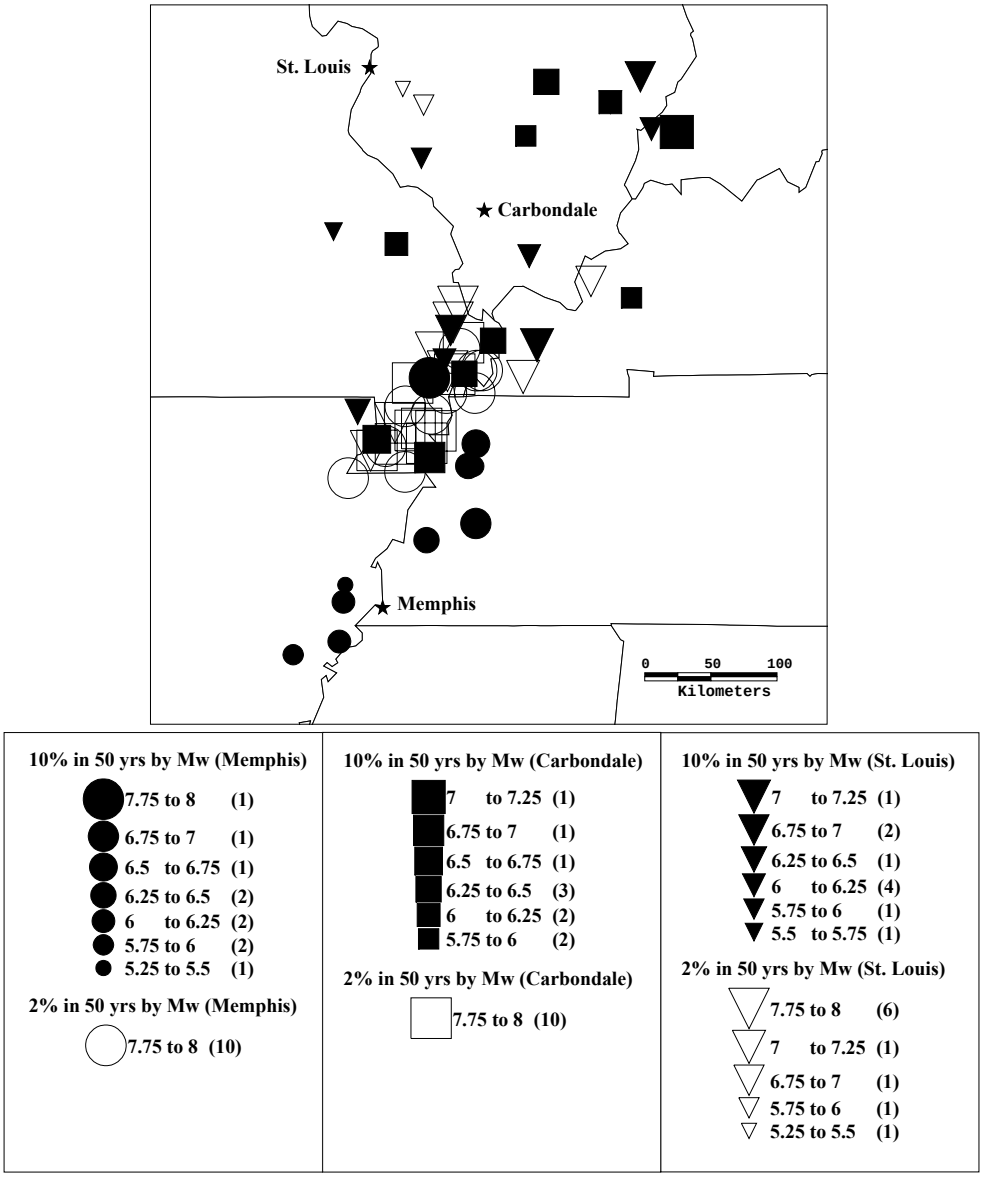

Figure 2.1.2 Epicenters and magnitudes of events contributing to uniform hazard ground motions for Memphis, Carbondale and St. Louis (number of events in the magnitude range is shown in the parentheses) (Wen and Wu 2001).

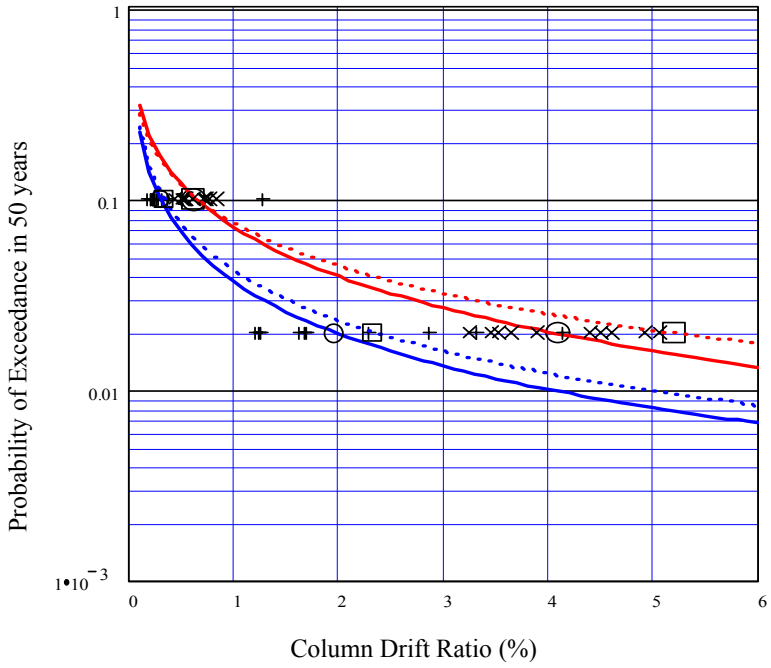

Figure 2.1.3. Probabilistic column drift ratio demand curve of a two-story steel moment frame building at Carbondale, IL before and after retrofit with shear walls (data points before retrofit [×], after retrofit [+], median value (o), and median including structural capacity uncertainty [□]; dashed and solid lines indicate performance curve with and without consideration of capacity uncertainty) (Wen and Wu 2001).

To consider all possible demands, simulation of future events can be used but is computationally impractical. To reduce computation cost, a method similar to the smart simulation method used in generating the uniform hazard ground motions looks promising. Events of various magnitudes and distances are first generated according to the regional seismicity and screened for each hazard level using the uniform hazard response spectra for the general location. The response spectra may be the averaged value of different sites if the system occupies a very large area such as a transportation network. As the response spectra are a good measure of demand on systems of wide range of frequency, the limited number of uniform hazard events after the screening (such as those given in Fig 2.1.2) would be representative of the future seismic demand on the spatially extended systems in a particular location. Given the magnitude and distance of such an event, the system response to the event can be then evaluated using the most suitable method to incorporate the effect of spatially correlation. For example, a coherence function matrix may be used in simulation of ground motions at different points. Alternatively, a physical wave propagation type of approach such as the broadband procedure (Saikia and Somerville 1997) can be used for this purpose. The spatial correlation in intensity may be accounted for via a simple procedure such as an intensity map for the given event. The median value of the system response to all events of the same hazard level will have a probability corresponding to the hazard level, from

which the system demand curve similar to Fig 2.1.3 can be obtained. The spatial correlation can be therefore properly accounted for.

2.1.6 Selection of Intensity Measure

Proper selection of the intensity measure to relate structural performance is an important step in the vulnerability analysis. A good intensity measure would predict the structural response and hence the vulnerability accurately and efficiently. In the past peak ground acceleration, peak ground velocity, peak ground displacement, and effective ground acceleration and velocity have been used for this purpose. A recent study (Luco and Cornell 2001) showed that measures consisting of the spectral displacement of the first two modes of linear elastic systems, modal participation factors and inelasticity are good measures in terms of "efficiency" and " sufficiency" for both far-source and near-source earthquakes. Efficiency is a measure of the scatter in a regression analysis of the response against the intensity measure. The smaller the scatter, the fewer the number of response analyses necessary to estimate the system capacity with the same accuracy. Sufficiency is a measure of the dependence of the response on the measure alone and not any other seismic parameters such as magnitude and distance of the event. The buildings used in that study are steel moment frames. The conclusion may not be strictly valid for other type of the constructions. The most effective intensity measure may be structure type dependent and needs to be investigated further.

2.1.7 Intensity Measure versus Uniform Hazard Ground Motions

The various intensity measures used by researchers such summarized in Luco and Cornell (2001) are all scalars derived from the ground motion time history and some of the structural properties such as natural period, participation factor, and inelastic response. Such intensity measures cannot predict all structural response characteristics, particularly higher mode contribution and very complex response behavior such as brittle member failure observed in pre-Northridge steel buildings and various failure modes of masonry structures. Such complex structural response behavior can be predicted only when the entire time history of the ground motions is used. This is the approach used in the uniform hazard ground motion method. The effectiveness of the two approaches in predicting the vulnerability in terms of total analytical and numerical effort versus accuracy of the vulnerability prediction is an important subject for investigation in this project.

2.2 Capacity Uncertainty and Modeling Errors

Structural capacity is the maximum force, displacement, velocity, or acceleration that a member or a system can withstand without failure, or more specifically, without reaching a prescribed limit state. The capacity is therefore dependent on the material properties, member dimensions, system configuration, the limit state under consideration, and methods and models used in describing the capacity. As in the case of demand, both

(aleatory) randomness and (epistemic) uncertainty are important elements in the evaluation of capacity and need to be carefully considered.

2.2.1 Material Properties

The member and system capacity depend directly on the material strengths and stiffnesses, which are inherently random. The randomness can be modeled by random variable based on test data. It is common to use the first two moments, i.e. the mean and standard deviation (or coefficient of variation), to describe the central value and the variability. Normal, lognormal or Weibull distributions are commonly used for convenience. The actual strength of the material of a given member generally differs, in some cases significantly, from the nominal values used in member capacity calculations during design. The relation between the nominal value and the actual value therefore needs to be established to estimate the real member capacity. The strength variability obviously depends on the material, manufacturing process, and sometimes the testing protocol. In general, the variability in masonry and timber material strength is larger than those in reinforced concrete and steel. Material property variability and test data up to 1980 can be found in the report by Ellingwood et al (1980). For example, the coefficient of variation of strength of timber varies in the range from 10 % to 30 % depending on species and in flexure or compression; and that of masonry walls from 10 % to 26 % depending on configuration and in compression or flexure. The coefficient of variation of compressive and tensile strength of concrete is around 18 % and that of the yielding strength of steel reinforcement and steel rolled shapes is around 10 % or less. Properties of construction material such as concrete and structural steel evolve over time. Strength statistics of newer material such as high-strength steel and concrete may be found in more recent literature. For example, statistics on yield and ultimate strength of structural steel under various environmental conditions can be found in the recent FEMA/SAC report (2001).

2.2.2 Member Capacity under Monotonic Load

The inherent randomness in the material property carries over to the structural members made of these construction materials. In addition, there is randomness in the dimensions of the members and also the capacity refers to a particular limit state such as shear, bending, or buckling failure under monotonic or cyclic loading condition. The randomness in terms of the bias (mean capacity/nominal capacity) and coefficient of variation of steel, reinforced concrete, masonry and glulam structural members (beams, columns, and walls) of various configurations and for various limit states can be found in Ellingwood et al (1980). The majority of the bias factors are between 1.0 and 1.2 and the coefficient of variation is under 20 %. The bias can be described by a normal distribution. The difference between the two models is small when the coefficient of variation is small.

2.2.3 Members Capacity under Cyclic Load- Damage Index

For seismic loading, one is especially interested in the member capacity under cyclic loading since members in a structural system generally undergo stress reversals of

various amplitudes and the member may reach a limit state under combined action of large deflection and cumulative damage. To account for both effects, various damage indices have been proposed. The most widely used is the index developed by Park and Ang (1985) based on test results of 403 reinforced concrete members. The index is a linear function of maximum displacement δ_m and total hysteretic energy dissipation normalized by member ultimate displacement and monotonic loading δ_u, and yield force Q_y.

$$D = \frac{\delta_m}{\delta_u} + \frac{\beta}{Q_y \delta_u} \int dE \tag{2.2.1}$$

Different value of the index corresponds to different limit states such as 0.4 for serious damage and 1 corresponding to complete damage (collapse). Test data show that the damage index capacity of reinforced concreted member can be modeled by a lognormal random variable with a mean value equal to 1.0 and a coefficient of variation of 0.53. It indicates that the randomness in the reinforced concrete member capacity is quite large. The index has been used in damage evaluation of buildings and other structures, e.g. Park et al (1985).

2.2.4 Rotation Capacity of Steel Connection Members

Following the large number of brittle fracture failures found in connections in steel moment frames of many buildings due to the 1994 Northridge earthquake, the capacity of connections against rotation demand under cyclic loading during earthquake excitations has attracted much attention in the structural engineering profession. In the FEMA/SAC project (SAC 2000), a comprehensive testing program of a large number (120) of welded and bolted connections of various configurations has been carried out according to pre-Northridge practice and for post-Northridge design in which many different improvements were incorporated. Test results of hundreds of experiments prior to 1994 were also analyzed. The connection rotation capacities for both pre- and post-Northridge connections were obtained. The capacity is defined in accordance with two limit states; θ_p the rotation limit when plastic deformation occurs and θ_g, the rotation limit corresponding to severe damage that the gravity load carrying capacity of the member is compromised. Test data generally show the dependence on the depth of the beam or the depth of the connection element of these capacities and large scatter. The mean values and standard deviations as linear functions of the depth of the beams were established from regression analyses of test results. Depending on the specific connection type and the depth of the beam, the rotation capacity and variability in terms of these two statistics shows large variation. Such large variation of coefficient of variation for different connections could partly due to the small number of samples used in the regression analysis. No distribution models were recommended for the capacity. In view of the small sample size and large coefficient of the variation, selection of the distribution model should be done with care. Note that with a distribution model, say a normal distribution, one can predict the probability of limit state of plastic deformation or loss of gravity load carrying capacity of the connection member when the rotation demand θ_d is

$$\text{known P(plastic deformation)} = P(\theta_p < \theta_d) = \Phi\left(\frac{\theta_d - \mu_{\theta_p}}{\sigma_{\theta_p}}\right) \quad (2.2.2)$$

$$P(\text{loss of gravity load carry capacity}) = P(\theta_g < \theta_d) = \Phi\left(\frac{\theta_d - \mu_{\theta_g}}{\sigma_{\theta_g}}\right) \quad (2.2.3)$$

The connection fragility is defined as the probability of capacity being exceeded given a specific demand.

2.2.5 Bayesian Models of Member Capacity

When calculating member capacity against a prescribed limit state, mathematical models based on mechanics are used. In all mathematical models, there are errors associated with the assumptions and approximations of such model that it needs to be calibrated against experimental results or field observations. Rigorous tracking of the uncertainty in the mathematical model based on our prior knowledge of the mechanical behavior of the components and calibrating the model against experimental data can be done via the Bayesian statistical method (Section 2.2.1). Such a models have been recently developed for structural members by researchers (e.g., Gardoni et al 2002, Sasani et al 2001). The basic concept behind this method can be illustrated by a simple example as follows. Consider a structural member model predicting the member capacity, y, against a prescribed limit state by the following equation

$$y = g(\boldsymbol{\theta}; \mathbf{x}) + \varepsilon \quad (2.2.4)$$

in which $\boldsymbol{\theta} = \theta_1, \theta_2, \ldots \theta_k$ denotes the set of the parameters for the mathematical model; $\mathbf{x} = x_1, x_2, \ldots x_n$ represents the sample values of y from experimental or field observations; ε is a random variable representing the unknown errors in the model assumed to follow a normal distribution. Within the context of such formulation, given the parameters $\boldsymbol{\theta}$, y is a normal random variable. Calibrating of the model parameters in view of observational evidence is formulated by regarding the model parameters as random variables governed by distributions based on prior knowledge (such as mechanics principles, structural analysis methods, and engineering judgment/experience). The parameters are calibrated (or updated in Bayesian terminology) in view of sample evidence of y as follows:

$$f''(\boldsymbol{\theta}) = k\, L(\boldsymbol{\theta}) f'(\boldsymbol{\theta}) \quad (2.2.5)$$

in which $f'(\boldsymbol{\theta})$ = the prior distribution of the model parameters; $L(\boldsymbol{\theta})$ is the sample likelihood function or the conditional probability of observing $\mathbf{x}$ given $\boldsymbol{\theta}$; and k is the normalizing constant. Note that the epistemic uncertainty such as those associated with knowledge and modeling errors including those due to small sampling (small n) is included in the formulation. In general, for small n and sharp $f'(\boldsymbol{\theta})$, i.e., strong knowledge based information and weak observational information, the prior distribution dominates. On the other hand, if $f'(\boldsymbol{\theta})$ is flat or diffuse and n is large, then $L(\boldsymbol{\theta})$ dominates. The overall uncertainty in the posterior distribution $f''(\boldsymbol{\theta})$ is less than

either $f'(\theta)$ or $L(\theta)$. One of the advantage of the Bayesian method is that even incomplete data of **x** such as those in the form of upper or lower bound due to certainty in the data collecting process or experimental procedure can be incorporated into $L(\theta)$ without difficulty. The method has been applied to evaluation of the capacity of circular reinforced concrete bridge columns and shear walls against deformation and shear demand due to cyclic loads. The advantage of this model compared with deterministic models was also shown. Fig. 2.2.1 shows the result of the probabilistic prediction of the capacity of RC column against drift ratio demand, i.e. the conditional probability of failure of the column given that it reaches a drift ratio (or fragility curve).

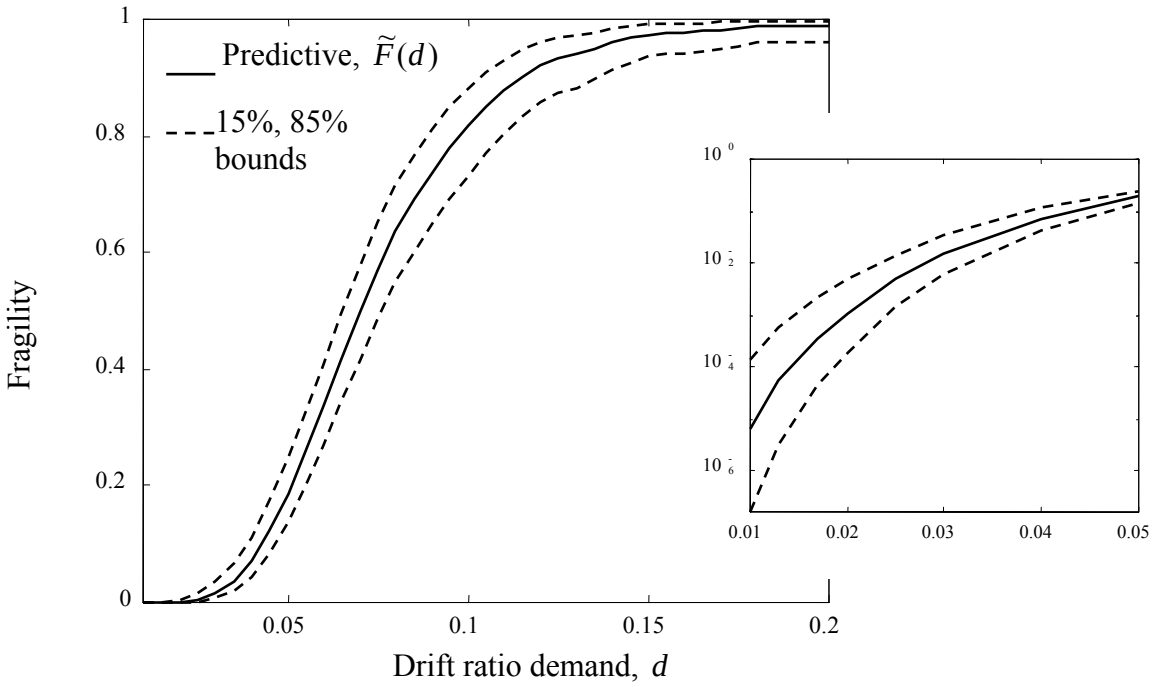

Figure 2.2.1. Probabilistic Capacity of RC Column against Drift (Gardoni et al 2002)

2.2.6 Uncertainty in System Capacity

The description of uncertainty in system capacity is more involved since a structural system consists of many components and the system behavior is complex under dynamic excitation, especially when the system goes into nonlinear range. The system capacity can be therefore more conveniently described in terms of the system limit states of interest.

2.2.6.1 System Capacity against Damage

Commonly used system limit states are those corresponding to different damage states and performance levels. For example in SEOAC Vision 2000 (1996), there are five performance(damage) levels: fully operational (negligible), operational (light), life safe(moderate), near collapse(severe), and collapse(complete) and each level is related to a structural (and nonstructural) response level indicated by a transient and a permanent drift limit. In the FEMA/SAC project for steel buildings, the performance/damage levels were reduced to two: immediate occupancy and collapse prevention. The system capacity is again described in terms of interstory drift angles. The uncertainty in the system capacity therefore can be described in terms of the drift capacity for different performance levels, such as the median drift capacity and its coefficient of variation. The commonly accepted distribution for the capacity is the lognormal distribution for its convenience in reliability analysis and reliability-based design, as will be seen in the next section. Structures of different construction material, configurations, and designs have different drift thresholds [e.g., FEMA 273]. Determination of drift capacities for different performance levels is largely a process of combination of analysis and judgment/experience. The determination of system collapse prevention capacity is discussed further in the following.

2.2.6.2 System Capacity against Collapse-Incremental Dynamic Analysis

Of all the limit states and the corresponding system capacities, system collapse is the most difficult to determine. The structural dynamics close to collapse is extremely complex and is still largely an unsolved problem due to nonlinear member and system response behaviors. The large record-to-record variation of ground motions and structural response behaviors further complicate the matter. Collapse of structures under random excitations is a difficult mathematical problem of stochastic stability. Engineers have used an inelastic static pushover analysis in the past to estimate this capacity. It provides insight into the structural response behavior at large displacement (Krawinkler and Sever 1997; Gupta and Krawinkler, 2000) but considers the first mode static response only, which is basically different from dynamic response. As a result, such analysis generally over-predicts the response and underestimates the capacity.

Improvements can be made by considering higher modes via modal pushover analysis as shown by Chopra and Goel (2002). Vamvatsikos and Cornell (2001) extended the concept of pushover analysis to dynamic response in the form of incremental dynamic analysis (IDA). The system capacity against collapse is evaluated by dynamic response analyses of the system under a suite of ground motion time histories such as the SAC ground motions, which are increased in intensity causing the structural response to increase from the linear elastic range into the nonlinear inelastic range and finally to the point where the structure finally becomes unstable, i.e. a large increase in response with a small increase in the spectral acceleration. The displacement at this final point is defined as the system displacement capacity against collapse. As mentioned earlier, due to the large record-to-record variation of the ground motions and extremely complex structural nonlinear behavior, the transition point is not always easy to pinpoint. Engineering judgments are often necessary and there are large scatters for different excitations with

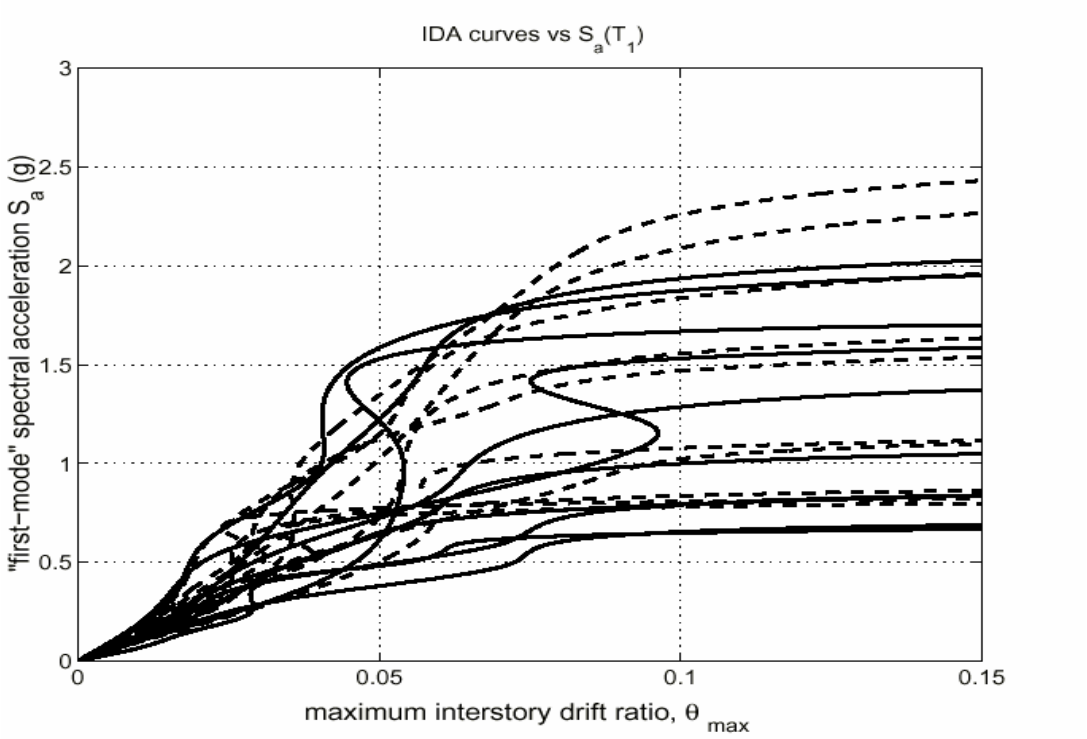

Figure 2.2.2. Results of Incremental Dynamic Analysis of 9-story Steel Moment-Resisting Frame with Fracturing Connection under SAC Ground Motions (Vamvasitkos and Cornell 2002)

the same spectral acceleration. Fig. 2.2.2 shows an example of the interstory drift using DIA of a 9-story steel frame under SAC ground motions. The uncertainty in capacity against collapse can be described in terms of the mean and standard deviation of the interstory drift capacity under multiple recorded ground motions from DIA. The coefficient of variation of this displacement capacity is generally on the order of 30%. Such a procedure has been used in the FEMA/SAC procedure.

2.3 Structural Systems Limit State Probability (Reliability) Analysis

In view of the large uncertainties in both demand and capacity, as shown in the previous sections, the performance of the structural systems can be described meaningfully only when these uncertainties are taken into consideration explicitly. In other words, evaluation of the performance needs to be described in terms of reliability of the structural system against various limit states over a given period of time. Since the earthquake occurrence and the ground excitations and structural responses are random functions of time, the reliability problem is therefore a problem of a vector random process in time passing from a prescribed safe domain to an unsafe domain defined by the limit state. A rigorous mathematical solution of the so-called "first passage" problem is generally difficult. In reliability analysis, the random process first passage problem is often replaced by a more tractable formulation in which a structural performance function

corresponding to a given limit state is constructed in terms of a vector of random variables representing the uncertainty in the problem. The reliability problem is then solved using the first two moments of the random vector and a first-order or second-order approximation of the performance function. Such methods are commonly referred to as the first order reliability method (FORM) or the second order reliability method (SORM). In earthquake engineering, an even simpler formulation of the problem is used in terms of two variables, demand versus capacity, as described in the previous sections, for a given limit state. Alternatively, depending on the problem, a simulation method may be more suitable to evaluate the reliability. These methods, their advantages and disadvantages in application to earthquake engineering are briefly described in the following.

2.3.1 Identification of Important Limit State

Performance levels or limit states for both structural and non-structural systems are defined in this document as the point in which the system is no longer capable of satisfying a desired function. There are many types of performance levels in the field of earthquake engineering. In addition, performance levels can be identified by qualitative and quantitative approaches. Both methods are summarized below.

Traditional Qualitative Approaches

Qualitative approaches for identification of performance levels have traditionally been used in building codes. In particular, most building codes require designers to ensure life safety of the occupants during factored loading and serviceability or functionality during unfactored loading. FEMA 273, and its update FEMA 356, has the most comprehensive documentation on performance levels that are defined qualitatively and is briefly summarized below.

FEMA 273/356 define *performance levels* related to the structural system as:

(1) *Immediate Occupancy (IO)* - occupants are allowed immediate access into the structure following the earthquake and the pre-earthquake design strength and stiffness are retained;
(2) *Life Safety (LS)* - building occupants are protected from loss of life with a significant margin against the onset of partial or total structural collapse;
(3) *Collapse Prevention (CP)* – building continues to support gravity loading, but retains no margin against collapse.

In addition to the discrete structural performance levels, FEMA 273/356 also define *structural performance ranges* such as:

(1) *Damage Control (DC)* – Range of structural damage between immediate occupancy and life safety;
(2) *Limited Safety Range (SR)* – Range of structural damage between life safety and collapse prevention;

FEMA 273/356 also defines non-structural performance levels as:

(1) *Operational* - non-structural components are able to function as prior to the earthquake;

(2) *Immediate Occupancy* – building access and life safety systems generally remain available and operable;
(3) *Life Safety* – non-structural damage that is not life threatening;
(4) *Hazard Reduced Range* - damage that includes potentially falling hazards, but high hazard components are secured and will not fall. Preservation of egress, fire suppression systems, and other life safety issues are not ensured;

In terms of identifying overall building performance levels, FEMA 273/356 utilizes both definitions of structural and non-structural performance levels. Analysis…uncoupled…
It is important to note that these traditional performance level definitions are based on *qualitative* definitions. For illustration purposes, FEMA 273/356 presents inter-story drift values that are typical for each structural performance level for the different types of structural systems in use. For example in reinforced concrete frame structures, inter-story deformations of 1%, 2%, and 4% of the story height may be acceptable for IO, LS, and CP, respectively. However, it is clear that deformation limits will depend on a variety of variables that include: degree of section confinement and detailing; level of axial column load (P-delta effect); non-structural participation; and pre-existing damage.

Quantitative Approaches
Although current building codes and state-of-the-art publications have attempted to define the various performance levels for structural and non-structural systems, performance levels have only been identified qualitatively. Therefore, designers have to determine quantitative response limits that correspond to the qualitative code descriptions. Another approach for defining structural performance levels might be based on quantitative procedures using nonlinear pushover techniques. These quantitative performance levels can be utilized by the designer and judged to supersede the qualitative performance levels in current building codes.
Example performance levels that can be identified analytically using nonlinear pushover procedures are:
(1) *First Yield (FY)* – Inter-story deformation at which a member of a story initiates yielding under imposed lateral loading;
(2) *Plastic Mechanism Initiation (PMI)* – Inter-story deformation at which a story mechanism initiates under imposed lateral loading;

For example, consider the portal frame in Fig.2.3.1(a). Under imposed lateral loading, the story shear force versus inter-story deformation can be calculated using pushover techniques and hypothetically shown in Fig. 2.3.1 (b). The FY performance level corresponds to an inter-story deformation at first member section yielding, shown at the base of the columns. The PMI performance level subsequently occurs after both ends of the beam yield. It is important to note that the sequence and form of member yielding during applied loading prior to the mechanism formation. Both can have significant effects on the levels of structural deformability (capacity) in building structures.
A key input parameter required in identifying such quantitative performance levels is the imposed lateral loading or deformations. Since multi-story buildings are susceptible to high mode response and impulse-type loading during earthquakes, loading patterns that have been typically used for determining structural demands as in current building codes

may not be appropriate for identifying performance levels, which are *capacities*. As such, the imposed lateral loading or deformation should be consistent with those that have the most critical consequence. Fig. 2.3.2 shows the deformation pattern in a framed structure during inverted triangular lateral loading (similar to loading proportional to the fundemental mode shape of the structure) and during loading that might be critical for the second story of the building. Fig. 2.3.2 (a) shows that the deformations are uniformly distributed throughout the building, where Fig. 2.3.2 (b) shows that the deformations on the second floor would be more impose more critical mechanisms on the second floor.

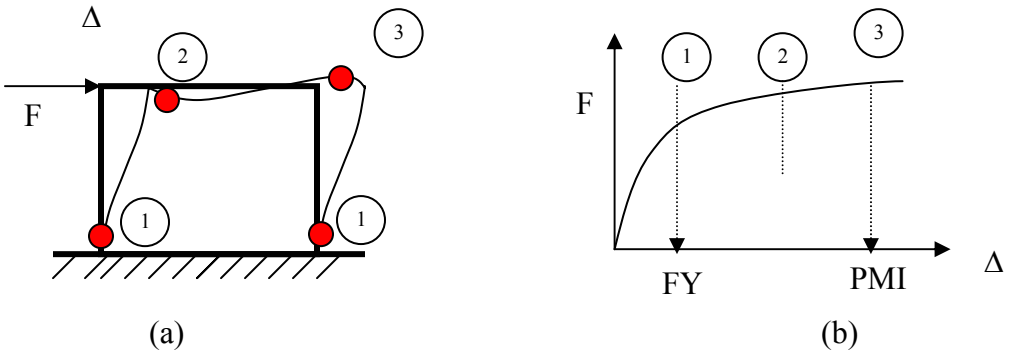

Figure 2.3.1 Pushover Analysis and Yield Formation

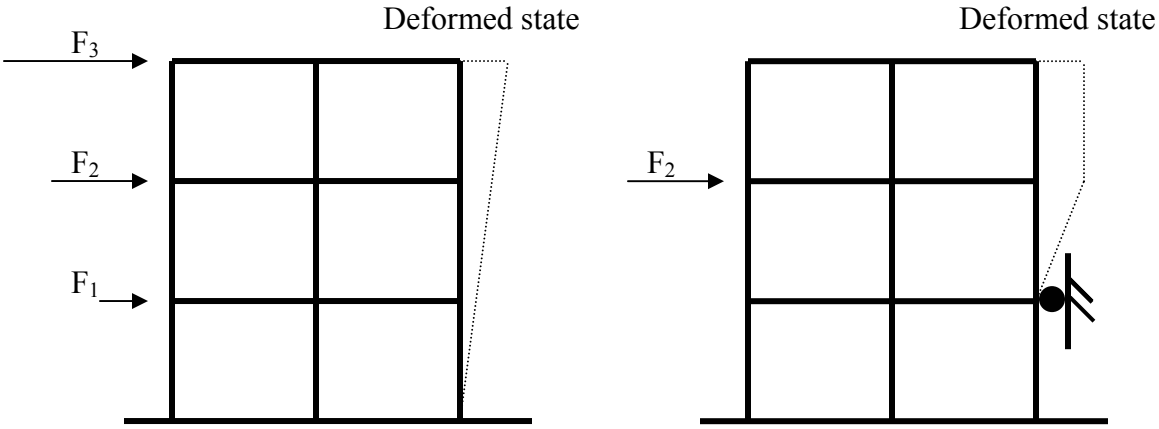

Figure 2.3.2. Loading Patterns for Pushover Analysis

From pushover analyses, a hypothetical comparison of the story shear vs. inter-story drift is shown in Fig. 2.3.3. The figure shows that the previously described FY and PMI performance levels will depend on the imposed lateral loading or deformation patterns.

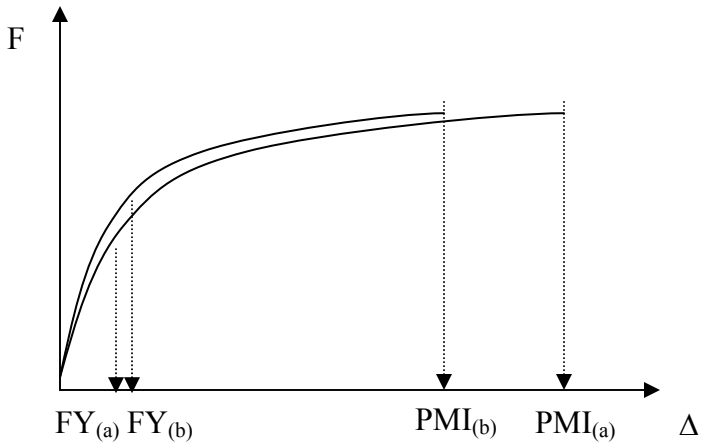

Figure 2.3.3. Comparison of Story Shear with Interstory Drift in Pushover Analysis

2.3.2 Demand versus Capacity Formulation

The reliability problem is simplified considerably if the limit state can be stated in terms of the demand exceeding the capacity. This statement may be an over-simplification, in that the capacity and demand may not always easily defined for certain limit states such as the case of system collapse discussed in the previous section. In earthquake engineering applications, simplicity nevertheless offers some advantages, especially in code procedure formulation. This is the method used in the reliability based, performance oriented design procedure proposed in the SAC/FEMA Steel Project (Cornell et al 2002), which is described in the following.

Considering now the limit state described in terms of only two random variables; C (capacity) and D (demand), the performance function is now g(**X**) = C-D a linear function. The probability of limit state over a given period of time, t , is then given by the probability integral

$$P_t = P_t\,(C < D) = \int P_t\,(C \le D \,|\, D = d) f_D\,(d)\,dd \qquad (2.3.1)$$

Simple closed form solutions of the integration can be obtained when both C and D can be modeled by normal or lognormal random variables.

$$P_t = 1 - \Phi(r) \qquad (2.3.2)$$

$$r = \frac{\mu_C - \mu_D}{\sqrt{\sigma^2{}_C + \sigma^2{}_D}}$$, when both C and D are normal

in which μ and σ denote mean and standard deviation

$$r = \frac{\lambda_C - \lambda_D}{\sqrt{\beta^2{}_C + \beta^2{}_D}}$$, when both C and D are lognormal

in which, $\beta_X = \sqrt{\ln(1+\delta_X{}^2)}$, and $\lambda = \ln\mu_X - 0.5\beta_X{}^2 = \ln\tilde{x}$. $\tilde{x}$ = median value of X and δ_X = coefficient of variation of X.

This is not the case when the demand described by Eq. 2.3.1 is not a simple normal or lognormal variable. The closed form solution, however, can still be obtained when the capacity variable C can be modeled by a lognormal random variable and the seismic hazard can be described by a power function as given in Eq. 2.1.7.

2.3.3 FEMA/SAC Formulation

When the uncertainty in the modeling and analysis is considered the limit state probability becomes a random variable and needs to be treated as such. Depending on the application, for example, one may want to evaluate the mean value of the limit state probability to perform a risk/benefit analysis or evaluate the percentile value for a confidence interval estimate. The uncertainty can be conveniently grouped into those in the hazard analysis, excitation/demand relationship, and structural capacity estimate. For example, the parameters k_0 and k in the seismic hazard model (Eq. 2.1.7), a and b in the regression equation for structural response (Eq.2.1.4), and the parameters in structural capacity models (Eqs.2.2.1 to 2.2.3) may all have uncertainty due to either modeling (e.g. incorrect functional form) or sampling (small number of test results) errors. For simplicity and tractability in analysis, the uncertainties in the seismic hazard, structural demand, and structural capacity models are assumed to be lognormal variables with a median values given by the model predictions and dispersion parameters β_{HU}, β_{DU}, and β_{CU}. The subscript H, D, and C denote hazard, demand, and capacity respectively and U denotes uncertainty. Similarly, the dispersion parameters of the randomness in the demand and capacity are denoted by β_{DR}, and β_{CR}. Incorporating the uncertainty as defined above into Eq. 2.18, one can obtain the mean estimate of the limit state probability as follows:

$$E[P_t] = E[H(a^{\tilde{C}})]\exp[\frac{1}{2}\frac{k^2}{b^2}(\beta^2{}_{DR} + \beta^2{}_{DU} + \beta^2{}_{CR} + \beta^2{}_{CU})] \qquad (2.3.3)$$

in which $E[H(a^{\tilde{C}})] = H(a^{\tilde{C}})\exp[\frac{1}{2}\beta_{HU}]$ (2.3.4)

In other words, effects of randomness and uncertainty are now combined. Note that the expected limit state probability is equal to the mean estimate of the hazard exceeding the median structural capacity multiplied by a correction factor that increases exponentially with the total uncertainty in the demand and capacity, and depends on the hazard and regression analysis parameters (k and b). The seismic hazard given in the USGS National Earthquake Hazard Maps is that of the mean hazard (Frankel et al 1997) with regard to modeling uncertainty, Eq. 2.3.3 is therefore compatible with the USGS hazard maps.

To estimate the percentile values for a confidence interval estimate, in principal all uncertainty dispersions need to be considered. In the FEMA/SAC procedure, it is assumed that the uncertainty in seismic hazard has been incorporated through the mean hazard curve in Eq.2.3.4. The confidence interval estimate is then obtained as function of the demand and capacity uncertainty using the mean hazard curve. The limit state probability corresponding to a percentile level q (probability of q not being exceeded) is given by

$$P_{q,t} = \tilde{P}_t \exp[K_q \beta_L] \tag{2.3.5}$$

$$\text{in which, } \tilde{P}_t = E[H(a^{\tilde{C}})]\exp[\frac{1}{2}\frac{k^2}{b^2}(\beta^2_{DR} + \beta^2_{CR})] \tag{2.3.6}$$

$$\beta_L = \sqrt{\frac{k^2}{b^2}(\beta^2_{DU} + \beta^2_{CU})} \tag{2.3.7}$$

$$K_q = \Phi^{-1}(q) \tag{2.3.8}$$

$\tilde{P}_t$ is the median (50%) value of P_t . Note that the median estimate is the same as that considering only the randomness in the demand and capacity. The q percentile limit state probability is equal to $\tilde{P}_t$ multiplied by a factor depending on the uncertainty dispersion parameters and the percentile value. K_q is the standard normal variate value corresponding to this percentile value.

2.3.4 Method of Simulation

2.3.4.1 Randomization of Capacity

The simulation method can be applied to reliability evaluation when the structural capacity uncertainty is considered. In a direct Monte-Carlo method, one needs only to randomize the capacity of the structure according to the randomness and uncertainty models as mentioned above in the time history analysis of the structure. The limit state probability can be then calculated from the response statistics of the repeated time history analyses. It is conceptually simple. The difficulty is obvious that the randomization needs to be done for each element. Also, as in the structural demand analysis, the computational effort may become excessive

2.3.4.2 Uncertainty Correction Factors

To incorporate the effect of capacity uncertainty into the simulation procedure and at the same time avoid the difficulty of detailed modeling at the component level as mentioned above, one can use a hybrid procedure. The structure is first regarded as deterministic and the smart simulation is performed at a given hazard level, e.g. 50%, 10%, or 2 % in 50 years to obtain the probabilistic structural demand curve, e.g., the median response to the set of uniform hazard ground motions (UHGM) corresponding to a hazard level as

shown in Fig. 2.1.3. At a given hazard level, the effect of the uncertainty can be then incorporated by multiplying the median estimate by a correction factor similar to that given in Eq. 2.3.3. As shown in Fig. 2.1.3, at a given hazard level such as 10% in 50 years or 2% in 50 years, the demand described by the median response to the UHGM corresponds to the probability of exceedance considering the randomness and uncertainty (if included in the simulation in Section 2.1.4) in the excitation only. To account for the randomness and uncertainty in the capacity and demand, the limit state probability is multiplied by a correction factor (Wen and Foutch 1997)

$$C_F = 1 + \frac{1}{2} S^2 \delta^2_T \tag{2.3.9}$$

in which S is the sensitivity coefficient to the change in structural capacity depending on the seismic hazard and the median structural capacity; δ_T is the coefficient of variation of the total randomness and uncertainty in the demand and capacity.

$$\delta_T \approx \sqrt{\delta^2_{RC} + \delta^2_{UC} + \delta^2_{RD} + \delta^2_{UD}} \tag{2.3.10}$$

in which RC, UC, RD, and UD denote randomness and uncertainty in capacity and demand. Alternatively, if the limit-state probability is kept the same, the median value can be multiplied by a correction factor C_D to reflect the effect of total uncertainty as follows:

$$C_D = 1 + \frac{1}{2} S \delta^2_T \tag{2.3.11}$$

The seismic hazard, e.g., in terms of 50-year probability of exceedance of the spectral acceleration, can be generally modeled by a lognormal distribution. If the hazard curve is not available, it can be determined directly from the UHGM. The median values of the spectral acceleration of the UHGM at 10% and 2% in 50 years allow one to determine the two lognormal distribution parameters λ and ζ. The sensitivity coefficient S is then given by

$$S = \frac{\ln a_C - \lambda}{\zeta^2} \tag{2.3.12}$$

in which a_C is the median capacity of the system in terms of spectral acceleration S_a. Note that when the hazard dispersion measure ζ is large, S is small indicating that the the uncertainty in hazard dominates and the result is not sensitive to the structural capacity uncertainty.

For example, in Fig. 2.1.3, the 50-year spectral acceleration hazard parameters for Carbondale Illinois are λ = -6.85 and $\zeta = 2.07$(Wen and Wu 2001), for the building with a fundamental natural period of T= 0.15 sec after retrofit. The sensitivity coefficient S at 10/50 and 2/50 hazard levels are calculated to be 0.618 and 1.0 respectively according to Eq.2.3.9. Assuming a total uncertainty of δ_T = 50 % for the structural drift capacity against all limit states, the correction factor C_F and C_D are respectively 1.05 and 1.07 at 10/50 hazard level 1.13 and 1.13 at 2/50 hazard level. It is seen that the effect of the

demand and capacity total uncertainty is small since it is overshadowed by the large uncertainty of the seismic excitation (large value of the dispersion parameter ζ in the Eastern United States. The median values can be then modified by the correction factors and fitted by a lognormal (dashed) curve as the risk curve of column drift capacity being exceeded as shown in Fig. 2.1.3.

3.0 Application to Consequence Based Engineering

The initial stage of the Consequence-Based Engineering (Abrams 2002) is rapid assessment of system performance. At this stage refined and detailed uncertainty and vulnerability analysis are not required. When the consequence determined from rapid assessement is not acceptable and parameters need to be refined, the damage synthesis consisting of more detailed analysis of the system demand, capacity, and vulnerability is then performed. The different methods of vulnerability analysis as mentioned in the foregoing can be used most efficiently at various stages of the CBE.

3.1 Fast evaluation of vulnerability (no time history response/ regression analysis required)

For region of low to medium seismicity, systems response may be within linear elastic range. For such linear elastic systems or nonlinear inelastic system that can be represented by an equivalent SDOF inelastic system, a relatively fast analysis of the vulnerability can be performed using the response spectrum without having going through repeated time history response analyses. The method outlined in Eqs. 2.1.1 to 2.1.3 can be used. The excitation intenisty measure to be used in this case is the spectral acceleration S_a. As shown in Eq. 2.1.1 the structural response demand parameter D can be expressed as a function of S_a multiplied by a correction factor for uncertainty due to uncertainty in the simple method of analysis.

For example, if the demand variable is maximum interstory displacement at a given floor and the excitation intensity measure is the spectral acceleration of the first mode,

$$D = Ng(S) \approx N\sqrt{\sum_{i=1}^{n}\gamma_i g_i (S^i{}_a)^2} \qquad (3.1.1)$$

in which g is the relationship between D and S; N is the correction factor for modeling and analysis error and uncertainty. g_i is the interstory drift due to i-th mode, and γ_i is the modal participation factor. S^i_a is the i-th mode spectral acceleration, which can be determined from the uniform hazard response spectra given the fundamental mode spectral acceleration and the corresponding hazard level. The square root of sum of squares is used for an approximate evaluation of the combined maximum. Once the function g and the bias and uncertainty in the correction factor N are established, the probabilistic demand curve of D can be detemined as shown in Eq. 1.2.2, where both the modeling errors and seismic hazard are considered. If the bias factor is assumed to a lognormal distribution and seismic hazard in terms of the annual maximum spectral

acceleration S_a, the probabilistic demand curve can be calcualted according to Eq. 1.2.2 as follows,

$$P_t(D>d) = \int \{1 - \Phi[\frac{\ln d - \lambda_{D|S=s}}{\beta_{D|S=s}}]\} f_{S_a}(s) ds \qquad (3.1.2)$$

in which $\lambda_{D|S=s} = \ln \mu_N g(s) - \frac{1}{2}\beta^2_{D|S=s}$

$$\beta_{D|S=s} = \sqrt{\ln(1+\delta^2_N)}$$

$f_{S_a}(s)$ = density function of maximum spectral acceleration in (0, t)

The uncertainty in the seismic excitation intensity measure and the bias (μ_N = mean value of N) and uncertainty (δ_N = coefficient of variation of N) in modeling and analysis are therefore properly combined by Eq.3.1.1. which can be easily integrated. Similarly, for an inelastic system which can be represented approximately by a SDOF inelastic system with a given deflection shape, the displacement demand can be approximated described by an uniform inelastic response spectrum. The spectrum in terms of the the system yield coefficient C_y (system yield force/system weight) and the system ductility ratio η can be obtained from the uniform hazard acceleration spectrum of the linear systems (Nassar and Krawinkler 1992, Miranda and Bertero 1994, Collins et al 1996). One can therefore establish the relationship between the ductility demand and the spectral acceleration for the linear systems as follows

$$\eta = Ng(S) \qquad (3.1.3)$$

in which g(S) is the functional relationship between η and S based on the uniform hazard inelastic response spectra. N is the correction factor for the bias and uncertainty in this approximate method. Once the statistical parameters and distribution for N have been established, the probabilistic ductility demand curve can be obtained as outlined in Eqs. 3.1.1 and 3.1.2. The probabilistic demand curve of the system can be used to evaluate the limit state probability as shown in Eq. 1.2.3 when the system capacity against a given limit state and its uncertainty are known.

3.2 SAC/FEMA Approach based on Time History/Regression Anlaysis

For a complex nonlinear inelastic system that cannot be satisfactorily approximated by an equivalent SDOF system, time history response analyses are required to evaluate the limit state probability. The SAC/FEMA approach (as outlined in Eqs. 2.1.4 to 2.1.8) may be used to determine the probabilistic demand curve based on regression analysis of the system response under selected ground excitaion of a wide range of excitation intensity measure. The capacity uncertainty and seismic hazard modeling error can be then

incorporated into the formulation to evaluate the limit state probability as outlined in Eqs. 2.3.1 to 2.3.8.

3.3 Vulnerability Evaluation Using Uniform Hazard Ground Motions

For complex nonlinear inelastic systems that simple intensity measure may not be adequate to predict the system demand, a direct prediction of the system displacement demand from time history analysis under uniform hazard ground motions may be used to evaluate the limit state probability. The method outlined in Section 2.1.4 may be used to evaluate the probabilistic demand curve. The system capacity and uncertainty can be then incorporated to determine the limit state probability as outlined in Eqs. 2.3.4 to 2.3.12.

4.0 Demonstration of Vulnerability Function Framework for Buildings

The proposed vulnerability analysis framework is demonstrated here by probabilistic displacement demand analysis, fragility curve analysis, and limit state probability analysis over a given period of some representative buildings structures in mid-America. The emphasis is on credible quantitative treatment of uncertainty in the chain of events from the seismic source to the structural limit state probability evaluation. Although only building structures are studied, the procedure and treatment of uncertainty can be easily extended to other structures such as bridges and industrial facilities without difficulty.

4.1 Masonry Buildings in Memphis

The procedure is first demonstrated by a masonry commercial/residential building located in Memphis. A finite element model based on ABAQUS was developed to describe the nonlinear response behavior of the components and building system. Four wall damage modes, diagonal tension, bed-joint sliding, toe crushing and rocking are considered. The performance of the building is measured by the wall drift ratio. Ground motions that were generated according to the regional seismicity and uniform hazard response spectra (discussed in Section 2.1.4) are used in this study. Structural response time histories are calculated for each of the ten uniform-hazard ground motions (UHGM). The UHGM based probabilistic demand analysis is also carried out. The wall drift ratio is assumed to follow a log-normal distribution at each hazard level. In addition, a power law is also used to establish the relationship between the spectral acceleration and the wall drift ratio (see Section 2.1.2, Eq. 2.1.4). Vulnerability of this building in terms of fragility curve under a given spectral acceleration and 50-year limit state probability to various extent of damage according to FEMA 273 damage classification are then calculated. To determine the capacity against collapse and its uncertainty for the incipient collapse fragility curve, Incremental Dynamic Analysis (IDA, Section 2.2.6.2) is also performed. The impact of the contribution from various uncertainty terms is discussed.

4.1.1 Uniform Hazard Ground Motions

Due to the lack of data for ground motion of engineering interest, the ground motions required for vulnerability analysis were modeled by simulation (Section 2.1.4). The uncertainties in occurrence time, source location, magnitude, attenuation, and soil amplification are modeled by random variables and are simulated using information on regional seismicity and up-to-date random vibration-based ground motion models. Both point-source and finite-source models that are used in the simulation allow incorporation of some of the important near-source effects of large events. The method can be used for fast simulation of large number of ground motions for a given site, from which suites of ten uniform hazard ground motions (UHGM) corresponding to a given probability of exceedance are selected by matching the response spectra with the uniform hazard response spectra. The UHGM are then used for structural response analysis. They represent events of various magnitudes, distance, and attenuation. Their frequency and intensity are such that the *median* response of the structure gives an accurate estimate of the demand on structure *for a given probability of exceedance*. In other words, the suite

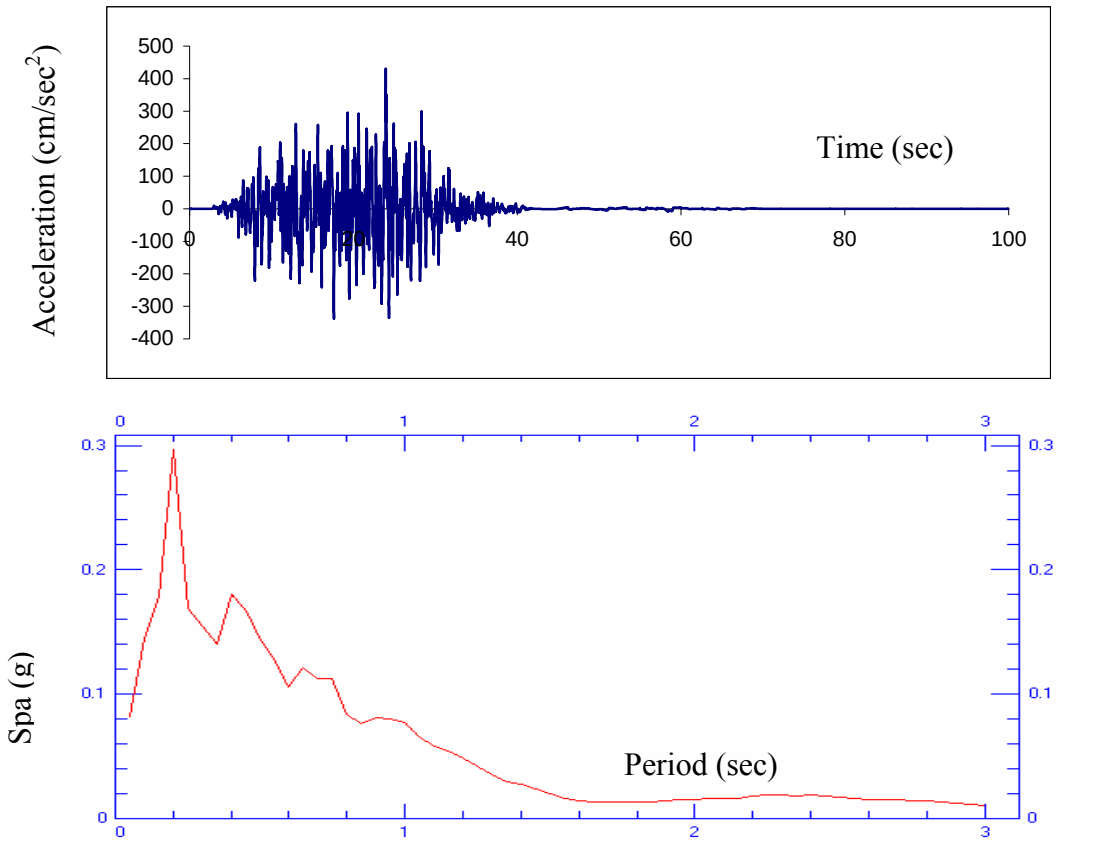

Figure 4.1.1 Sample time history and acceleration spectrum of the simulated 2/50 ground motion at Memphis, Tennessee.

of ten ground motions allows one to evaluate the structural response of small probability of exceedance that normally required much larger number (thousands) of structural response analyses. Two sets of ground motion corresponding to 10% in 50 years and 2% in 50 years exceedance probability were generated. Figure 4.1.1 shows one sample of the time history and spectral acceleration response spectrum of the 2% in 50 years ground motions generated for Memphis, Tennessee. Details of the method and results of can be found in Wen and Wu (2001).

4.1.2 Modeling of Masonry Walls

The nonlinear in-plane response behavior of unreinforced masonry (URM) walls is difficult to predict accurately. A general knowledge of the in-plane behavior of a solid wall, which does not have any opening, is a good start in understanding the in-plane behavior of a URM wall. The response behavior of an individual solid wall may be elastic in the beginning stage of the excitation, but as the intensity of ground motion increases, the response of the structure becomes inelastic and nonlinear. Based on FEMA-273 (NEHRP, 1997), four damage types common to a solid wall i.e., diagonal tension, toe crushing, bed-joint sliding, and rocking, (see Figure 4.1.2) are considered. The damage type of each individual wall is determined by factors such as wall aspect ratio, gravity loads, and the strength of the wall. The damage types mentioned above adequately describe the behavior of a wall that is solid.

In reality, however, the walls of most masonry buildings are often perforated. The mechanics and behavior of a perforated wall are more difficult to describe analytically. For this reason, a rational but simplified lumped-parameter model is often used that can reasonably and efficiently describe the non-linear in-plane response of URM walls. The simplification of an in-plane URM wall response carries the assumption that the critical case (e.g. bed-joint sliding or other damage type) will dominate the non-linear behavior of the wall. The critical case is determined by examining the sum of lateral strengths for each damage type of each single component (solid wall). The component that has a minimum lateral strength is then chosen as the dominant type of wall damage.

4.1.3 Modeling of Building

The building that was chosen for this study is a typical mid-America un-reinforced masonry commercial/residential building of 1930 vintage (Figure 4.1.3). It is assumed that the building is located in Memphis, TN. The building has two-stories, with footprint dimensions 83 ft (NS) by 26.9 ft (EW). Its total height is 39 ft. The thickness of all masonry walls is assumed to be 12 in. The elastic modulus and the Poisson's ratio for the walls are 515 ksi and 0.25, respectively. The mass of the building was calculated by summing the weight of the floor, the roof slabs, the walls and 20 % of the live load. The mass was lumped at the center of each diaphragm, and at the intersection of the central axes of walls and diaphragms. The diaphragms of the residential building and its walls are assumed to be rigidly connected. The finite element model of the building is shown in Figure 4.1.4. Table 4.1.1 below shows a typical setup for calculation of the lateral strength of the building's south wall (second floor, as shown in Figure 4.1.3). The

rocking mode is the dominant type of damage since it occurs at the lowest lateral force. Based on the lateral strength value and the corresponding lateral stiffness, which is determined by the 2-D finite

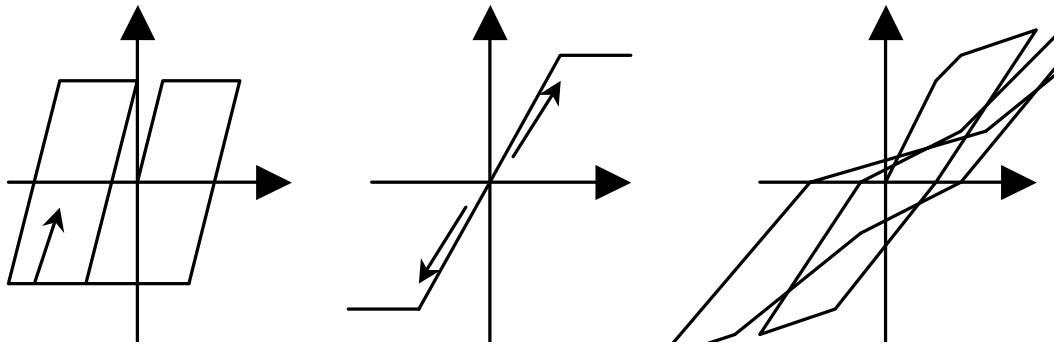

Figure 4.1.2. Hysteretic Behavior of Each Damage Mode.

Figure 4.1.3. South Wall – Second Floor of a Commercial/Residential Building

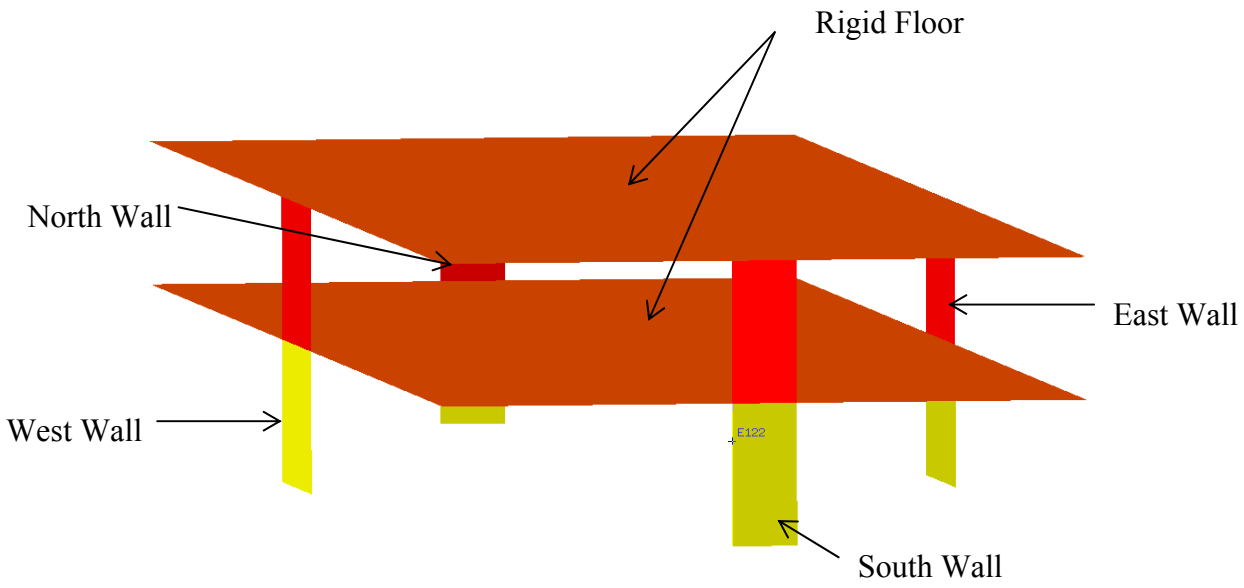

Figure 4.1.4. Finite element model for un-reinforced masonry commercial/residential building, all walls are modeled by the ABAQUS user-defined-element.

Table 4.1.1 Lateral Strength Calculation of South Wall of residential building

South Wall_2nd	(Unit: Kips)			
Pier No.	Bed-joint sliding	Rocking	Diagonal tension	Toe compressive
1	34.29	13.46	25.77	14.62
2	38.34	30.79	58.93	33.45
Total	72.63	44.26	84.71	48.07

element analysis (SAP2000), the finite element model of URM wall based on ABAQUS is developed following the model generated by White and Kim (2001). The validity of this model has been verified by comparison of structural response using this model with the recorded response of a fire station during the Loma-Prieta earthquake.

4.1.4 Structural Response Analysis

Structural response time histories were calculated for each of the ten uniform-hazard ground motions. Figure 4.1.5 shows an example of the time history of the response and the force-displacement (bed-joint sliding mode) relationship of the south wall of the residential building under a 2% in 50 years ground motion. Figure 4.1.6 shows the responses (rocking mode) of the north wall of the building under the same ground

motion. The different energy dissipation characteristics of the two failure modes are obvious. The response analyses were carried out for each of the uniform hazard ground motions for both 10% and 2 % in 50 years hazards. The drift ratio (in %) statistics of these two walls are shown in Table 4.1.2. The median response represents the demand on the structures corresponding to a given probability of exceedance. The east and west walls have much smaller response and are not shown here. The south wall has an opening in the first floor for the gate of the building. It has a much smaller stiffness and the response is large and mostly elastic. The force demand at the wall/diaphragm interface is very high, especially for the 2% in 50 years ground motion. For example, the force demand at the top of the north wall of the building is 87,000 lb under the 2% in 50 years ground motions. It indicates that the connection components at the interface would not be strong enough to withstand such large force. The implication is that when the connection fails the collapse of the structure is quite likely to occur.

4.1.5 Uncertainty Treatment

In vulnerability analysis of structures, i.e., the fragility curve (FC) and limit state (LS) probability calculation, both the randomness (aleatory) and uncertainty (epistemic) of the ground motion intensity demand, displacement demand, and structural capacity need to be considered, as shown in Section 2. The procedure is demonstrated in the following.

The displacement demand on the structures is described in terms of the drift response statistics under the uniform hazard ground motions (Section 2.1.4). In a UHGM motion-based approach, these uncertainties are incorporated in the limit state probability analysis by a correction factor applied to the median response (Wen and Foutch 1997) as shown in Section 2.3.4.2. The correction factor is given by Eq. 2.3.11. The total uncertainty is given by Eq. 2.3.10, in which both aleatory and epistemic uncertainties of the demand and capacity are considered. The sensitivity factor as shown in Eq. 2.3.12 depends on the seismic hazard parameters at the site. Different values of the coefficient of variation of the structural capacity were assumed to examine the sensitivity of the limit state probability to the capacity uncertainty. To determine the capacity against collapse, the Incremental Dynamic Analysis (IDA) was performed to determine the drift ratio capacity against incipient collapse and its uncertainty. The fragility analysis of the conditional probability of limit state given the excitation intensity of spectral acceleration was then performed in which a power law relationship between the displacement demand and the excitation intensity was determined from regression analysis of the building responses under the UHGM.

4.1.6 Displacement limit state probability using UHGM

The displacement limit states in terms of drift ratio of the walls of the building are considered. The median responses at the two hazard levels (10% and 2% in 50 years), such as those shown in Table 4.1.2, are multiplied by the correction factor in which the uncertainty due to record-to-record variation of the response and the structural capacity uncertainty against a given limit state (assumed to have a coefficient of variation of 50%)

are considered. The probabilistic displacement performance curves are obtained for each structural element of the building. Figure 4.1.7 shows the performance curve of first-floor north wall of the building. The sample responses (□) to the uniform hazard motions and the median point (O) are shown. The performance curves with and without consideration of the system capacity uncertainty are shown by solid and dashed lines. It is seen that in spite of the large uncertainty assumed for the capacity

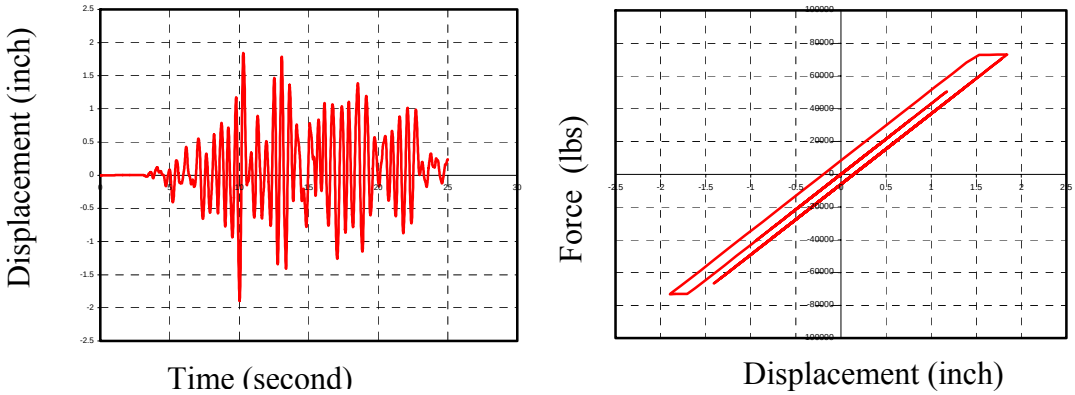

Figure 4.1.5. Time history and force-displacement relationship of Bed-Joint Sliding mode of first floor south wall under a 2% in 50 years ground motion.

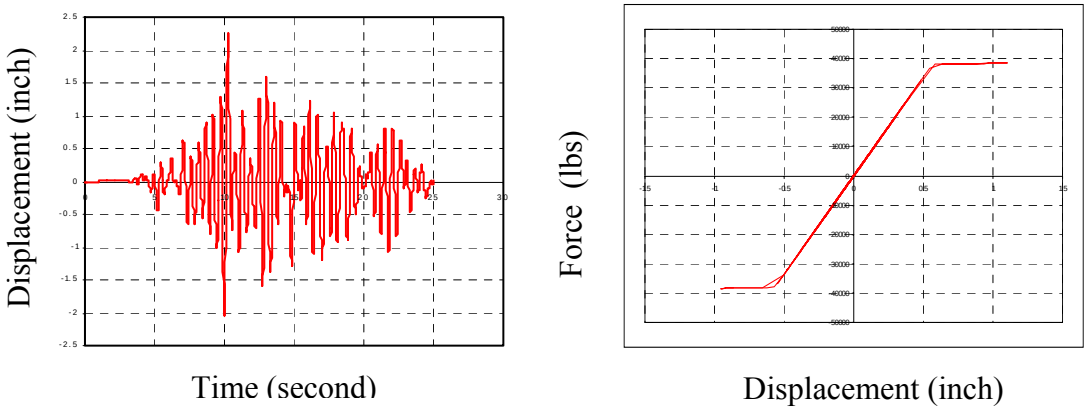

Figure 4.1.6. Time history and force-displacement relationship of rocking mode of first floor north wall under a 2% in 50 years ground motion.

Table 4.1.2. Medians and coefficient of variation (COV) of spectral acceleration S_a and wall drift ratio (%) of the URM Building, Memphis.

		10/50		2/50	
		Median	COV	Median	COV
South Wall – First Floor	Drift Ratio	0.09	0.21	0.61	0.15
	S_a	0.11g	0.15	0.78g	0.1
North Wall – First Floor	Drift Ratio	0.1	0.2	0.62	0.17
	S_a	0.11g	0.15	0.78g	0.1

the results are not too sensitive to it due to the dominance of the uncertainty in the seismic hazard in Mid-America as mentioned in Section 2.3.4.2. The performance curve of the first floor south wall of the building is shown in Figure 4.1.8. The limit state probability in terms of maximum story drift ratio can be therefore determined from the performance curve. For example, according to FEMA 273, the drift ratio limits for un-reinforced masonry construction for Immediate Occupancy (IO), Life Safety (LS), and Collapse Prevention (CP) are 0.3%, 0.6 %, and 1%, respectively.

4.1.7 Capacity against Collapse by Incremental Dynamic Analysis (IDA)

Collapse prevention is one of the most important objectives in vulnerability analysis and seismic design. The limit state of incipient collapse can be described by an Incremental Dynamic Analysis (IDA) as shown in Section 2.2.6.2. Following Vamvatsikos and Cornell (2001), a single-record IDA is a series of dynamic nonlinear analysis of the building under excitations of a single ground motion scaled to various intensities according to the spectral acceleration. The result of an IDA is highly dependent on the record chosen; therefore, to capture the full characteristic of uncertainty, IDA of the building under multiple ground motions is necessary. The IDA is therefore performed under the UHGM to evaluate the system capacity and uncertainty for the vulnerability analysis. Figure 4.1.9 show ten IDA curves of the masonry

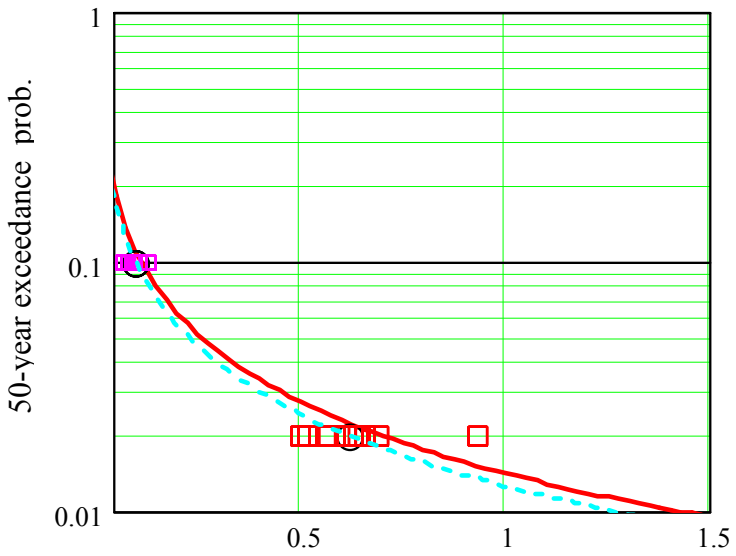

Figure 4.1.7. Probabilistic displacement performance curve of first-floor north wall, of the building (response □, median ○, solid line includes capacity

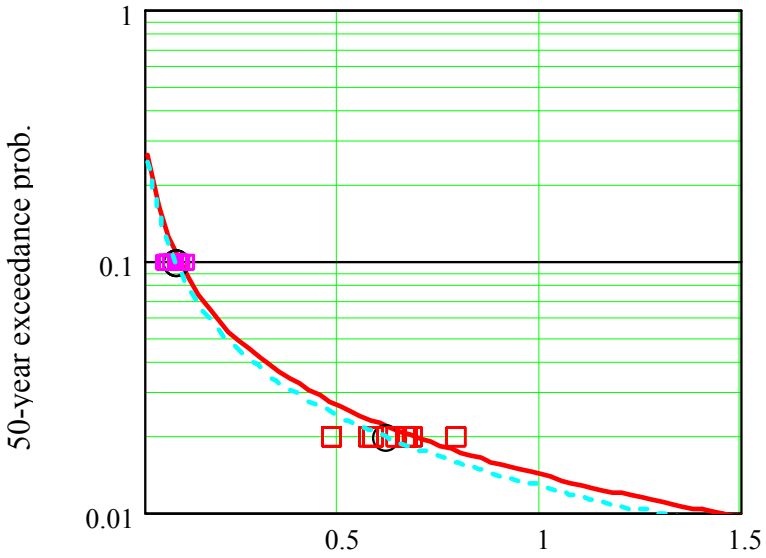

Figure 4.1.8. Probabilistic displacement performance curve of first-floor south wall of the building (response □, median ○, solid line includes capacity

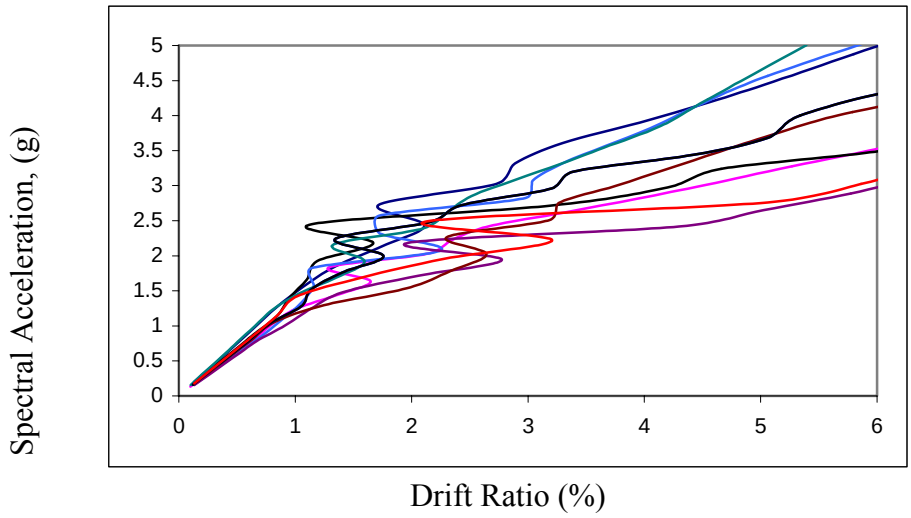

Figure 4.1.9. IDA curves of the building (maximum drift ratio for all walls) under 2/50 ground motions.

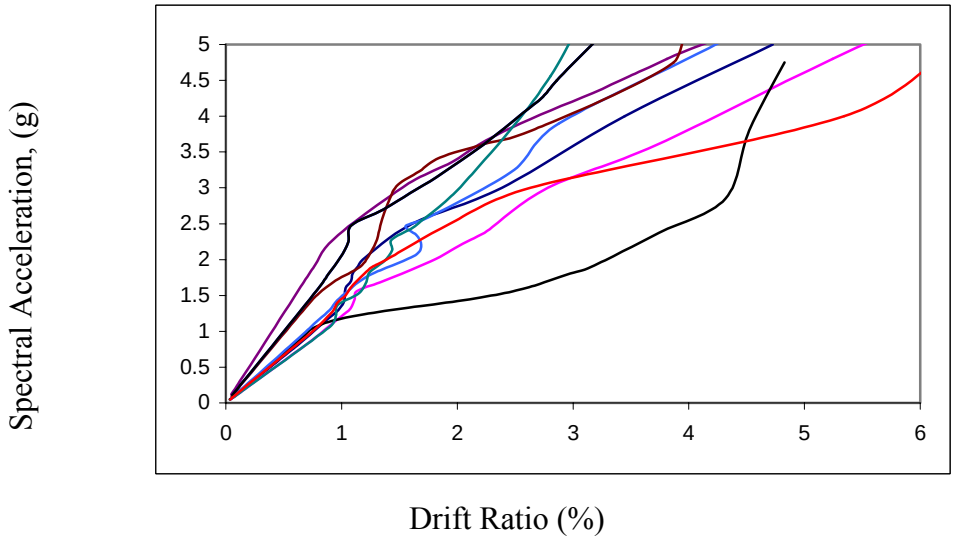

Figure 4.1.10. IDA curves of the building under 10/ 50 ground motions

building under the 2/50 ground motions in Memphis. Figure 4.1.10 show the IDA curves under the 10/50 years ground motions. When the slope of the IDA curve becomes flat, it indicates a large increase in structure displacement at a small intensity (spectral acceleration) increment, i.e. instability or incipient collapse. The drift ratio threshold for the slope to drop to 20% of the elastic stage has been suggested by Vamvatsikos and Cornell for incipient collapse of steel moment frames. This value is used for the IDA

curve under 2% in 50 years (2/50) motions. A threshold corresponding to a 50% drop is also used under both 2/50 and 10/50 motions. The resulting incipient collapse drift ratio thresholds generally show large scatter. Figures 4.1.11 and 4.1.12 show the drift capacity data points and fits by a lognormal distribution. A straight line would indicate a perfect fit. The fits are good in view of the small number of data. The lognormal distribution with parameters $(\lambda_{ICC}, \beta_{ICC})$ is used here in the ensuing reliability analysis where ICC denote incipient collapse capacity. The standard deviations of the capacity of two cases are 0.33 and 0.29, respectively. The cumulative lognormal functions of the collapse drift capacity for the two cases are shown in Fig 4.1.13. These are also the fragility curves against incipient collapse. The FEMA 1% deterministic collapse criterion is also shown as step function in these two figures for comparison.

4.1.8 Fragility Curve Using Excitation Intensity

As shown in Section 1.1, the fragility curve (FC) is the conditional probability of a prescribe limit state given the displacement or seismic excitation intensity demand. The limit state capacity controls the central location of the FC and the uncertainty in the capacity controls the shape (or dispersion) of the FC. The previous section shows the calculation of FC given the displacement demand. The FC for given intensity demand is also commonly used and is demonstrated as follows.

When the limit state is described in terms of drift ratio, one needs the relationship between the drift ratio and spectral acceleration to construct the FC. A convenient relationship is the power law as given in Section 2.1.3.

$$D = aS_a^{\,b} \tag{4.1.1}$$

in which, D is drift ratio, S_a is spectral acceleration, a and b are constants determined from regression analysis of D on S_a. The regression analysis is carried out using the response to the UHGM. Fig. 4.1.14 and Table 4.1.3 show the results of the analysis. The regression line predicts the mean value of D given S_a. The scatter around the predicted value (or uncertainty of the prediction) due to record-to-record variation is assumed to have a uniform coefficient of variation (does not depend S_a). The distribution of the scatter of drift for a given spectral acceleration is again assumed to be lognormal. The two clusters show the data points under 10/50 and 2/50 ground motions. It is seen that the relation is almost linear and the scatter are not very large in either case. In addition to the above uncertainty due to earthquake record-to record variation, the there are also inherent uncertainty in the system capacity such as those due to material strength variability and workmanship. With the lognormal model one can calculate the conditional probability (or fragility curve) of a given limit state in terms of drift ratio threshold being exceeded given the spectral acceleration as follows.

$$P(D \geq d_0 \,|\, S_a) = 1 - \Phi\left(\frac{\ln d_0 - \lambda_{D|S_a}}{\beta_T}\right) \tag{4.1.2}$$

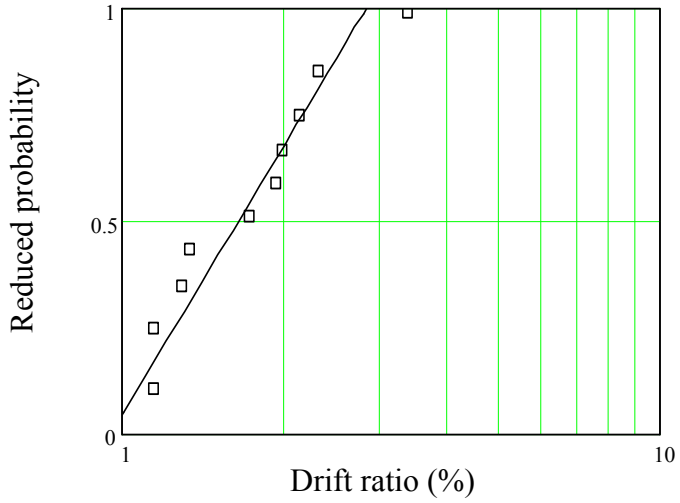

Figure 4.1.11. IDA incipient collapse capacity and lognormal fit, using 2/50 excitations only.

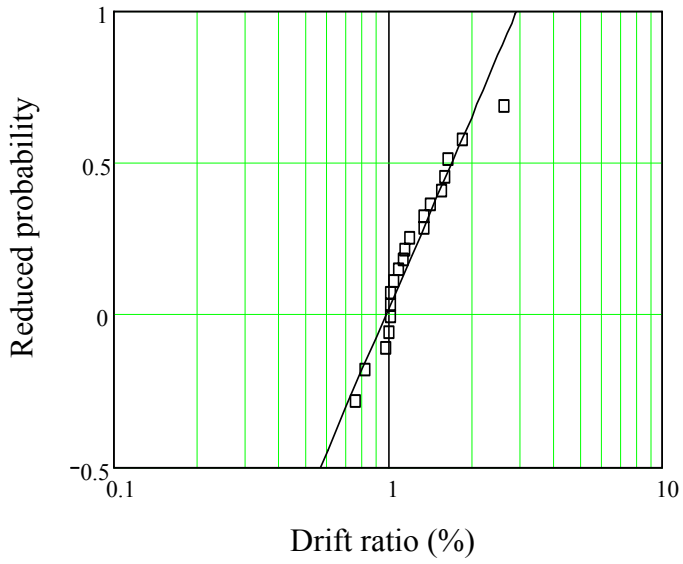

Figure 4.1.12. IDA incipient collapse capacity and lognormal fit, using 2/50 and 10/50 excitations.

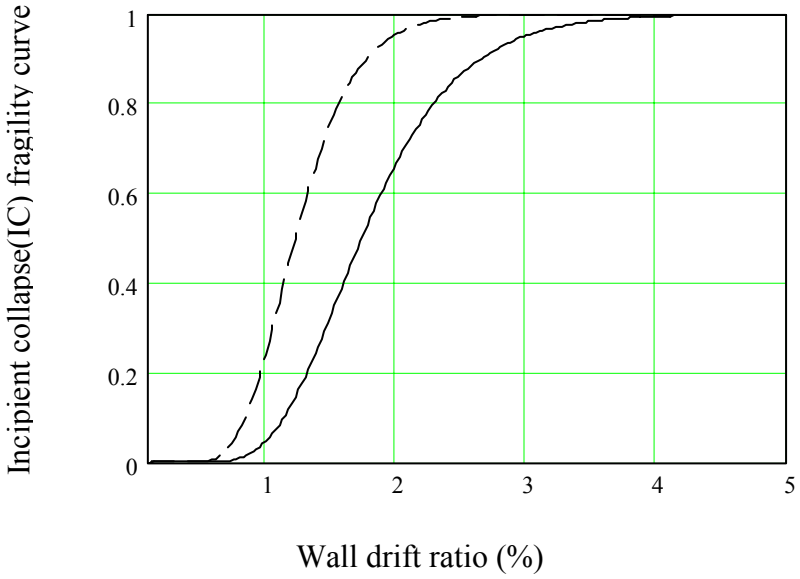

Figure 4.1.13. Building IDA incipient collapse fragility curve: dashed line, using both 10/50 and 2/50 excitation; solid line, using 2/50 excitations only. FEMA 1% deterministic capacity would be a step function at 1%.

in which $\lambda_{D|S_a}$ and β_T are lognormal distribution parameters calculated from the mean value from the regression equation and the overall uncertainty $\delta_T = (\delta_{D|S_a}{}^2 + \delta_C{}^2)^{0.5}$ where $\delta_{D|S_a}$ denotes uncertainty due to record-to-record variation as seen in the regression curves in Figures 4.1.14 and δ_C denotes inherent capacity uncertainty. The FC for incipient collapse according to the IDA procedure as a function of the drift can be converted to that in terms of the spectral acceleration as follows. For a given value of S_a, the drift demand as shown in the scatter of Figures 4.1.14 can be assumed to follow a lognormal distribution. Since the capacity against IC is also lognormal, the probability of IC given S_a, or the fragility curve for IC can be given by

$$P(IC|S_a) = 1- \Phi\left(\frac{\lambda_{ICC} - \lambda_{D|S_a}}{\sqrt{\beta^2_{D|S_a} + \beta^2_{ICC} + \beta^2_C}}\right) \qquad (4.1.3)$$

in which λ_{ICC} and β_{ICC} are the lognormal distribution parameters for structural capacity against incipient collapse (IC) evaluated from IDA analysis (see Fig. 4.1.12), β_C denotes the modeling uncertainty in the IC capacity evaluation by IDA method. The conditional probability (FC) of the three limit states, IO, LS, and CP according to FEMA 273 are calculated and shown in Fig. 4.1.15. The effect of δ_C is seen by comparing the top,

middle and bottom figure with δ_C = 20%, 30% and 40% respectively. FC for incipient collapse is also calculated and shown in the figure for comparison. Note that only uncertainty due to ground motion record-to-record variation is considered in the FC shown in this figure. Other uncertainties in structural capacity such as those in material properties, due to design errors and poor workmanship etc. have not been considered. They can be significantly larger and will cause a much larger dispersion in the FC.

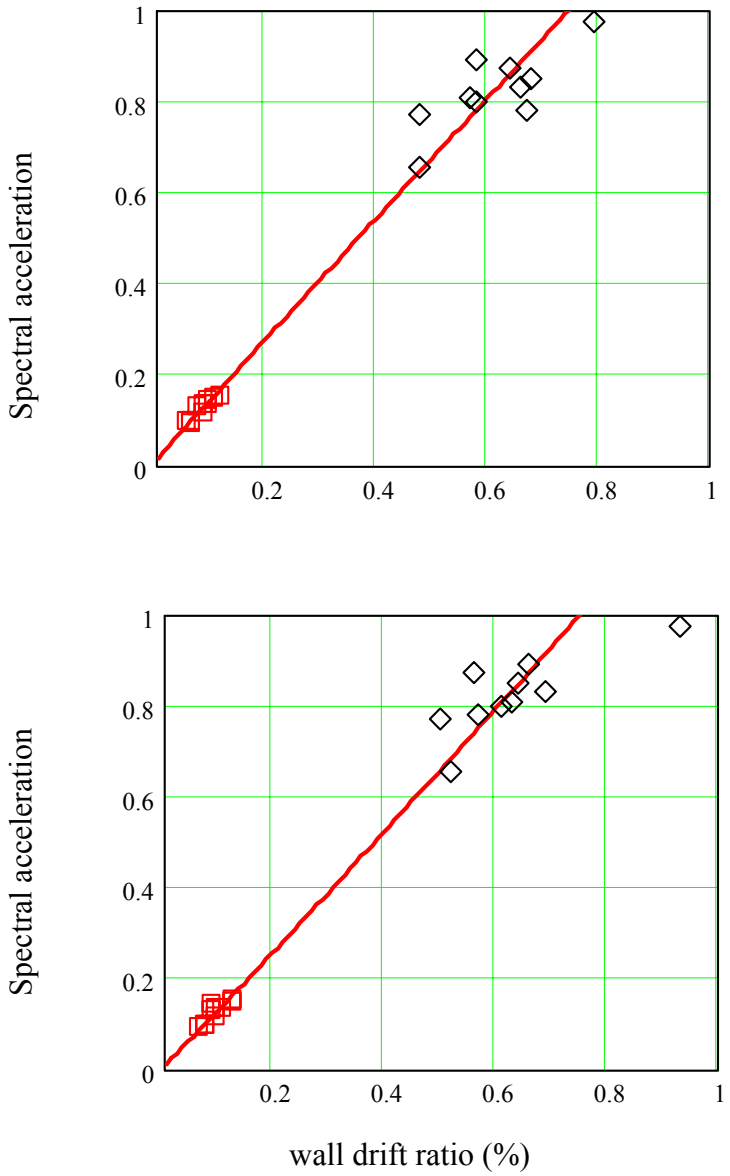

Figure 4.1.14. Regression analysis of wall drift ratio versus spectral acceleration: top, first-floor south wall; bottom, first-floor north wall.

Table 4.1.3. Regression coefficients

Wall Location	a	b	Coefficient of variation
South Wall (First Floor)	0.747	1.02	0.107
North Wall (First Floor)	0.752	0.97	0.123

4.1.9 Limit State Probability

Following Section 1.2, the 50-year probabilities are calculated for the above four limit states by integration of the FC with respect to the density function of the spectral acceleration as follows

$$P(LS) = \int P(LS|S_a) f_{S_a}(a) da \qquad (4.1.4)$$

in which f_{Sa} is the probability density function (assumed to be lognormal in this study) of the 50-year maximum spectral acceleration function based on the UHGM for Memphis.

To examine the sensitivity of the result to capacity uncertainty assumptions used in conjunction with the FEMA 273 limit states, different coefficients of variations of the capacity are assumed. The annual probabilities of limit states according to FEMA 273 classification of IO, LS, and CP are shown in Tables 4.1.4 and 4.1.5. A standard deviation of 0.3% drift ratio was assumed in Table 4.1.4 for the FEMA limit state thresholds. The uncertainties were increased by a factor of two in Table 4.1.5. A lognormal distribution was assumed again for the capacity uncertainties. For comparison, the Incipient Collapse (IC) limit state probability according to IDA analysis is also shown and no additional uncertainty is considered ($\beta_C = 0$). It is seen that the results are not too sensitive to the capacity uncertainty assumption due to the dominance of the uncertainty in seismic excitation in Memphis. Comparison of Table 4.1.5 with the 50-year probability of Fig. 4.1.7 at drift ratios of 0.1 for IO, 0.3 for LS and 1.0 for CP shows that the two different approaches give results that are very close.

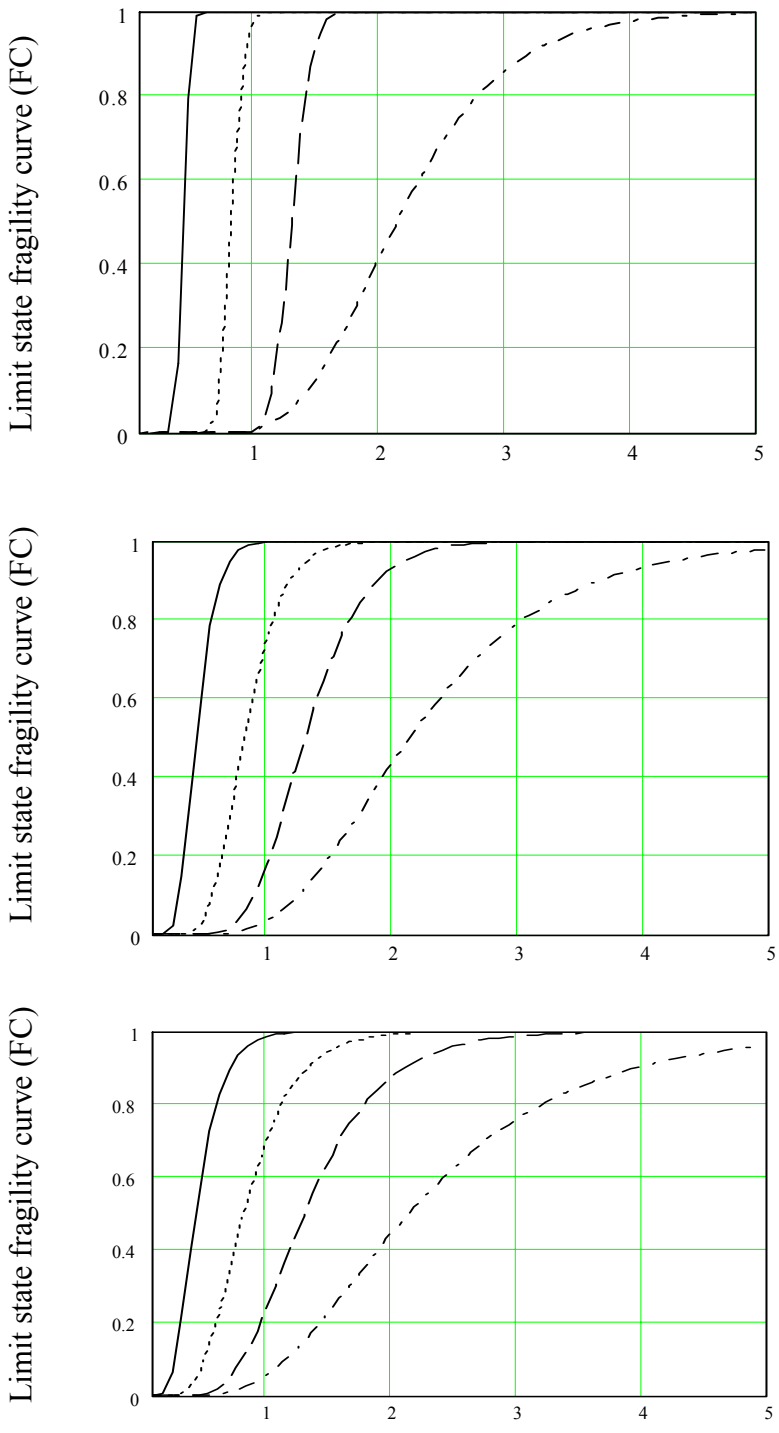

Figure 4.1.15. Fragility curve of the building for different limit states: solid line, IO (Immediate Occupancy); dashed line, LS (Life Safety); broken line, CP(Collapse Prevention) according to FEMA 273, and broken-dashed line, IC (Incipient Collapse) according to IDA; system capacity uncertainty δ_C assumed to be 0.2, 0.3 and 0.4 in top, middle and bottom figure.

Table 4.1.4. 50-year limit state probability

Limit State	Immediate Occupancy (IO)	Life Safety (LS)	Collapse Prevention (CP)	Incipient Collapse (IC)
Reference	FEMA 273	FEMA 273	FEMA273	IDA analysis
Capacity (Median Drift Ratio, %)	0.3	0.6	1	1.74
Standard Deviation of Capacity	0.3	0.3	0.3	0.33
Limit State Probability	$3.75X10^{-2}$	$2.11X10^{-2}$	$1.35X10^{-2}$	$8.36X10^{-3}$

Table 4.1.5. 50-year limit state probability

Limit State	Immediate Occupancy (IO)	Life Safety (LS)	Collapse Prevention (CP)	Incipient Collapse (IC)
Reference	FEMA 273	FEMA 273	FEMA273	IDA analysis
Capacity (Median Drift Ratio, %)	0.3	0.6	1	1.74
Standard Deviation of Capacity	0.6	0.6	0.6	0.33
Limit State Probability	$4.06X10^{-2}$	$2.30X10^{-2}$	$1.49X10^{-2}$	$8.36X10^{-3}$

4.2 Reinforced Concrete Frame Structures

4.2.1 Research Objectives

The objective of this work was to quantify the vulnerability of older reinforced concrete (RC) frame structures located in the Mid-America region, specifically near Memphis, TN, due to potential earthquakes. The seismic vulnerability of such construction is described by means of fragility curves, which relate the probability of exceeding a particular limit state given an imposed seismic demand. In this work, seismic demand is defined as the spectral acceleration of a particular earthquake event at the fundamental period of the structure under consideration. Story limit state capacities are identified using FEMA guidelines (immediate occupancy, life safety and collapse prevention) and using quantitative nonlinear analysis methods (first yield, plastic mechanism initiation, and incipient collapse). In addition, this research attempts to quantify the improved vulnerability of retrofitted RC structures using column strengthening.

4.2.2 Introduction

Historical Review of Model Building Code Requirements

The earliest model building code provisions for seismic design are in the 1927 Uniform Building Code (Olshansky, 1993). However, earthquake resistant design provisions were not fully considered nor implemented until after the 1971 San Fernando earthquake (Nordenson, 1993). Since that time, seismic provisions have been included, modified, and implemented continuously in our current building codes. For example, the 1988 version of the Standard Building Code provided seismic design provisions (Olshansky, 1993). However, state, county, or local entities rarely adopted these provisions. This resulted in building designs where the lateral load demand forces were small in comparison to the gravity load demands (Nordenson, 1993).

Review of ACI 318 Building Code Requirements

In the United States as well as throughout the work, the American Concrete Institute (ACI) 318 building code provisions and commentary are predominantly followed for the design of reinforced concrete buildings. The historical development of the ACI 318 with respect to seismic design provisions was presented in Dooley and Bracci (2001). A partial summary of that work is provided below.

Seismic provisions were first established in an appendix of ACI-318 following the San Fernando earthquake event in 1971. For special ductile frames, the sum of the column moment strengths was required to be greater than the beam moment strengths at any beam-column joint intersection (ACI 318-71, 1971) to promote desirable beam hinging. In addition, there were transverse reinforcement requirements in beam and column sections near the joint regions, beyond the standard non-seismic detailing, to enhance the ductility of the frame members. In the ACI 318-83 (1983) provisions, the design flexural strengths (ϕM_n) of the columns were required to exceed the design flexural strengths of the beams at the beam-column joint *centers* by at least 20%. The intent of the additional column strength requirement was to reduce the likelihood of yielding in the columns of frame structures. However, the beam strengths in monolithic construction could be

interpreted as the nominal flexural strength of the rectangular beam sections, neglecting contributions from the slab and slab reinforcement, which can significantly impact beam strength. More elaborate transverse reinforcement was also required, especially near beam-column joint regions, since columns might still develop significant yielding during earthquakes. ACI committee 352 (1991) on joints made recommendations for the seismic design of frame structures that the sum of the nominal flexural strengths (M_n) of the columns above and below the joint exceed the sum of the nominal flexural strengths of the beams framing in to the joint in a particular horizontal direction by at least 40%. In this report, it was clearly emphasized that no strength reduction factors were to be utilized and that the beam strength was to be determined with contributions from the slab in compression for positive moment and slab reinforcement for negative moment within the effective flange width as defined in ACI 318.

ACI 318-99 (2003) currently requires that the nominal flexural strength of columns exceed the nominal flexural strength of beams at beam-column joint faces by at least 20%. In this provision, the beam nominal flexural strength should consider the contributions of the slab in compression for positive moment (T-beam) and slab reinforcement for negative moment within the effective flange width defined in ACI 318. In other countries, such as New Zealand and Mexico, higher minimum nominal column-to-beam strength ratios at joint regions (between 1.5 and 2.0) are required. And even though the columns are much stronger than the beams at the frame joints, significant transverse detailing in potential hinge regions, including the columns and beam-column joints, is still required.

Older Reinforced Concrete Frame Structures

Low-rise RC frame buildings located in regions historically considered of low to moderate seismic risk were typically designed without consideration of lateral loading, since wind load seldom governed for low-rise construction. Therefore, such structures have been categorized as gravity load designed, or GLD, structures (Bracci et al., 1995a). In general, GLD RC frame structures have no special reinforcing details in the beam, column, and joint regions (El-Attar, 1997, Pessiki, 1990, Aycardi, 1994, and Bracci, 1995a). Another characteristic that distinguishes these structures from others designed in areas of higher seismic risk is the existence of strong beams and weak columns, which can lead to soft story failure mechanisms that are composed primarily of column hinging. The lack of sufficient column strength leads to column hinging at relatively low lateral loads, causing the formation of a story mechanism once all columns located on one story have hinged. Once the mechanism develops, the building's resistance is provided solely by the post-yield strength of the hinging column ends and inherent section ductility. Combining the lack of sufficient column strength with the lack of sufficient detailing in column sections for ductility, brittle soft story failure mechanisms may be prominent during strong earthquakes.

4.2.3 Prototype Building Design

The first task in the research was to design a three-story RC frame structure located in an area historically considered to be of low-to-moderate seismicity. As previously

discussed, buildings located in such areas were designed for gravity loads only. Therefore, the controlling design equation was U = 1.4D + 1.7L (ACI 318, 1999), where U is the total factored demand; D is the effect of dead load, including self weight, 20 psf for superimposed dead weight, and 500 lb/ft of cladding around the building perimeter; and L is the effect of live load, which was taken 50 psf for a typical office building loading.

The overall geometry of the building and member sections are shown in Fig. 4.2.1. The building system is a two-way slab, space frame building for resisting gravity and lateral loading. Column spacing (26 ft.) was determined and maximized based on using an 8" thick RC two-way slab designed according to the direct design method specified in ACI 318-99. Based on demand gravity loading, the minimum required slab reinforcement, #4 at 12" cc, governed the design for both the column and middle strip regions. Beams were designed as T-beam sections, with effective slab flange widths of 78" and 42" for the interior and exterior beams, respectively. The final beam sections at the beam-column joint face based on factored gravity loading were 16" wide and 24" deep from the top of slab to the bottom of the beam with 4#7 and 2#7 for top and bottom bars, respectively. Columns were 16" by 16" with 4#8 bars (1.2% reinforcement). Based on an average level of axial loading among columns and consideration of the slab and slab reinforcement within the effective flange width for the beams, the approximate column-to-beam strength ratio for the prototype building at an interior joint was 0.60, which is well below the current ACI 318 seismic requirements of 1.2. For a typical story, the ratio of total column strength to beam strength was about 0.8. From an eigenvalue analysis of the building numerical model, the fundamental period of the building was 0.87 seconds taking into account cracked sections per ACI 318.

4.2.4 Fragility Curve Development

The fragility curves for the RC frame building were developed according to the following equation:

$$P\left(LS / S_a\right) = 1 - \phi\left(\frac{\lambda_c - \lambda_{D/S_a}}{\sqrt{\beta_{D/S_a}^2 + \beta_c^2 + \beta_m^2}}\right) \tag{4.2.1}$$

where: $P(LS/S_a)$ = Probability of exceeding a limit state given the spectral acceleration at the fundamental period of the building; ϕ = standard normal distribution; λ_c = ln(median drift capacity for a particular limit state); $\lambda_{D/Sa}$ = ln(calculated median demand drift given the spectral acceleration from the best fit power law line); $\beta_{D/Sa}$ = demand uncertainty = sqrt(ln(1+s^2)), where s^2 = standard error = $\Sigma[(\ln(Yi)-\ln(Yp)]^2/(n-2)$; Yi, Yp are the observed and power law predicted median demand drifts, respectively, given the spectral acceleration, and n is the number of sample data demand points; β_c is the capacity uncertainty, which is taken as sqrt(ln(1+cov^2)) for the IDA and taken as 0.3 for FEMA and pushover limit states; and β_m is the modeling uncertainty, which is taken as 0.2, 0.3 and 0.4 for comparison.

Below the demand and capacity variables in Eq. 4.2.1 are defined and described below.

4.2.4.1 Inter-Story Drift Capacities (Limit States)

Based on observations during past earthquakes and previous research, the imposed inter-story drift on structures has been well correlated with the level of structural damage. As a result, this study will emphasize inter-story drift as the key parameter in the development of vulnerability functions. In this section, three different methods for developing inter-story drift capacities or limit states are presented in conjunction with different levels of uncertainty. The first set of limit state capacities was based on suggested story drift limitations using qualitative descriptions for Immediate Occupancy, Life Safety, and Collapse Prevention in FEMA-273 (1997). The second set of limit state capacities was determined quantitatively, specifically first yield and plastic mechanism initiation of the stories, from the results of nonlinear pushover analyses. Finally, incremental dynamic analyses were used to obtain the incipient collapse limit state.

FEMA-273 Limit States

Qualitative structural limit states described in FEMA-273 are: Immediate Occupancy (IO), where the structure would have minimal damage and occupants would have access to the structure following the earthquake event; Life Safety (LS), where the structure would have significant damage, but the life safety of the occupants would be preserved; and Collapse Prevention (CP), where the structure would be on the verge of structural collapse. For RC frame structures, these qualitative limit states can be represented by deterministic inter-story drift limits of 1%, 2%, and 4% of the story height for IO, LS, and CP, respectively. Although these suggested limits are approximate, they are considered fairly accurate for buildings properly designed for seismic loading. For GLD buildings, the limits for life safety and collapse prevention are probably not conservative due to insufficient column strength and insufficient section detailing for ductility as described previously. In this work, the uncertainty parameter (which is similar to the coefficient of variation) related to these limit state capacities, β_c, was taken as 0.3 for all fragility curve development and λ_c was taken as ln(1.0), ln(2.0), and ln(4.0) for IO, LS, and CP, respectively.

Quantitative Pushover Analyses

Pushover analyses are commonly used in seismic design and evaluation of structures as indicators of structural yielding and potential failure mechanisms. These types of analyses subject a nonlinear numerical model of a structure to prescribed forces or displacements until failure or some limit is reached. Results of pushover analyses demonstrate a building's resistance in terms of story shear force versus inter-story drift. In this work, force control loading analyses consisted of applying incremental inverted triangular and uniform loadings. In addition, displacement control analyses were used by prescribing incremental story displacements onto the structure. In order to identify critical story mechanisms, these analyses consisted of incrementally displacing an individual story and restricting the displacement of the story below. Individual story resistances are important because the lateral resistance of an entire structure is often dependent on the performance of a single story of the structure, especially for GLD

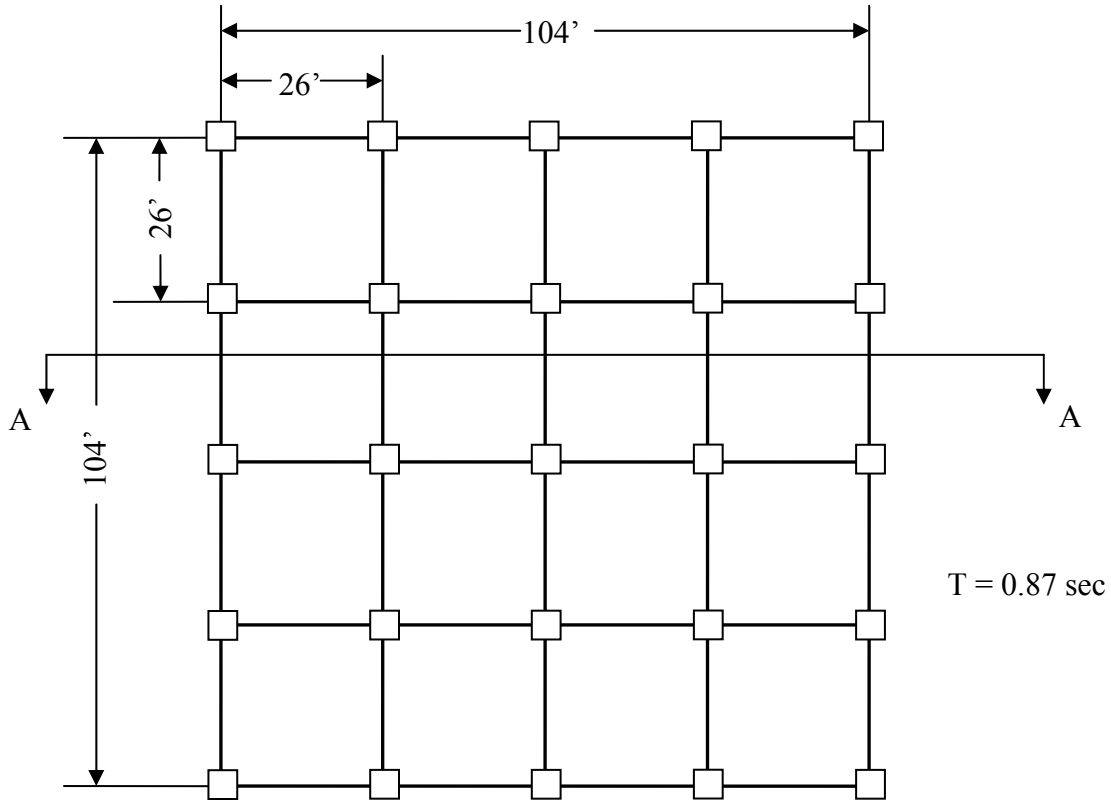

(a) Plan View

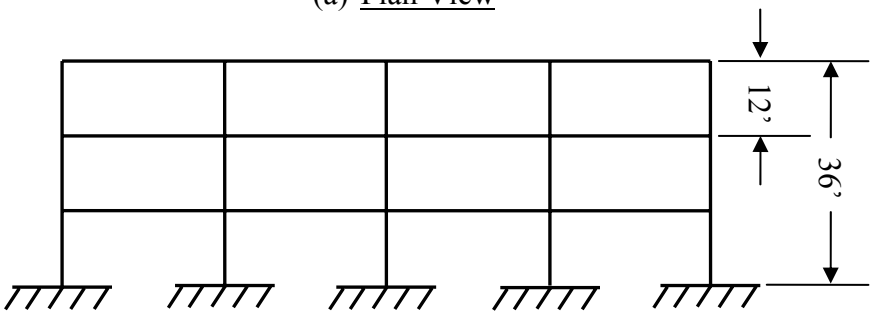

(b) Section A-A

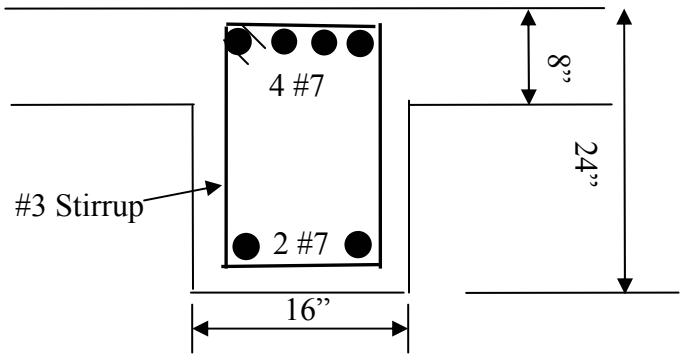

(c) Beam with Monolithic Slab Section

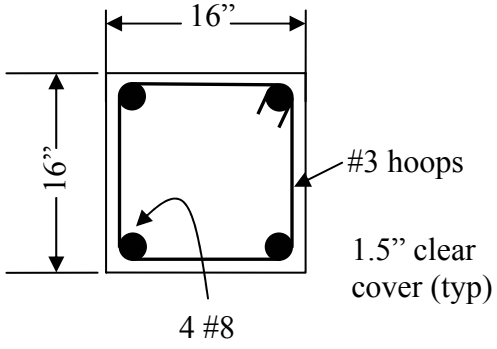

(d) Column Section

Figure 4.2.1 Prototype Structure

buildings. Finally, the upper-most story was displaced without restriction in lower stories to identify potential beam-sidesway mechanisms.

The results from the pushover analyses are presented in terms of story shear force vs. inter-story drift as shown in Fig. 4.2.2 and the sequence of member yielding as shown in Fig. 4.2.3. The first yield and plastic mechanism initiation drift limits (described previously) for the particular story of interest are shown in Fig. 4.2.2 and the final hinge section at which the mechanism develops is noted in parenthesis and corresponds with the sequence in Fig. 4.2.3. Similarly, the displacement control results are shown in Figs. 4.2.4 and 4.2.5. It should be emphasized that the results shown are based only on first order analyses and that P-delta loading is neglected. A significant observation from these results is that most yielding members were the columns, which was expected because of the small column-to-beam strength ratio, 0.6, in GLD structures. Second, the uniform force control analysis induced more critical first story limit states than the inverted triangular loading, and yielding was mainly restricted to the first story as shown in Fig. 4.2.3. The results from the displacement control loading further emphasize the potential for development of a story mechanism and more critical limit state values. The limit state capacities identified by nonlinear pushover methods are summarized in Table 4.2.1. Comparing the first yield and plastic mechanism limits from nonlinear pushover analyses with the immediate occupancy and life safety limit from FEMA, respectively, it can be concluded that the pushover limit states are significantly less than similar qualitative FEMA limits, for example comparing immediate occupancy with first yield and life safety with plastic mechanism initiation. However, the FEMA limits are intended for seismically designed structures.

Table 4.2.1 Pushover Drift Limits for First Yield and Plastic Mechanism Initiation

Pushover Loading	Story	FY Limit (% drift)	PMI Limit (% drift)
Force-Triangle	1	0.35	0.99
	2		1.22
	3		
Force-Uniform	1	0.34	0.70
	2		1.40
	3		
Displacement 1	1	0.32	0.52
	2		
	3		
Displacement 2-1	1		
	2	0.29	0.61
	3		
Displacement 3-2	1		
	2		
	3	0.26	0.74
Displacement 3	1	0.31	0.83
	2		0.51
	3		1.05

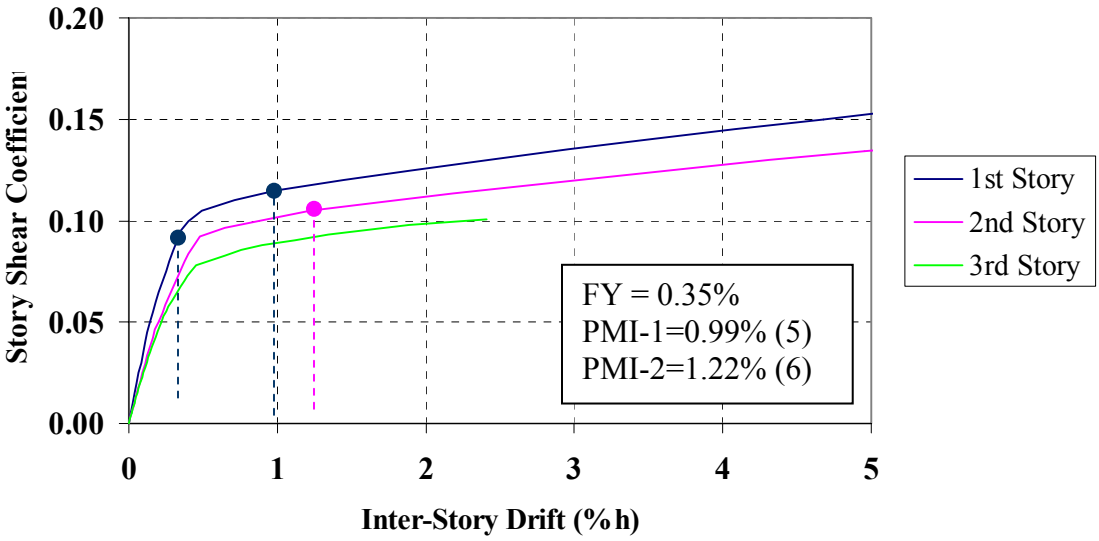

(a) Inverted Triangular Distribution

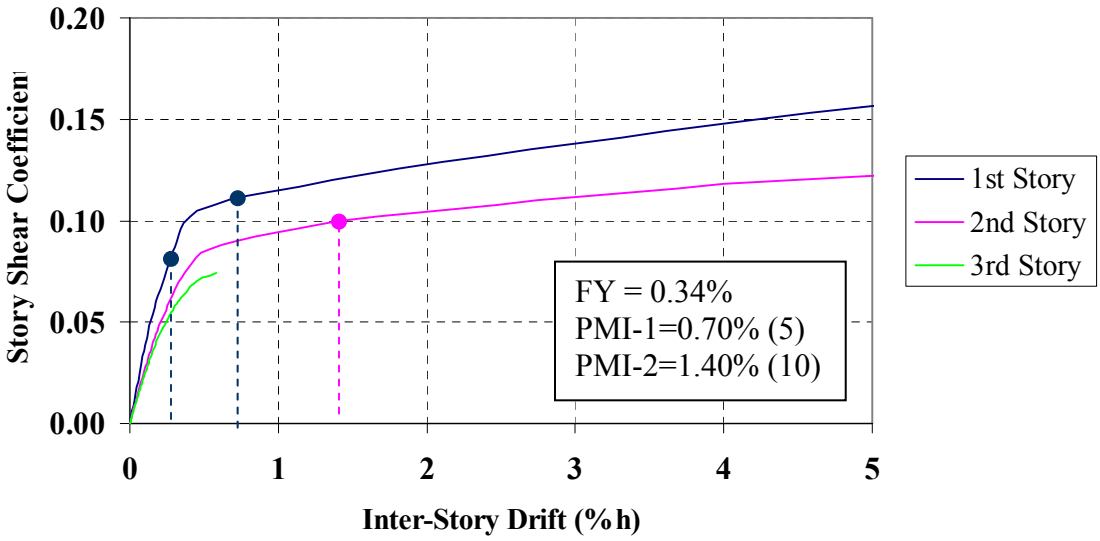

(b) Uniform Distribution

Figure 4.2.2 Pushover Analyses - Force Control Loading

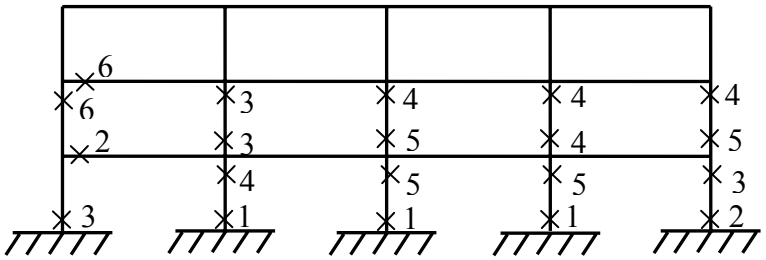

(a) Force Control - Inverted Triangular

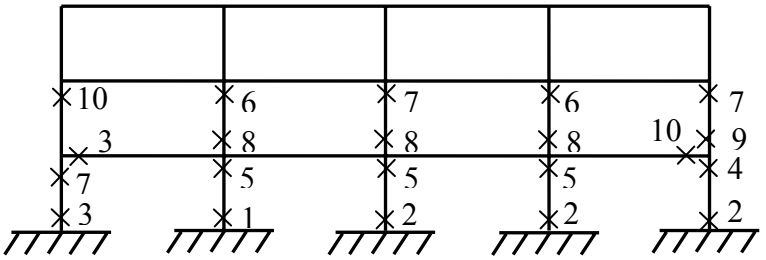

(b) Force Control - Uniform Distribution

Figure 4.2.3 Sequence of PMI – Force Control Loading

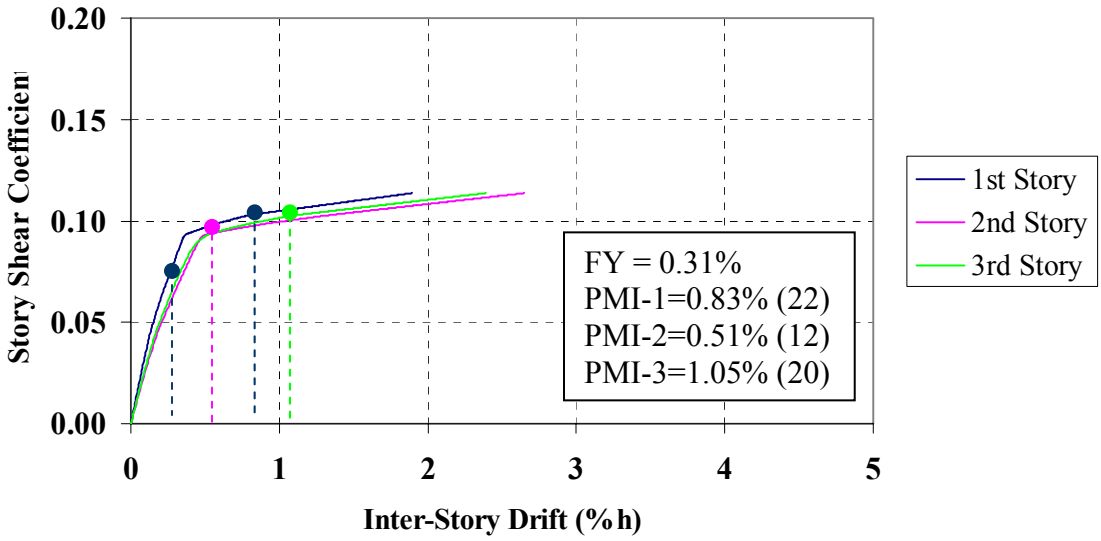

(a) 3rd Story – No restrictions

Figure 4.2.4 Pushover Analyses - Displacement Control Loading

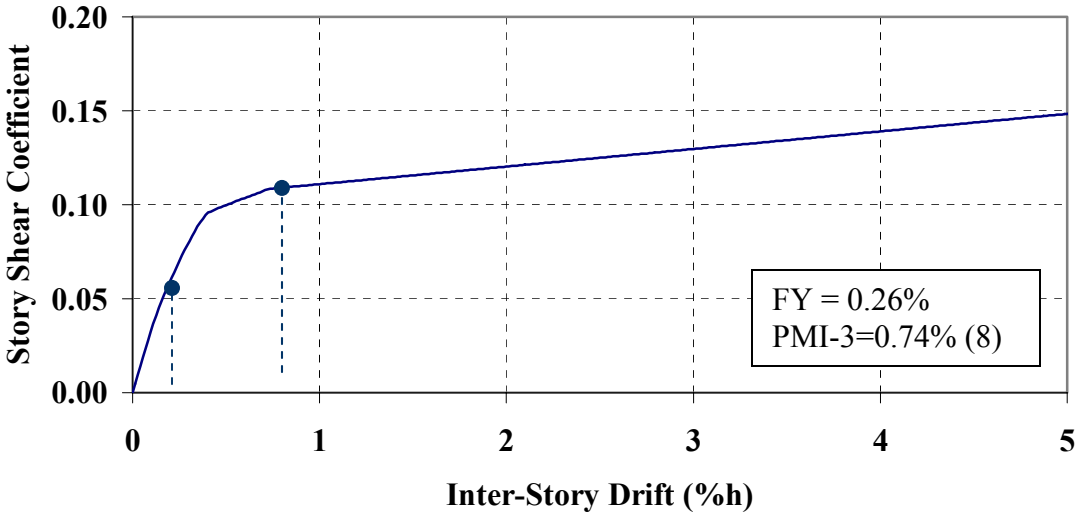

(b) 3rd Story – Restrict 2nd Story

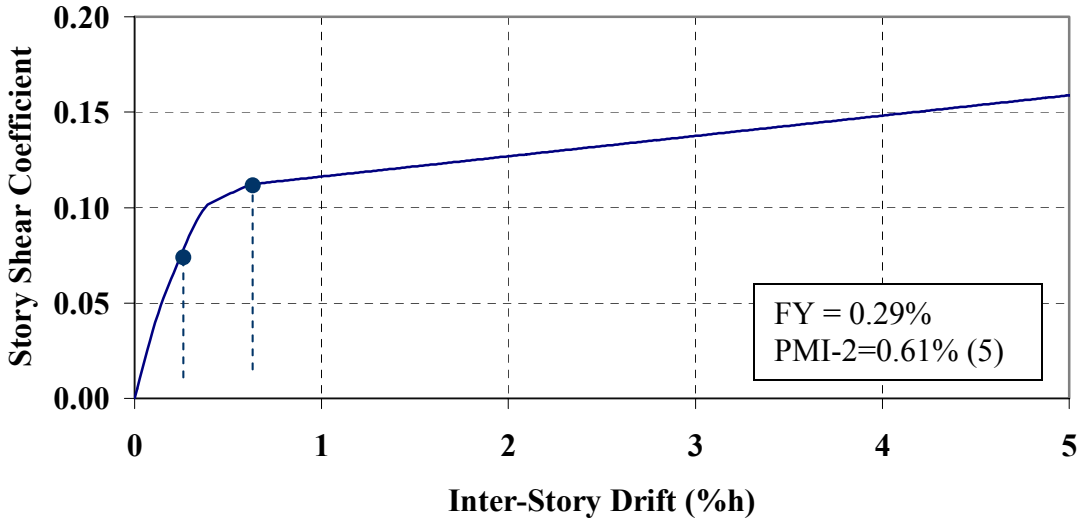

(c) 2nd Story – Restrict 1st Story

Figure 4.2.4 Continued

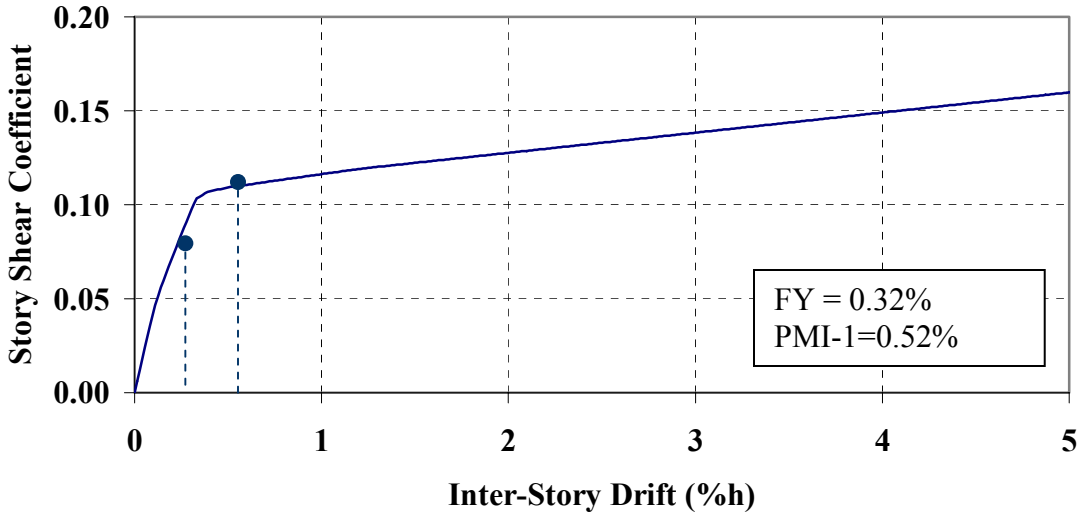

(d) 1st Story

Figure 4.2.4 Continued

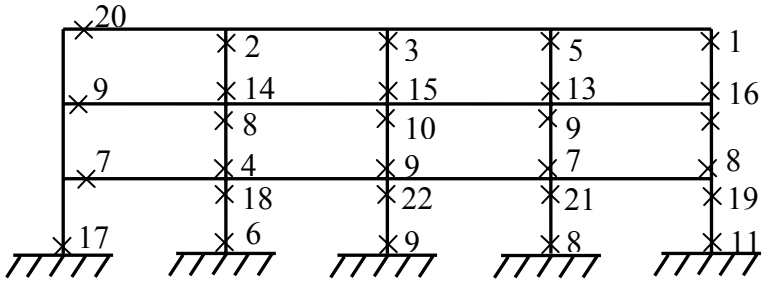

(a) 3rd Story – No Restrictions

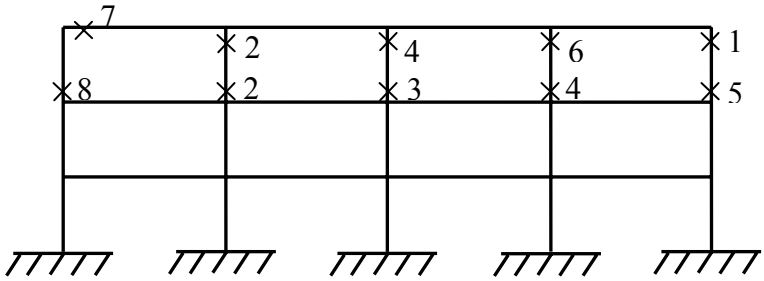

(b) 3rd Story – Restrict 2nd Story

Figure 4.2.5 Sequence of PMI – Displacement Control

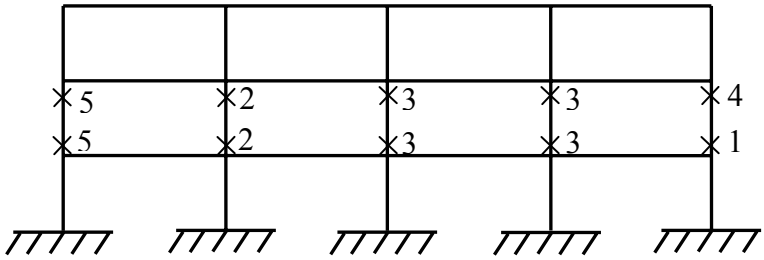

(c) 2nd Story – Restrict 1st Story

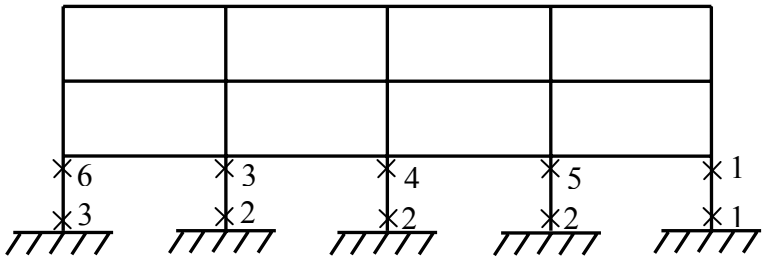

(d) 1st Story

Figure 4.2.5 Continued

For limit states determined from nonlinear pushover analyses, the uncertainty parameter related to these limit state capacities, β_C, was taken as 0.3 for all fragility curve development. Since the displacement control loading produced the most critical drift limits for first yield and plastic mechanism initiation, λ_C was taken as ln(0.32) and ln(0.52) for FY and PMI, respectively.

Incremental Dynamic Analyses

Incremental dynamic analysis (IDA) was next used to identify the Incipient Collapse limit state. IDA is basically an analytical procedure were the spectral acceleration of a ground motion at the fundamental period of the structure is incrementally increased and maximum inter-story drift demand is calculated by means of nonlinear time history dynamic analysis at each increment. In this work, Incipient Collapse was defined when the slope of the story drift vs. spectral acceleration decreases by 50% of the initial slope. Since 2 suites of 10 ground motions are utilized to represent the seismic demand (described later), IDA was conducted for the entire 20 records and a statistical estimate of incipient collapse was identified in terms of a story drift limit. Sample response curves from the IDA up to 5% inter-story drift demand are shown in Fig. 4.2.6a. The incipient collapse drift limit, as defined above, was identified for 14 of the 20 records, and is shown to fit a lognormal distribution in Fig. 4.2.6b. For the fragility curve parameters, the uncertainty parameter (which is similar to the coefficient of variation) related to these limit state capacities, β_C, was calculated by sqrt(ln(1+cov^2)) = 0.46, where cov is the coefficient of variation of the calculated IC limit state capacities. λ_C was taken as ln(median drift = 2.38%).

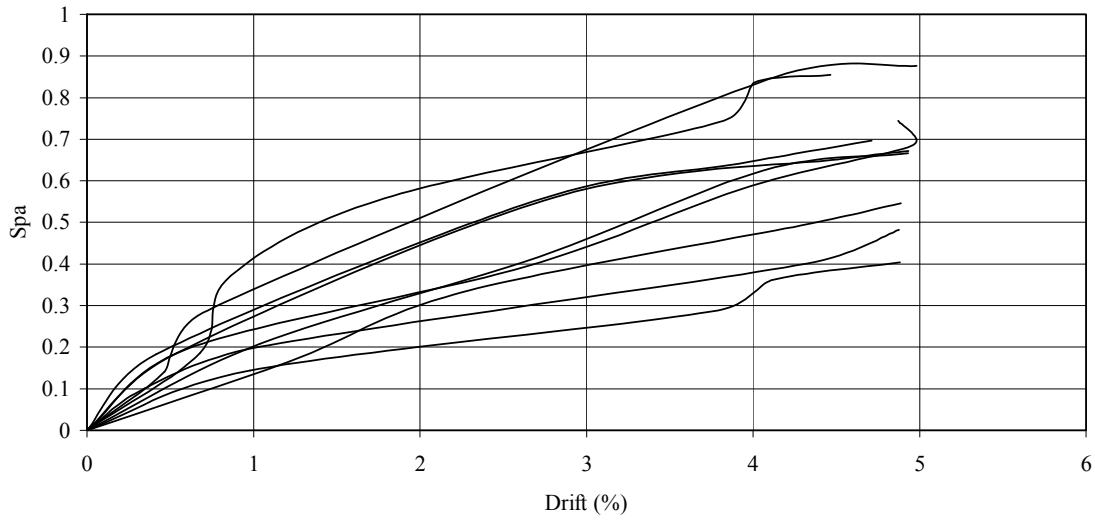

(a) Critical Response Curves

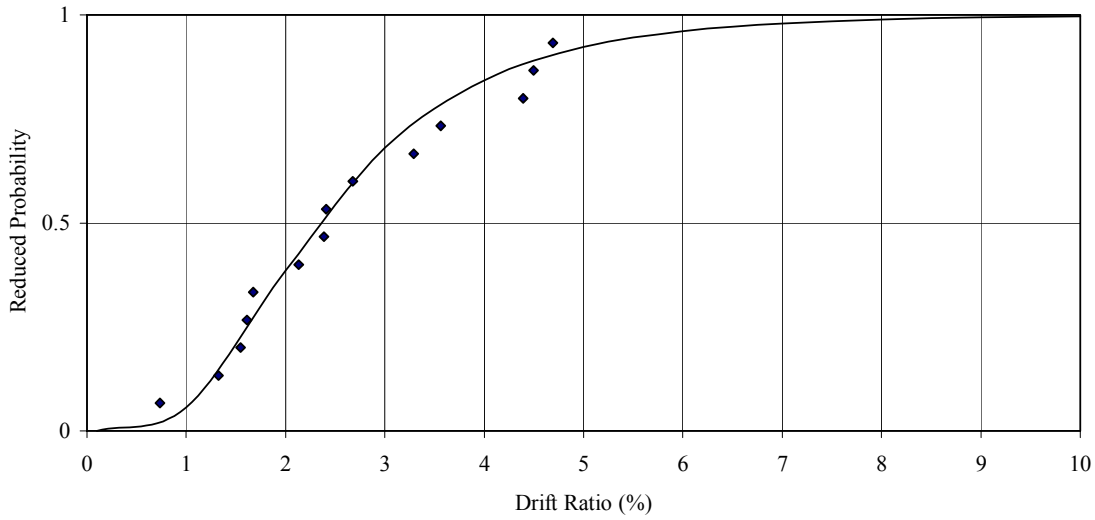

(b) Incipient Collapse Limits

Figure 4.2.6 Incremental Dynamic Analyses

Summary
Table 4.2.2 shows the β_C and λ_C capacity factors needed for the creation of fragility curves.

Table 4.2.2 Capacity Factors

	FEMA-IO	FEMA-LS	FEMA-CP	IDA-IC	Pushover-FY	Pushover-PMI
β_C	0.3	0.3	0.3	0.46	0.3	0.3
λ_C	0.00	0.69	1.39	0.87	-1.14	-0.65

4.2.4.2 Seismic Demand

Inelastic time history dynamic analyses using the program IDASS (Kunnath, 2003) are used to find the seismic demand of the given RC frame structure during earthquake ground motions of variable intensity. Since recorded ground motions for the Mid-America region are not available, synthetic ground motions developed by Wu and Wen (2001) were used as the seismic excitations. The ground motions, developed for the Memphis region with representative soil conditions, consist of a suite of 10 records with 10% and 2% probability of exceedence in 50 years. Figs. 4.2.7 and 4.2.8 shows the elastic acceleration and displacement response spectra, respectively, for the records used throughout inelastic time history dynamic analyses.

Nonlinear time history dynamic analyses were used to find the expected seismic inter-story drift demands for the 2 suites of ground motions. Fig. 4.2.9 shows the peak story drift demand vs. spectral acceleration at the fundamental building period for every ground motion and the best-fit power law trend line. The figure shows significant scatter in the demands with the 2% ground motion records, but still an overall good fit is obtained.

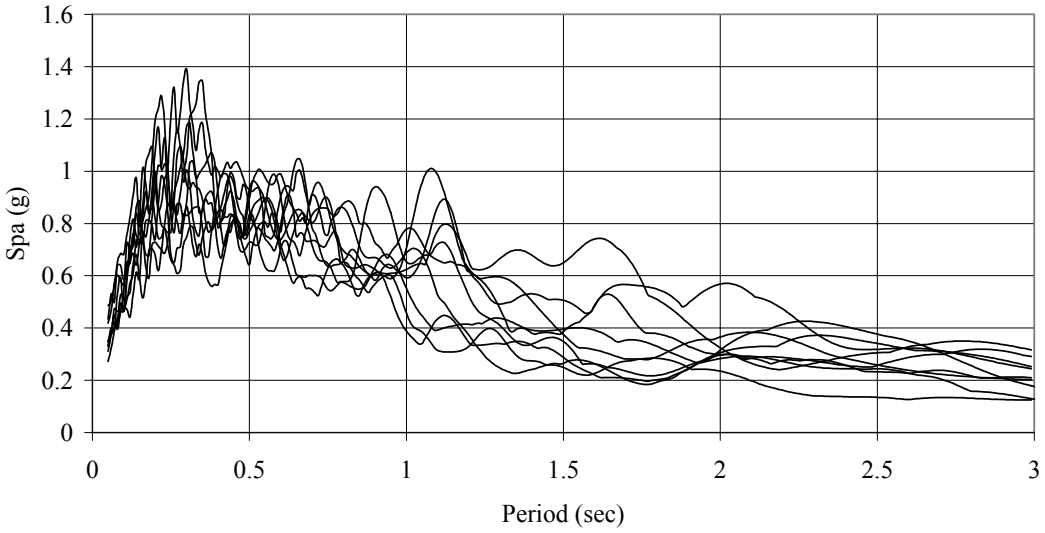

(a) 2% in 50 Years Records

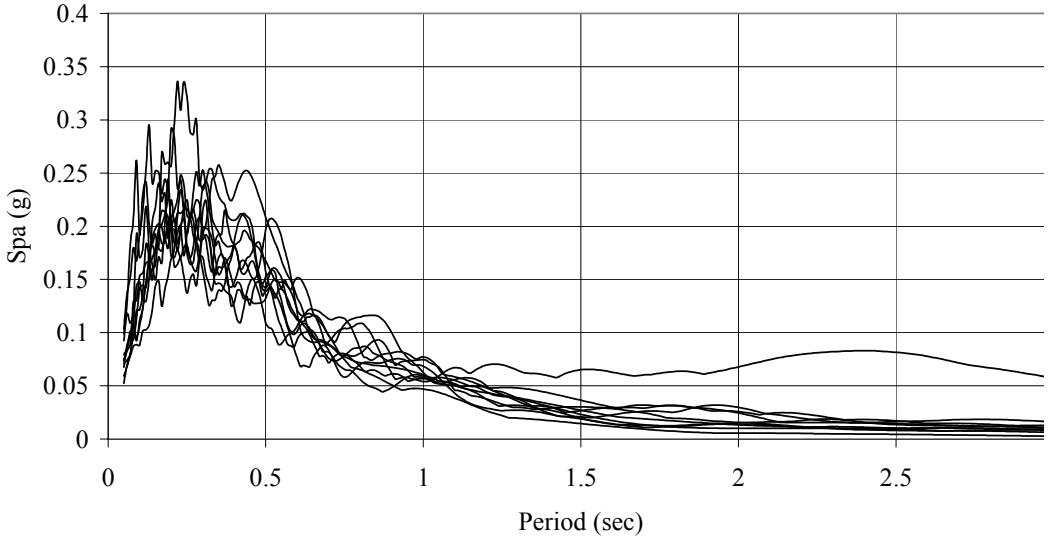

(b) 10% in 50 Years Records

Figure 4.2.7 Acceleration Response Spectra

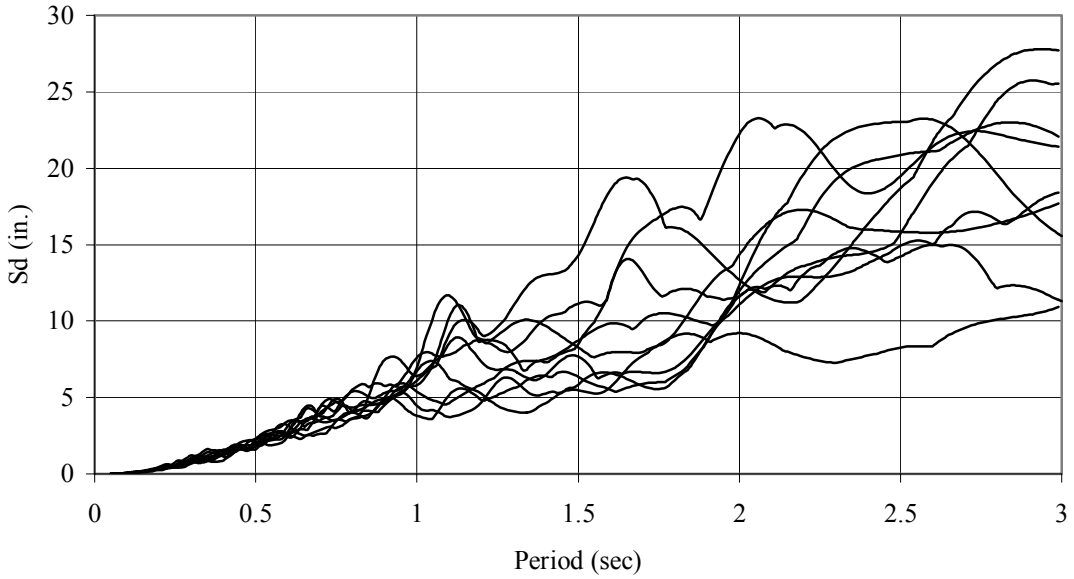

(a) 2% in 50 Years Records

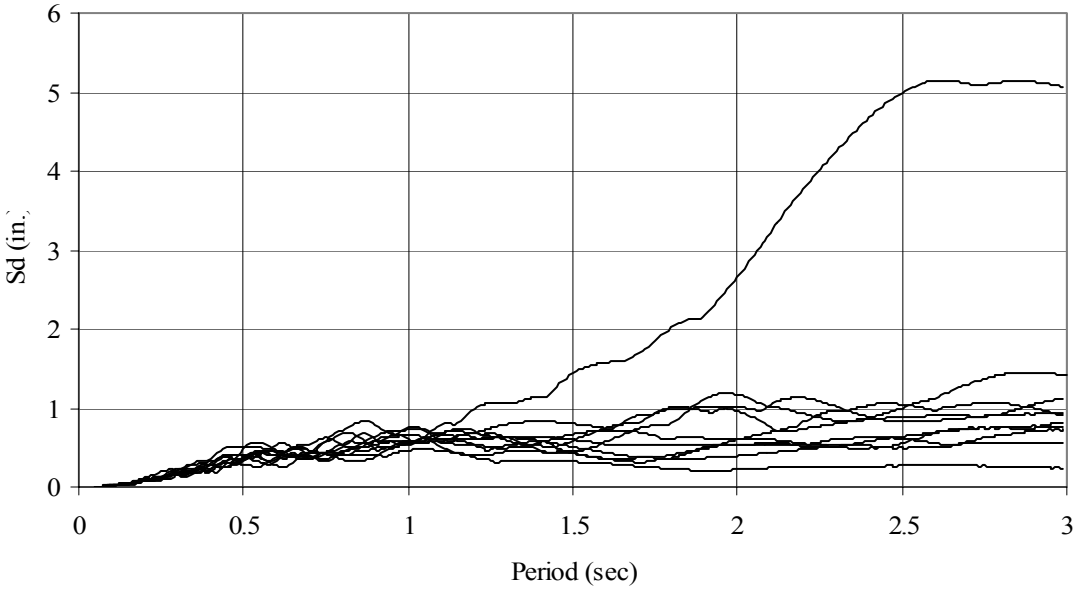

(b) 10% in 50 Years Records

Figure 4.2.8 Displacement Response Spectra

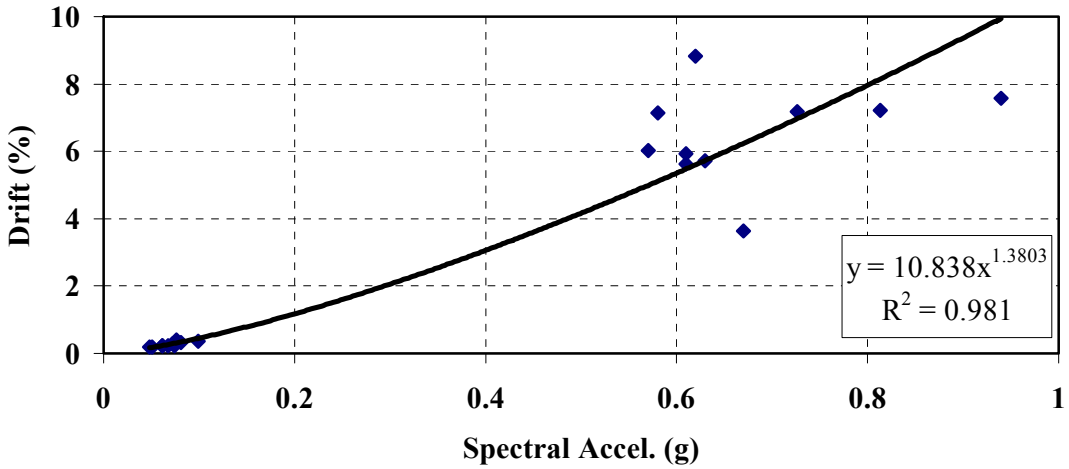

FIGURE 4.2.9 Inter-Story Drift Demand vs. Spectral Acceleration at 0.87 Sec. Period

Based on the results of these analyses, the fragility curve parameters related to the seismic demand are calculated as follows: $\lambda_{D/Sa}$ = ln(calculated median demand drift for a given spectral acceleration of an earthquake at the fundamental period of the structure); and $\beta_{D/Sa}$ = sqrt(ln(1+s^2)), as described previously. In this work, the demand drifts are calculated from the best-fit power law line and the scatter of the demand drifts about the same best-fit line are accounted for in the uncertainty parameter $\beta_{D/Sa}$ which was equal to 0.23.

4.2.4.3 Fragility Curve Results

Figs. 4.2.10-4.2.12 show the fragility curves for a typical older RC frame building, with three different levels of modeling uncertainty, β_m = 0.2, 0.3, and 0.4. The top portion of the figures show the fragility curves for the FEMA drift limit states and the lower portion shows the fragility curves for incipient collapse, first yield, and plastic mechanism initiation. Comparing the results between the 20%, 30%, and 40% modeling uncertainty, it can be concluded that the level of modeling uncertainty is relatively insignificant. For this reason, all further results discussed will deal only with a 30% modeling uncertainty.

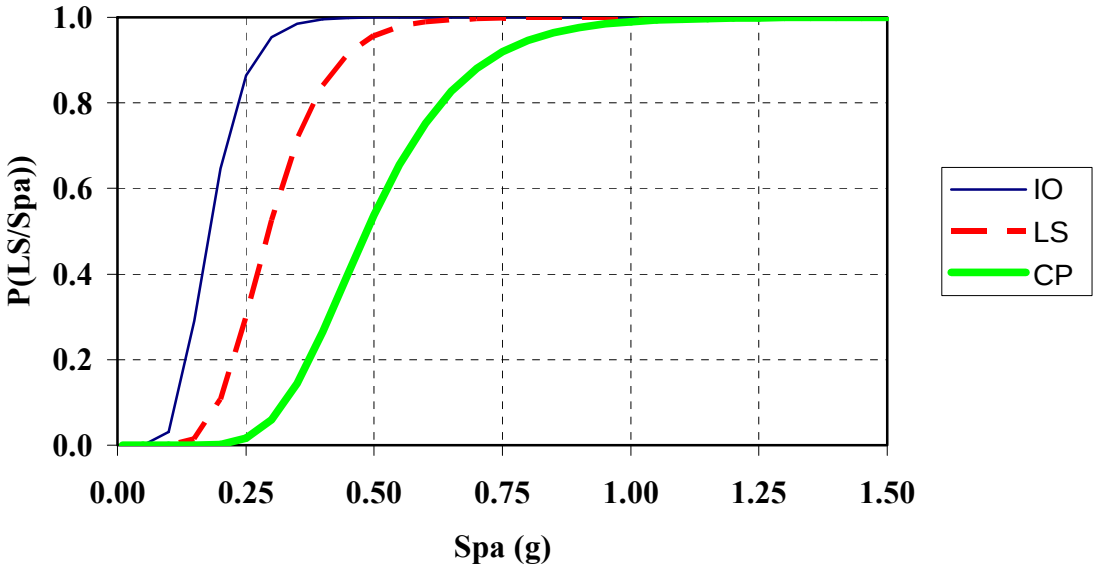

FEMA Limit States

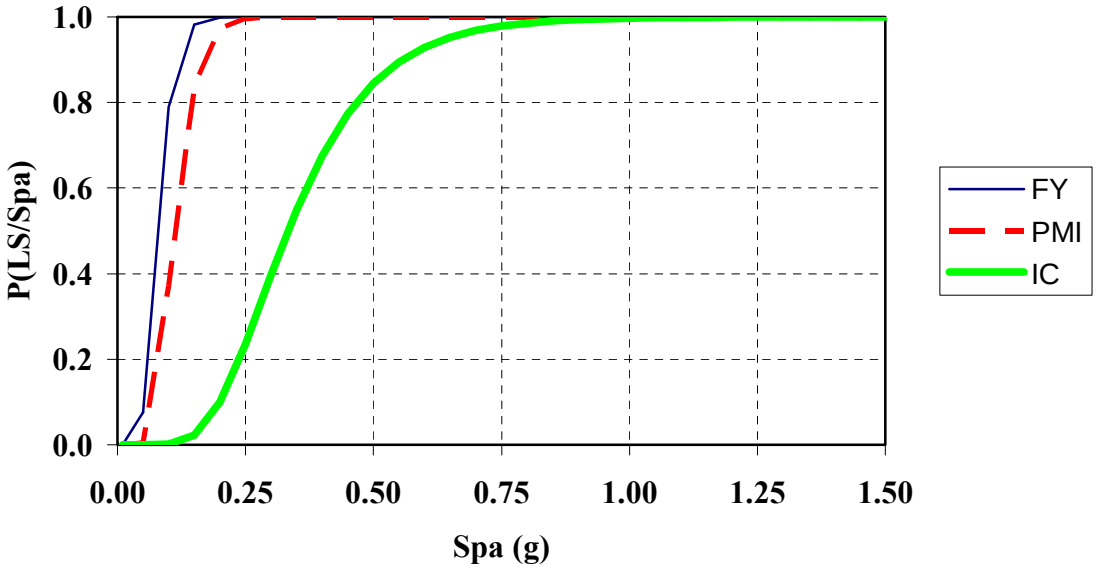

Quantitative Limit States

Figure 4.2.10 Fragility Curves with $\beta_m = 0.2$

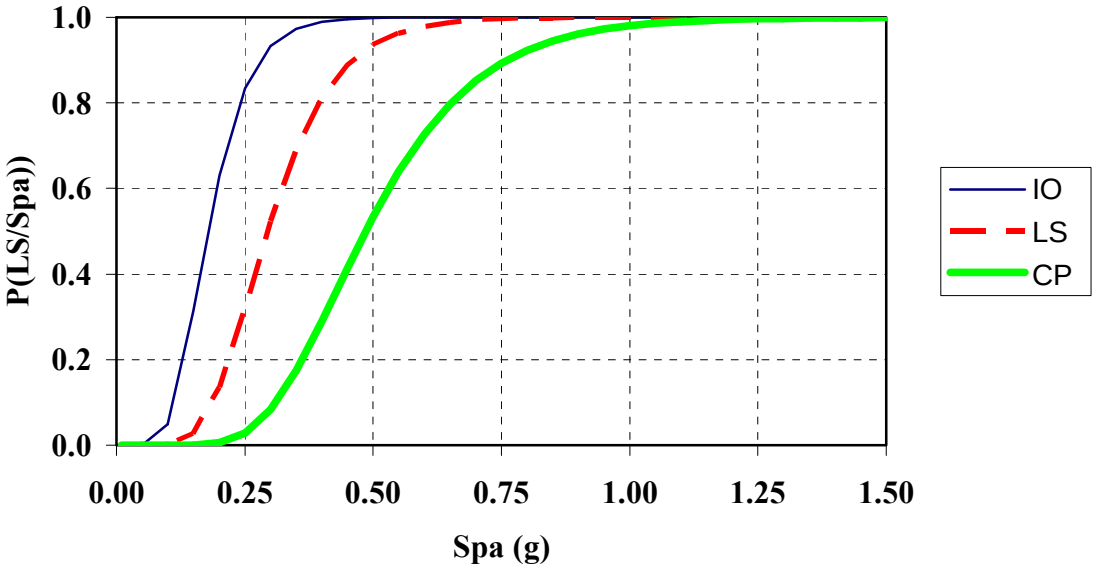

FEMA Limit States

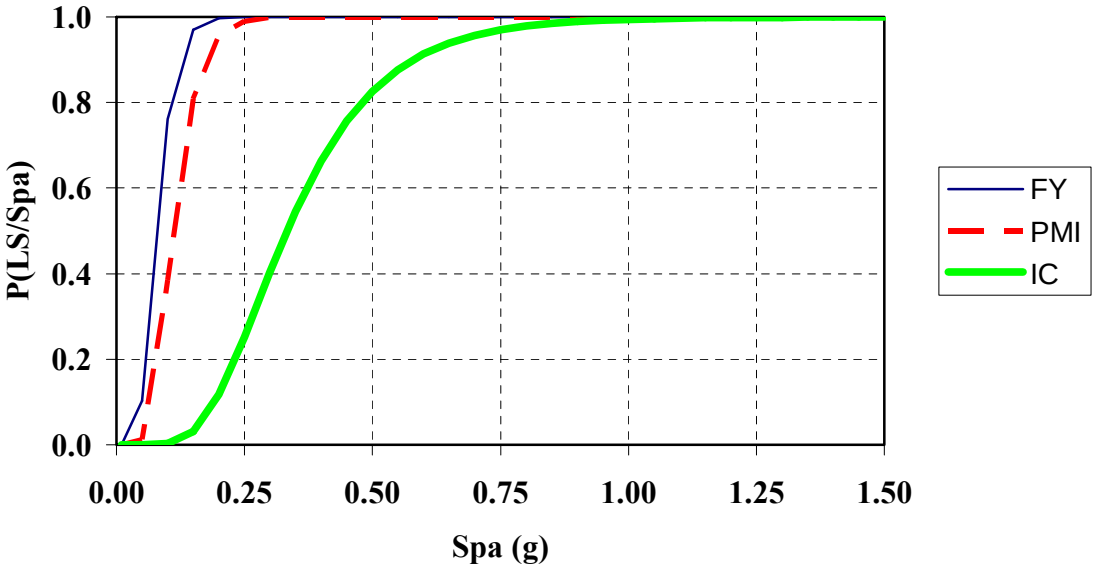

(b) Quantitative Limit States

Figure 4.2.11 Fragility Curves with $\beta_m = 0.3$

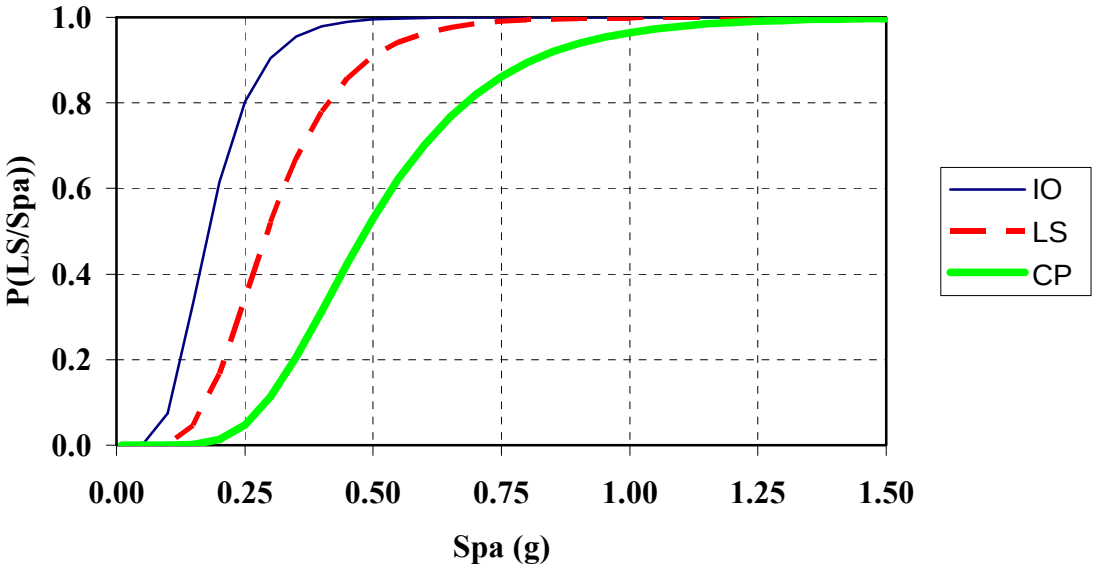

(a) FEMA Limit States

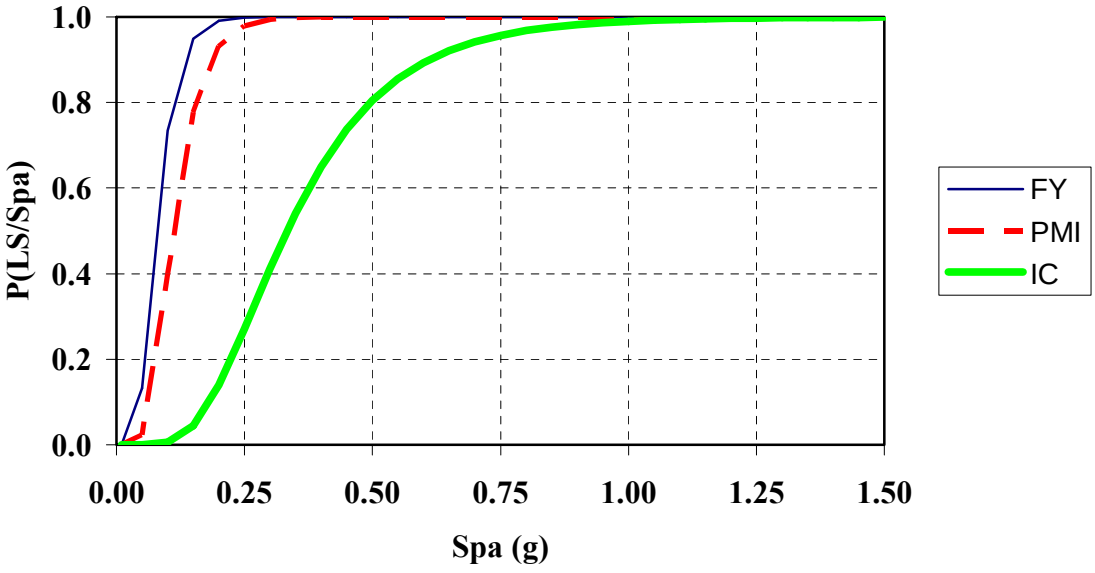

Quantitative Limit States

Figure 4.2.12 Fragility Curves with $\beta_m = 0.4$

Given the fragility curves, the seismic vulnerability of older RC frame structures can be evaluated based on given seismic event scenarios. For example, the IBC (2003) model building code specifies that new construction of similar buildings near Memphis, TN should be designed for a spectral acceleration of 0.74 g with fundamental building period of 0.87 sec. (using S_s =3.0 g and S_1 = 1.0 g). This acceleration would be representative of a very large intensity earthquake with 2% probability of exceedance in 50 years. Given the spectral acceleration of 0.74 g and the fragility curves developed, it can be concluded that older RC frame buildings will be extremely vulnerable to severe damage. For example, the probabilities of exceeding the FEMA defined limits are 99% for immediate occupancy, 99% for life safety, and 88% for collapse prevention. Using the nonlinear pushover and incremental dynamic analyses, the probability of exceeding the first yield and plastic mechanism initiation limit states are 99%, and 96% for incipient collapse.

4.2.5 Retrofit Fragility Curves for older RC Frame Structures

As summarized previously, GLD RC frame structures inherently have strong beams and weak columns (column-to-beam strength ratio of 0.6 for the prototype structure), which make them prone to story mechanisms at same inter-story drift levels. The fragility curves presented in Section 4.4.4 are basically controlled by response at the first story. Previous work by Bracci et al. (1995b) and Dooley and Bracci (2001) have shown that a key variable in controlling seismic damage to RC frames structures is the column-to-beam strength ratio at beam column joints. Therefore, a parametric study was conducted to evaluate the seismic performance of RC frame structures using column-to-beam strength ratios of 1.2 and 1.8. The former ratio is the current seismic design requirement specified in ACI 318 (2002) and the latter is a ratio recommended by Dooley and Bracci to deter story mechanisms. To accomplish the objective of evaluating the influence of column-to-beam strength ratio, two additional sets of fragility curves are developed according to the same methodology previously presented, for column-to-beam strength ratios of 1.2 and 1.8. The manner in which this was accomplished was by altering the column moment strength vs. curvature in the nonlinear analysis model to achieve the desired strength ratio. Fig. 4.2.13 shows the input column moment strength vs. curvature relationship input into the computer code IDASS for the originally GLD model (0.6), as well as relationships for the 1.2 and 1.8 strength ratios. It is important to note that the initial stiffness of the column response is constant in order to evaluate the influence of increasing column strength alone on the fragility curves.

4.2.5.1 Inter-Story Drift Capacities (Limit States)

Inter-story drift limit states for the computation models using column-to-beam strength ratios of 1.2 and 1.8 are defined below for each method used:

FEMA-273 Limit States
Since FEMA defines qualitative limit states which can be represented by deterministic inter-story drift limits of 1%, 2%, and 4% of the story height for IO, LS, and CP, respectively, for RC frame structures, the same drift limits will be considered for the two retrofit models. Therefore, as previously for the GLD building model, the uncertainty

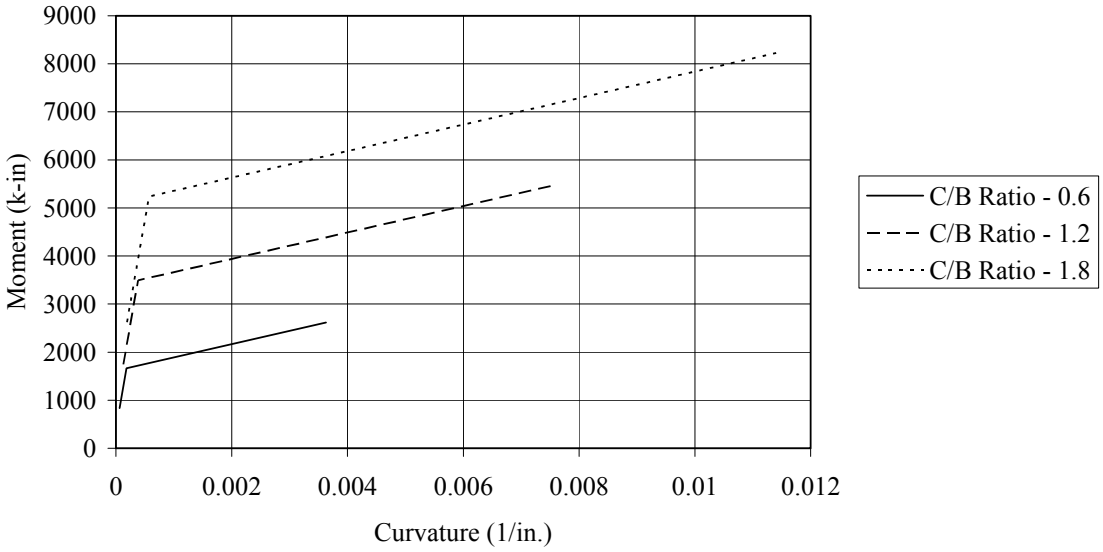

Figure 4.2.13 Nonlinear Moment vs. Curvature Relationships for Columns

parameter, β_C, was taken as 0.3 for all fragility curves and λ_C was taken as ln(1.0), ln(2.0), and ln(4.0) for IO, LS, and CP, respectively.

Quantitative Pushover Analyses

Since displacement control loading of individual stories was the critical loading mechanism for developing first yield and plastic mechanism initiation limit states, displacement control loading of the first story is only presented. The force-drift response and sequence of member yielding for the building models with 1.2 and 1.8 column-to-beam strength ratios are presented in Figs. 4.2.14 and 4.2.15, respectively. It can be observed that as the strength ratio of the building model increases that more yielding occurs in beam sections and the yielding mechanism in the structure is significantly distributed throughout the structure. This results in larger drift limits for plastic mechanism initiation. However, the first yield limit state is similar to the original GLD building. Therefore, the uncertainty parameter, β_C, was again taken as 0.3 for both building models and λ_C was taken as ln(0.61) and ln(0.57) for FY and ln(2.40) and ln(4.94) for PMI, respectively for the building models with column-to-beam strength ratios of 1.2 and 1.8.

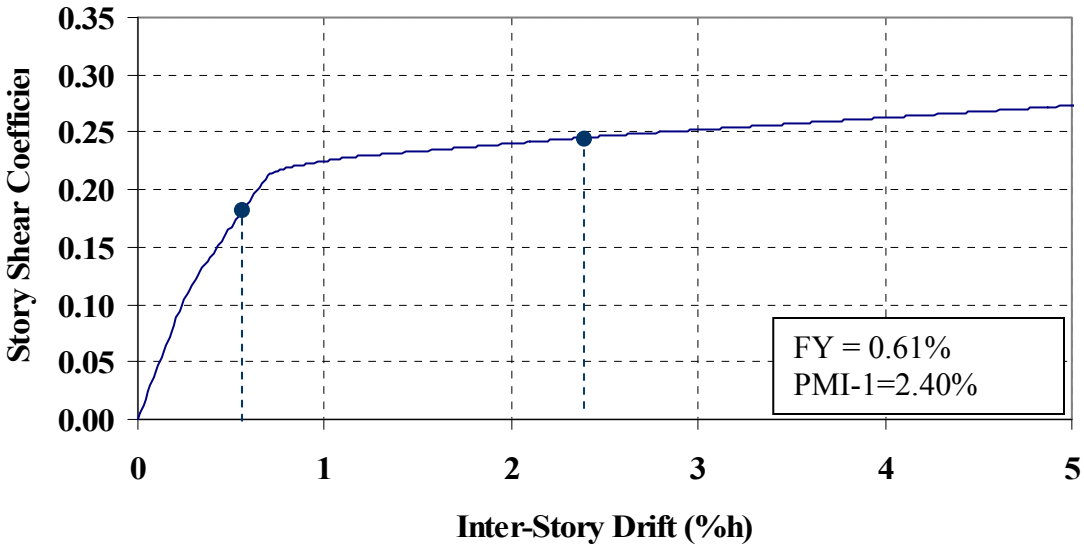

(a) Story Shear vs. Drift Response

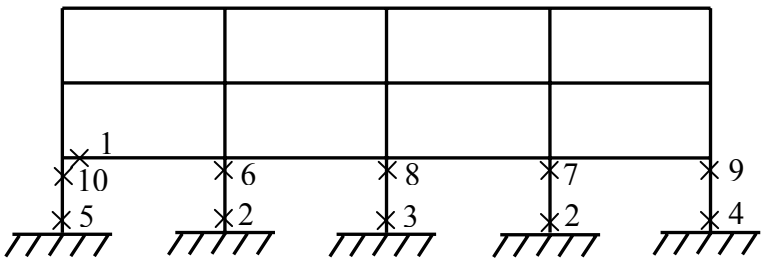

(b) Sequence of PMI

Figure 4.2.14 Pushover Analyses - Displacement Control Loading – 1.2 Strength Ratio

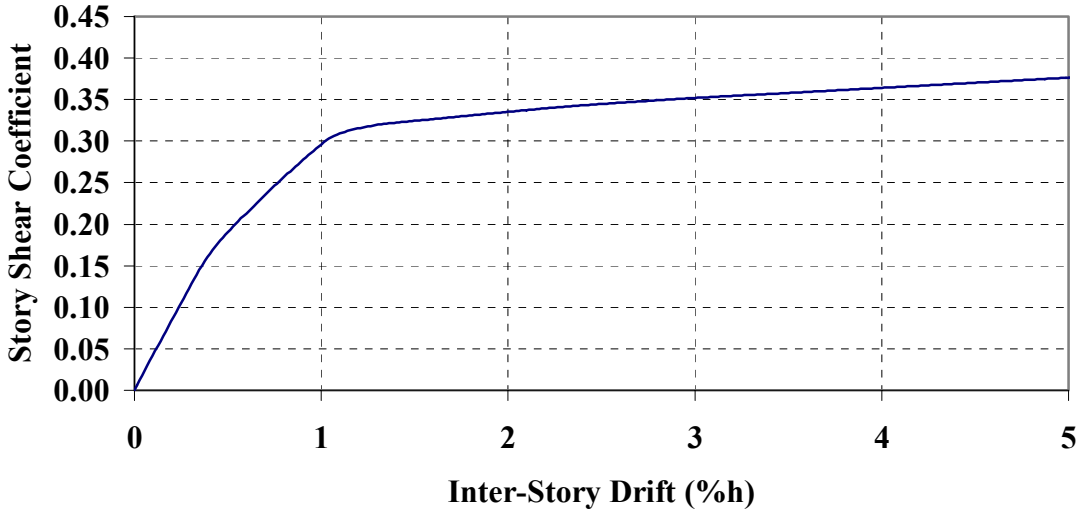

(a) Story Shear vs. Drift Response

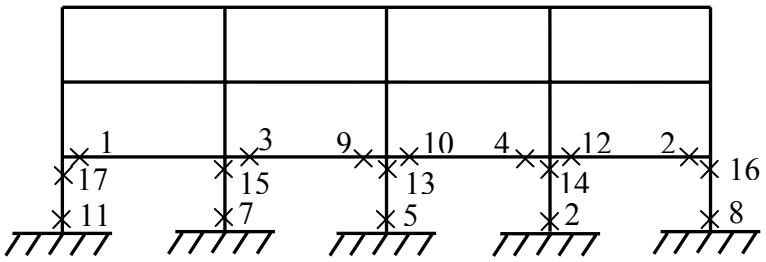

(b) Sequence of PMI

Figure 4.2.15 Pushover Analyses - Displacement Control Loading – 1.8 Strength Ratio

Incremental Dynamic Analyses

The critical incipient collapse drift limits from the IDA for the two retrofitted models are shown in Figs. 4.2.16 and 4.2.17. β_C was determined to be 0.34 and 0.42, and λ_C was taken as ln(median drift = 2.20%) and ln(median drift = 2.65%), respectively for the 1.2 and 1.8 ratio building models.

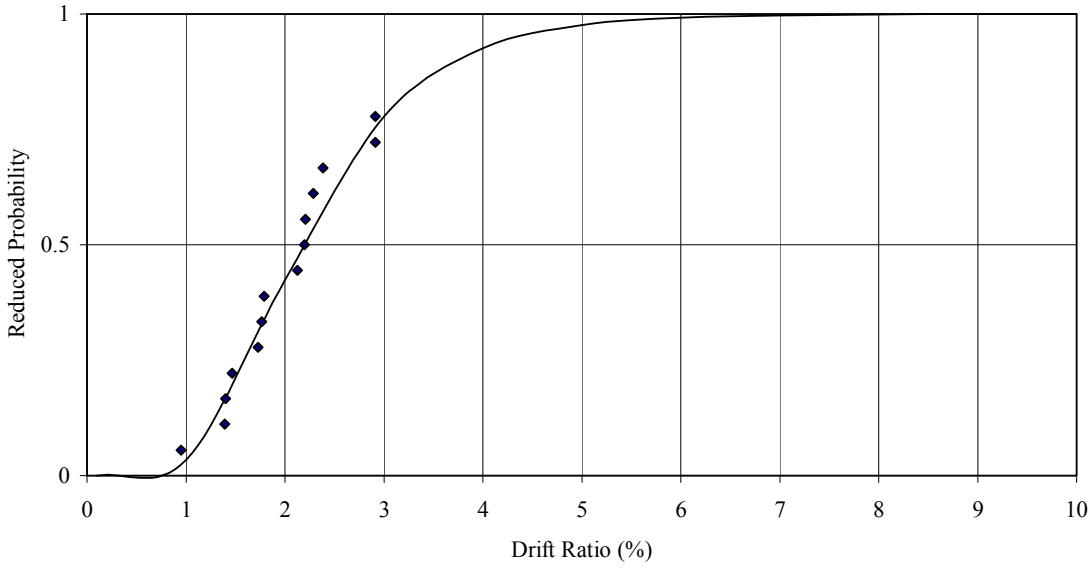

Figure 4.2.16 Incremental Dynamic Analyses – 1.2 Strength Ratio

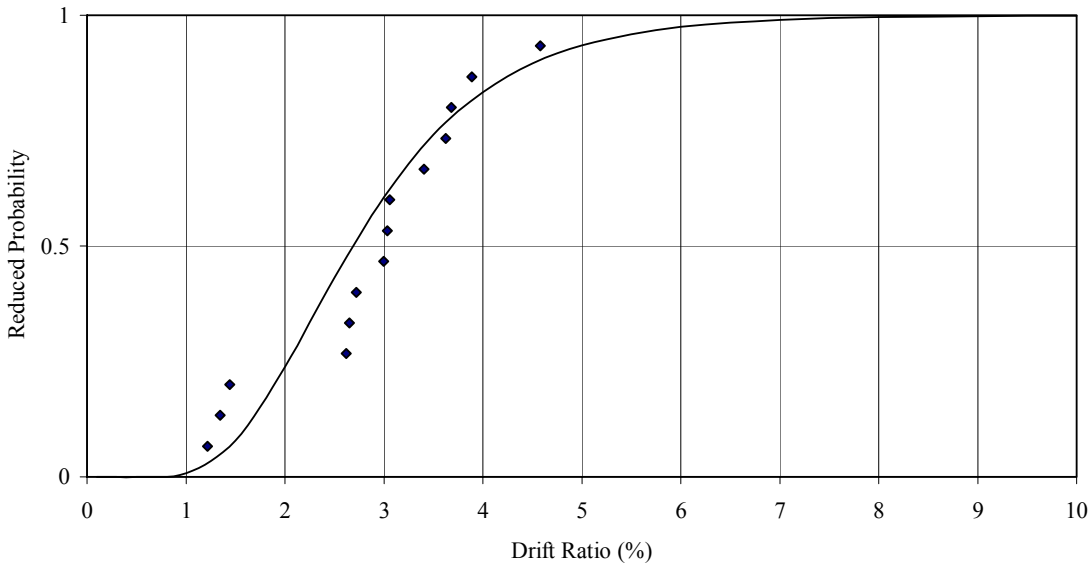

Figure 4.2.17 Incremental Dynamic Analyses – 1.8 Strength Ratio

Summary
Table 4.2.3 shows the capacity factors for the 1.2 and 1.8 models for the fragility curves.

Table 4.2.3 Capacity Factors for 1.2 and 1.8 Models

	FEMA-IO	FEMA-LS	FEMA-CP	IC	Pushover-FY	Pushover-PMI
β_C (1.2)	0.3	0.3	0.3	0.34	0.3	0.3
λ_C (1.2)	0.00	0.69	1.39	0.79	-0.49	0.88
β_C (1.8)	0.3	0.3	0.3	0.42	0.3	0.3
λ_C (1.8)	0.00	0.69	1.39	0.98	-0.56	1.60

4.2.5.2 Seismic Demand

Inelastic time history dynamic analyses using IDASS (Kunnath, 2003) were used to find the seismic demand for the RC frame structures with 1.2 and 1.8 column-to-beam strength ratios during the same earthquake ground motions used for the GLD building. Figs. 4.2.18 and 4.2.19 show the peak story drift demand vs. spectral acceleration at the fundamental building period for every ground motion and the best-fit power law trend line, respectively for the 1.2 and 1.8 ratio building models. The figures again shows significant scatter in the demands with the 2% ground motion records, but still an overall good fit is obtained.

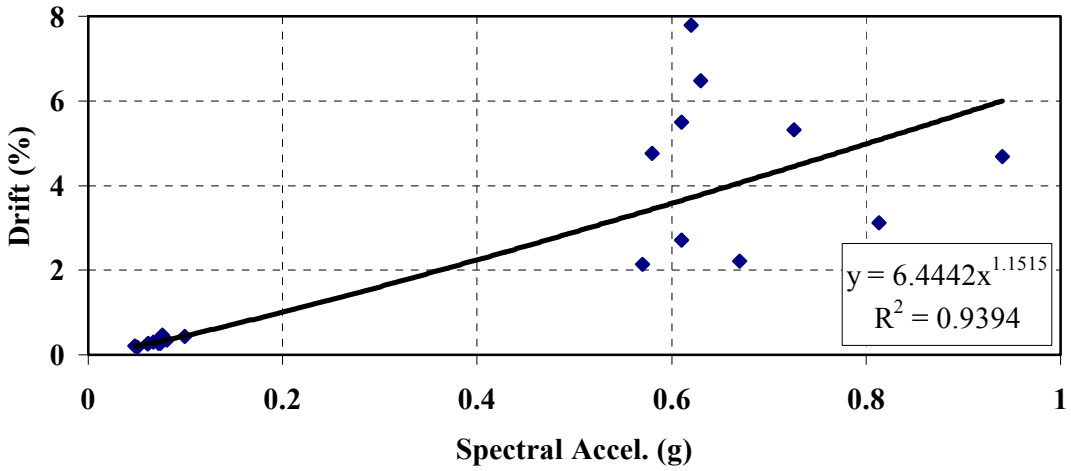

Figure 4.2.18 Inter-Story Drift Demand vs. Spectral Acceleration – 1.2 Strength Ratio

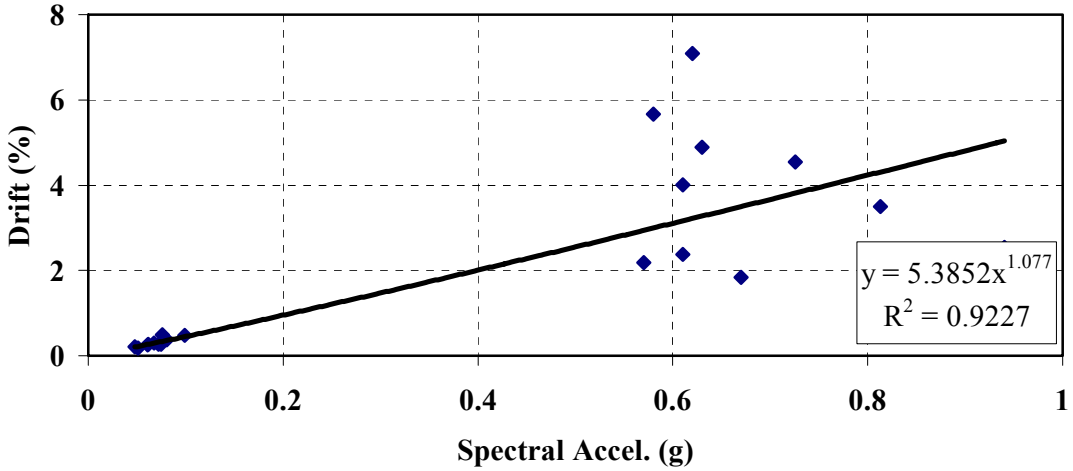

Figure 4.2.19 Inter-Story Drift Demand vs. Spectral Acceleration – 1.8 Strength Ratio

Based on the results of these analyses, the fragility curve parameters related to the seismic demand are calculated as follows: $\lambda_{D/Sa}$ = ln(calculated median demand drift for a given spectral acceleration of an earthquake at the fundamental period of the structure); and $\beta_{D/Sa}$ = sqrt(ln(1+s^2)), as described previously. As before, the demand drifts are calculated from the best-fit power law line and the scatter of the demand drifts about the same best-fit line are accounted for in the uncertainty parameter $\beta_{D/Sa}$ which was equal to 0.35 and 0.37, respectively for the 1.2 and 1.8 building models.

4.2.5.3 Fragility Curve Results

Figs. 4.2.20 and 4.2.21 show the fragility curves for 1.2 and 1.8 column-to-beam strength ratio building models. The top portion of the figures show the fragility curves for the FEMA drift limit states and the lower portion shows the fragility curves for incipient collapse, first yield, and plastic mechanism initiation. It can be observed by comparing the FEMA drift limit state fragilities that the probability of exceedance is improved with building retrofit based on column strengthening. However, the two retrofitted models have similar probability of exceedence. Since the capacity limit states were constant for all three model building, it can be concluded that the inter-story drift demands were significantly reduced with column strengthening of 1.2 strength ratio as compared to the existing building, and only slightly reduced with additional column strengthening at the 1.8 strength ratio. However, column strengthening using the 1.8 column-to-beam strength ratio also significantly affects the quantifiable limit state capacities of first yield and plastic mechanism initiation. This results in enhanced building performance and better fragility curves.

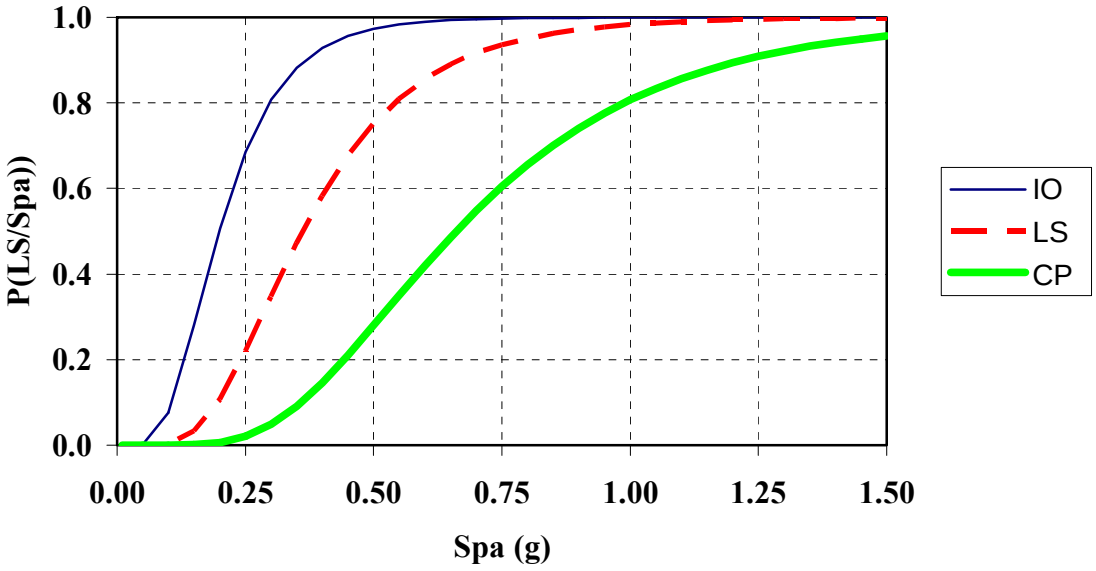

(a) FEMA Limit States

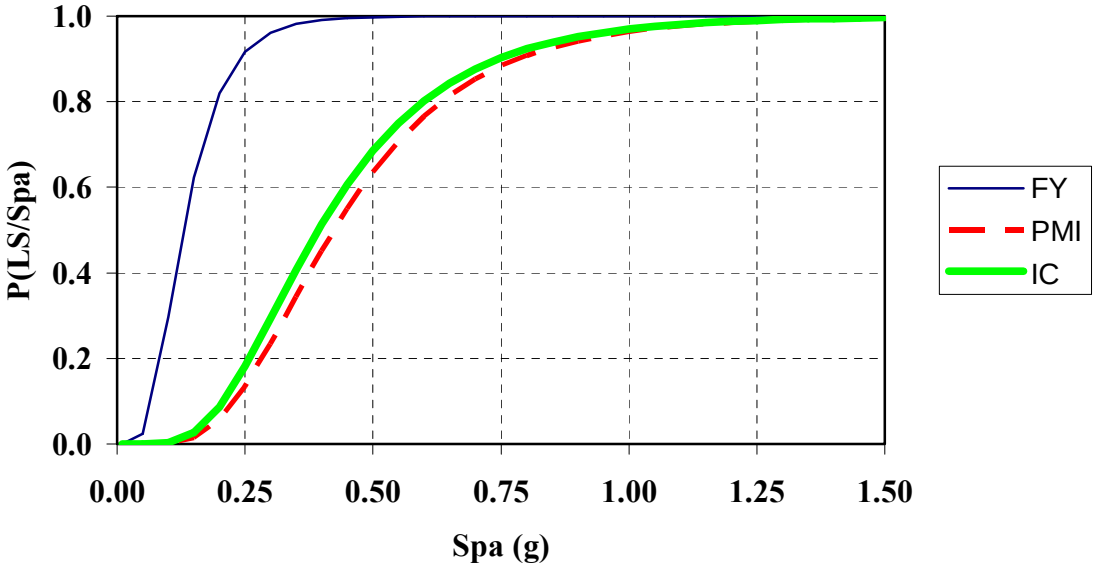

(b) Quantitative Limit States

Figure 4.2.20 Fragility Curves – 1.2 Strength Ratio

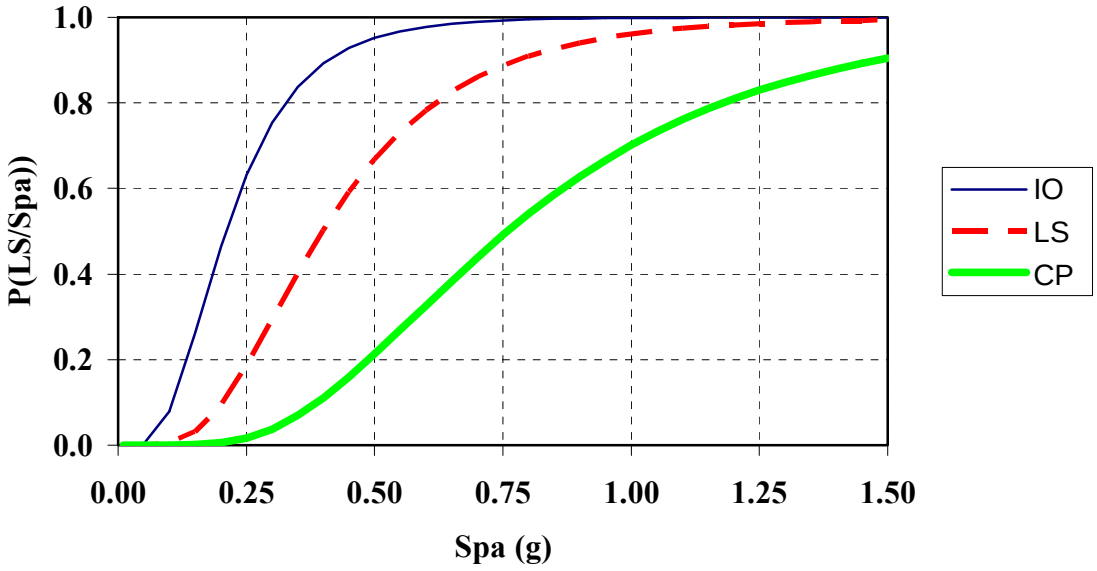

(a) FEMA Limit States

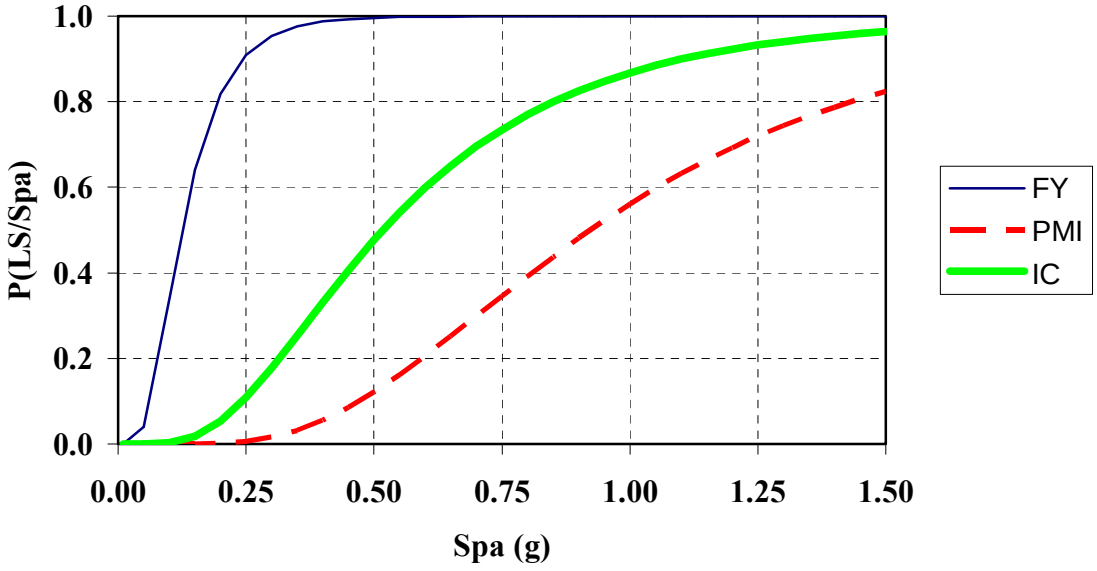

(b) Quantitative Limit States

Figure 4.2.21 Fragility Curves – 1.8 Strength Ratio

4.2.6 Conclusions

The seismic vulnerability of older reinforced concrete (RC) frame structures located in the Mid-America region, specifically near Memphis, TN, due to potential earthquakes was quantified by means of fragility curves, which relate the probability of exceeding a particular limit state given an imposed seismic demand. Seismic demand is defined as the spectral acceleration of a particular earthquake event at the fundamental period of the structure under consideration. Story limit state capacities were identified using FEMA guidelines (immediate occupancy, life safety and collapse prevention) and using quantitative nonlinear analysis methods (first yield, plastic mechanism initiation, and incipient collapse). The fragility curve results imply that such construction will be vulnerability to severe damage during large magnitude earthquakes that are probable for the region. As a method of retrofit, column strengthening was considered to improve the seismic vulnerability of such structures. The results showed that the fragility curves were improved with column strengthening. Building seismic response demands were significantly reduced with column strengthening of 1.2 strength ratio as compared to the existing building, and only slightly reduced with additional column strengthening at the 1.8 strength ratio. However, column strengthening using the 1.8 column-to-beam strength ratio also significantly affects the quantifiable limit state capacities of first yield and plastic mechanism initiation. This results in enhanced building performance and better fragility curves.

4.3 Steel Building Frames

Steel moment frames in buildings play a key role in mitigating the impact of extreme earthquakes and winds. Their importance to the performance of the overall building system is amplified by the so-called common cause effect, in which inadequate performance of the structure may lead to failure or loss of function of nonstructural items such as roofing and cladding, as well as damage to mechanical or electrical components and systems.

In this section, fragility-modeling procedures are developed for steel frames, components and systems subjected to earthquake ground motions. These quantitative methods provide a basis for evaluating structural performance and the role of the structural system in mitigating earthquake hazards and in developing damage and loss estimation procedures. The study is centered on the following three tasks:

- Fragility modeling
- Database requirements
- Risk perspectives derived from fragility estimates

4.3.1 Review of fragility modeling concepts

As noted in Section 2, fragility analysis is a technique for assessing and displaying, in probabilistic terms, the capability of an engineered component or system to withstand a

specified seismic event. Fragility modeling requires a focus on the behavior of the structural system as a whole and, specifically, on what can go wrong with the system. The fragility modeling process leads to a median-centered estimate of system performance, coupled with an estimate of the uncertainty in performance. This uncertainty has both aleatory and epistemic components, as discussed below. While the control variable in the current application is the spectral acceleration at the fundamental period of the structure, $S_a(T_1)$, other demand variables, such as spectral velocity or Modified Mercalli Intensity, can also be used. The selection of the control variable depends on the manner in which the hazard is specified, the nature of the decision process, and the mode of risk communication to the stakeholder group.

The fragility of a structure commonly is modeled by a lognormal cumulative distribution function (CDF). If the structural capacity is described as the product of a large number of statistically independent random variables, the central limit theorem provides some justification for this choice of CDF. Using this model, the fragility is described by,

$$F_R(x) = \Phi[\ln(x/m_R)/\beta_R] \qquad (4.3.1)$$

in which $\Phi[\ ]$ = standard normal probability integral, m_R = median capacity (expressed in units that are dimensionally consistent with the control variable used to define the seismic hazard, e.g., spectral acceleration,), and β_R = logarithmic standard deviation, which is approximately equal to the coefficient of variation (COV) in capacity, V_R, when $V_R \leq 0.3$. The 5-percent exclusion limit on the system capacity, which might serve as a threshold for decision purposes (as illustrated subsequently), is

$$R_{0.05} = m_R \exp(-1.645\ \beta_R) \qquad (4.3.2)$$

Equation (4.3.1) depicts the conditional limit state probability of the system when the state of knowledge is essentially perfect (within the bounds of normal engineering structural mechanics). In this case, parameters m_R and β_R measure inherent randomness (or aleatory uncertainty). Such uncertainties are essentially irreducible under current engineering analysis procedures. As an example, the yield strength of steel sampled from the flange of an ASTM A992 W-section (specified yield stress of 50 ksi), tested in accordance with standard ASTM procedures, is a random variable that can be modeled by a lognormal distribution with a mean of approximately 56 ksi (386 MPa) and COV of approximately 0.08, depending on the Shape Schedule (AISC, 1999). These statistical estimates are relatively stable from sample to sample, assuming that the sample sizes are not too small. This inherent variability is characteristic of aleatory uncertainty; additional data or other information does not change the probabilistic model in any significant way.

Additional sources of uncertainty in estimated capacity arise from assumptions made in the analysis of the system and from limitations in the supporting databases. In contrast to

aleatory uncertainties, these knowledge-based (or epistemic) uncertainties depend on the quality of the analysis and supporting databases, and generally can be reduced, at the expense of more comprehensive (and costly) analysis. Sources of epistemic uncertainty in analysis of steel structures include two-dimensional models of three-dimensional structures, structural models based on beam and column centerline dimensions that neglect beam-column panel zones, support conditions and connections that are neither fully rigid nor simple, neglect of shear deformations, and limitations in the supporting databases.

The presence of epistemic uncertainty means that the structural fragility actually is described by a *family* of curves, reflecting incomplete knowledge regarding the parameters used to model the structural fragility: in the median, COV, and the CDF itself. To first order, these uncertainties can be assumed to be vested in the estimate of the median capacity, m_R, in Eq. 4.3.1. [This is the customary of modeling epistemic uncertainty in seismic PSA of critical facilities; unpublished studies have shown that the contribution of uncertainty in β_R is of secondary importance in comparison to that of uncertainty in m_R.] Under this assumption, m_R is replaced by a (Bayesian) random variable, M_R, which is assumed to be modeled by a lognormal distribution with median m_R and logarithmic standard deviation β_U. Then, the overall uncertainty in capacity (aleatory and epistemic) is displayed by the *family* of lognormal CDFs, defined by parameters (m_R,β_R,β_U). With this model, the 5-percent exclusion limit in Eqn 4.3.2 becomes a random variable as a result of the uncertainty in M_R, modeled by β_U. The lower 5-percent confidence interval on $R_{0.05}$, R_k, is defined by,

$$R_k = m_R \exp[-1.645(\beta_R + \beta_U)] \qquad (4.3.3)$$

One might say (with a Bayesian interpretation) that the probability of surviving an earthquake event with intensity R_k is at least 95% with 95% confidence.

Distinguishing between the different sources of uncertainty may create accounting difficulties in database management. Moreover, in many applications, it is desirable to have one overall estimate of fragility for review, assessment and decision purposes that reflects both aleatory and epistemic uncertainty. Such an estimate is provided by the *mean* fragility, defined as (Ellingwood, 1998)

$$E[F_R(x)] = \Phi[\ln(x/m_R)/\beta_C] \qquad (4.3.4)$$

in which

$$\beta_C = [\beta_R^2 + \beta_U^2]^{1/2} \qquad (4.3.5)$$

At the usual levels of aleatory and epistemic uncertainty found in the assessment of steel (or reinforced concrete) structures, R_k in Eqn 4.3.3 corresponds to roughly the 1 to 2-percentile value of $E[F_R(x)]$.

Limit state(s) of structural performance must be identified before the fragility model(s) can be constructed. This is also a key step in the development of loss estimation methodologies. Such limit states depend on the performance objectives of the building or other infrastructure system in which the structure must function or preserve its overall integrity, and the assessment of limit states requires a system reliability approach. Performance objectives usually are qualitative in nature: the system must remain operational under normal or moderate hazards; the system must not endanger life safety under extreme hazards; etc. Such goals must be transformed into structural limit states that can be verified by analysis or test. The focus in design of steel frames according to the AISC *LRFD Specification* (AISC 1999) has been on ultimate strength because the key focus in building codes is life safety. However, the structural strength limit state may be of lesser importance than a deformation-related limit state, especially when the structural frame is an integrated component of a complex building system in which structural, nonstructural, mechanical and electrical systems all must interface properly. Modern approaches to earthquake-resistant design of buildings and other structures are based on deformation capacity rather than on strength (e.g., Priestley, 1996; BSSC, 1997; 1998). Properly designed steel frames, particularly those that are highly redundant, may behave in a ductile manner under extreme loads, and yet the building may suffer damage to appurtenant systems at structural deformations well below those at incipient structural collapse.

The fragility analysis of a steel frame requires a thorough understanding of the mechanics of structural response and the interactions between structural and nonstructural behavior to challenges over a wide range, including those at and beyond the design basis. At such levels, the behavior of the structural system usually is highly nonlinear in nature. Because of the complexity of structural behavior in this range, closed-form models generally are not sufficient to describe their response to extreme earthquake events, and one must resort to nonlinear finite element analysis to support the fragility model (Song and Ellingwood, 1999).

4.3.2 Databases to support fragility assessment

Supporting databases and statistics must be developed to model aleatory and epistemic uncertainties in all parameters known to affect the capacity of the structure. Databases to describe some variables can be identified through a review of the literature. Other parameters may have to be identified and estimated through expert opinion. Proper construction of a consensus estimation survey (sometimes called a Delphi) and careful analysis of the results can lead to statistical models that subsequently can be updated using Bayesian techniques, if and when further information becomes available. It must be emphasized that fragility modeling requires "best estimates" of performance rather than the (generally) conservative estimates that would be obtained from code formulas and nominal

material strengths; otherwise, these conservatisms may propagate through the analysis in an unpredictable way.

Summaries of statistical data to describe strength of steel members (beams and columns, and connections) and structures subjected to static forces are available in published literature [e.g., Ellingwood and Hwang (1985); Dexter (2000)]. Some of these statistics are different from those used to develop the first-generation of LRFD specifications in the 1970's because changes in the interim have occurred in steel making and rolling practices. Most steel strengths (yield and ultimate tensile strengths) presented in the published literature are based on mill tests conducted in accordance with ASTM standard procedures. Mill tests of steel (and standard-cure concrete cylinder tests, for that matter) are conducted at a strain rate than is atypical of either static or dynamic loading of the structural system. The strength that should be used to assess reliability of frames under gravity load is the static strength in situ, i.e., the strength when loading to failure takes over a period of several minutes to one hour. The mill test data for steel strength are adjusted to static conditions by the approximate relation $F_{y,stat} = F_{y,mill}$ - 4 ksi (Galambos and Ravindra, 1978). Similarly, when the structural component or system is subjected to dynamic forces, the statistical properties of strength of steel for use in developing fragility curves should be adjusted for the increased rate of load. The steel "dynamic" strengths presented correspond to loading to "failure" in approximately 1 - 5 seconds. Mill tests of steel are conducted at a strain rate that falls somewhere between "static" and "dynamic" rates of application of structural actions. Since the precise rate of loading to failure in a steel frame subjected to earthquake ground motion is uncertain, it is conservative to ignore the increase in strength for dynamic load effects in seismic fragility assessment.

Furthermore, while mill tests for A36 steel historically were performed using specimens taken from the webs of W-sections, for modern A992 structural W-shapes coupons now are taken from flanges rather than from the web, where the values of F_y are approximately 5% lower under the same test conditions. Finally, although some studies have indicated that yield strength decreases with increasing size or thickness, the data reviewed in this study indicate that this effect is negligible.

The uncertainty in the finite element-based structural analysis that supports the fragility assessment should also be taken into account, as recent research has shown that this source is at least as important as variability in steel strength in a fragility assessment. This uncertainty is epistemic in nature, as it arises from idealizations made in modeling the behavior of the structure analytically. One can visualize this uncertainty by: (1) imagining that all properties of the structure are known from companion tests or independent measurement; (2) using these properties to analyze the ultimate capacity of the structure; (3) testing the structure to failure; and (4) comparing the predictions to test results. The ratio of the test to calculated capacities is the (uncertain) modeling factor. Refined structural models (e.g., nonlinear FEA) in the hands of a skilled analyst usually predict behavior more accurately than do design code models, and in such cases the mean of this modeling factor will be close to 1.0 (implying an unbiased estimate) and the COV usually will be on the order of 0.05. When an approximate structural model is used, this source of

uncertainty can be at least as important as other sources that traditionally have been included in system reliability assessment.

4.3.3 Description of Frame

A three-story, four-bay steel moment-resisting frame was considered to illustrate the fragility modeling concepts. This frame is typical of steel frames in urban areas of the Eastern United States, such as Boston, MA, Memphis, TN, or Charleston, SC that are exposed to moderate seismic hazards. The studies herein were performed as a demonstration of concept, and the structural models were intentionally simplified. The frame was modeled as a planar frame. Centerline dimensions of the frame were used in the structural model, and the contribution of beam-column panel zones was neglected for simplicity. On the other hand, both material and geometric nonlinearities (P-Δ effects) were included in the assessment. The possibility of cracking or deterioration in the connections was not considered. Other studies (Song and Ellingwood, 1999) have shown that cracking of welds in the connections may have a significant impact on response at larger intensities of ground motion, particularly if the connection deterioration is concentrated at one story.

The fragility analysis requires a system reliability approach involving Monte Carlo simulation and repeated finite element analyses. Because of the cost of performing nonlinear FE analysis, the number of simulations, N, necessary to model the uncertainties and to construct the fragility must be kept to a minimum. In the present study, the yield strength, ultimate strength, and modulus of elasticity of the steel were modeled as deterministic and were set equal to their respective mean values. The total uncertainty in behavior thus is vested in the ground motions, modeled by suites of appropriately scaled natural or synthetic ground motions. In a subsequent phase of the study, the uncertainties in structural properties (including structural damping) will be included and an analysis of variance (ANOVA) will be performed to determine the dominant contributors to seismic fragility of frames designed in non-seismic regions. As part of this phase, efficient random sampling plans aimed at minimizing the standard error associated with numerical experimentation (variance reduction techniques) will be employed (e.g., Imam and Conover, 1980; Rubenstein and Melamed, 1998); such plans currently are under development.

The finite element analyses of the frame were performed using OpenSees, an open-source computational platform currently under development at the University of California at Berkeley. The static nonlinear structural response of the frame (pushover) and eigenvalue extraction were checked independently using SAP 2000NL to gain insight on the epistemic uncertainties associated with the choice of finite element platform. The general procedure was to first perform a static nonlinear "pushover" analysis of the frame to identify general characteristics of system behavior, i.e., redistribution of forces within the system subsequent to initial yield, locations of plastic hinging, and overall system ductility. Following the pushover analysis, the system responses to a suite of earthquake ground motions were determined, and the uncertainties in response and performance were

assessed. Finally, an incremental dynamic analysis was performed to determine the capacity of the frame to withstand increasing levels of ground motion.

The building with this frame is assumed to be located in Memphis, TN. The plan and elevation of the frame are illustrated in Figure 4.3.1. The frame was one of three "Pre-Northridge" frames in Boston that were modeled as part of the recently completed SAC Project (Gupta and Krawinkler, 2000a; Yun, et al, 2002; Lee and Foutch, 2002). It was designed by a consulting structural engineering firm using the *National Building Code, 1993 Edition*. The design of the lateral force-resisting system for this frame was governed by seismic effects. Its capacity to withstand the wind forces stipulated in ASCE Standard 7-98 and 7-02 in Memphis, TN was checked. The maximum inter-story drift under (unfactored) design wind force is roughly h/1,300, in which h = story height. Since common design office practice is to limit interstory drifts to h/500 - h/400, these frames meet the lateral stiffness requirements and, in fact, would be overly stiff if wind alone were the governing design consideration.

4.3.4 Structural Response to Static Lateral Forces

As a first step, a static nonlinear pushover analysis of this frame was performed. The pushover results depend on the distribution of lateral forces. It is customary to assume that the lateral forces are approximately proportional to those in the fundamental mode with shape $(z/H)^k$, in which z = elevation, H = building height, and k = constant. Here, both linear (k = 1) and quadratic (k = 2) distributions of lateral force were assumed. (In the SAC program, all pushover analyses were performed assuming that k = 2.) The results of these static nonlinear pushover analyses are illustrated in Fig. 4.3.2. The onset of nonlinear action begins at a drift of approximately 0.01H**,** at which point nonlinear response initiates at the right-hand ends of the beams in spans AB and BC of the roof and third story. It was assumed in the SAC project that at the point where the tangent stiffness is 20% (or less) of the initial stiffness, small additional deformations will lead to large P-Δ moments and the possibility of incipient collapse. The stiffness of this particular frame decreases to 20% of its initial value at an overall drift of approximately 0.023.

4.3.5 Ground Motion Models

Two sets of ground motions were used in this study. The first set was generated in the SAC project for Boston, MA. That ensemble contains 20 records corresponding to an earthquake with 2% probability of being exceeded in 50 years (denoted a 2/50 ensemble). The ensemble was a mix of natural (appropriately scaled) and synthetic ground motions, with 14 natural and 6 synthetic accelerograms. The second set of ground motions were generated as part of MAE Center research (Wen and Wu, 2001) for three sites in Mid-America: Memphis, TN, Carbondale, IL, and St. Louis, MO (believed to represent a cross-section of earthquake-prone sites in the central United States). Ensembles of 10 ground motions corresponding to a 2/50 event were generated for each of these three sites. In contrast to the SAC ground motions, all 30 ground motions derived by Wen and Wu were synthetic in nature. Firm soil conditions were assumed in all cases. None of the ensembles

selected contains "near-field" records (less than 10 km from the building site), the frequency contents of which are different from far-field records.

Seismic fragility and risk assessment of buildings in Mid-America must utilize synthetic ground motions. Unlike the Western United States, there are few ground motion records in Mid-America, and there are none that correspond to the large earthquakes that are likely to challenge modern building construction in that region. Current research has raised some question as to the sensitivity of the fragility models to the ground motion ensembles selected for their development; hence, the selection of these two different ensembles. These and other issues related to fragility development are presented in the following section.

4.3.6 Dynamic Response of Steel Frame to Earthquake Ground Motions

The development of vulnerability functions requires characterization of ground motion by a suite of appropriate ground motions, determination of structural response (structural demand), and identification of performance limits (structural system capacity) and degrees of structural damage and losses associated with specific damage levels. The first three are addressed in this section, providing the opportunity to discuss some specific current research issues that must be addressed in developing vulnerability functions and loss estimation methodologies for civil infrastructure in Mid-America. Losses associated with specific damage levels will be considered in a later phase of the research program.

We first characterize structural system response (measured by interstory rather than overall drift) to earthquake demand in a relatively simple way. The model structure in Figure 4.3.1 is a regular, 3-story, 4-bay moment frame. Its fundamental period is T_1 = 1.86 sec; the shape of the first mode is approximately linear, and its system behavior is determined (in the elastic range) mainly by its first mode. Contributions of higher modes in this structure are relatively insignificant. In such cases, Shome and Cornell (1998) have suggested that the ground motion intensity can be characterized by the spectral acceleration at the fundamental period, $S_a(T_1)$. Vamvatsikos and Cornell (2001) showed subsequently that plots of maximum interstory drift ratios vs first mode spectral acceleration produced less dispersion than similar plots against peak ground acceleration for a steel moment frame in which T_1 = 2.2 sec. The smaller dispersion implies that ensembles with fewer ground motion records can yield the same confidence level in the response analyses.

Thus, it is assumed that the seismic demand on this structural frame can be characterized by the following simple relation between interstory drift, θ, and $S_a = S_a(T_1)$:

$$\theta = a\, S_a^{\,b}\, \varepsilon \qquad (4.3.6a)$$

or, in transformed linear form,

$$\ln \theta = \ln a + b \ln S_a + \ln \varepsilon \qquad (4.3.6b)$$

in which a and b are model constants and ε is a zero-median error that describes the uncertainty in the relationship. Estimates of these model constants and the standard error can be determined by performing nonlinear dynamic analyses of the building frame using an appropriate ensemble of ground motions, determining the resulting maximum interstory drift, and performing a linear regression analysis of $\ln\theta$ on $\ln S_a$ utilizing eq (4.3.6b) to determine constants a, b and the standard error, $\sigma_{\ln\varepsilon}$.

To establish a frame of reference for the range of spectral accelerations assumed in the following results, the median seismic hazard curve for Memphis, TN is presented in Figure 4.3.3. This hazard curve is obtained from the U.S. Geological Survey website indicated in the figure, which presents spectral accelerations as a function of return period for T_1 = 0.2 sec and 1.0 sec. These spectral accelerations are used to anchor a 5-percent damped response spectrum, from which the spectral accelerations at other fundamental periods can be determined. As noted above, fundamental period for the frame in this study is 1.86 sec. The range of return periods covered in Figure 4.3.3 is approximately 600 to 6,000 years.

The results of this analysis are presented in Figures 4.3.4 using the 14 unscaled natural SAC ground motions for Boston, MA and in Figure 4.3.5 using the synthetic Wen/Wu motions for Carbondale, IL, St. Louis, MO and Memphis, TN. The results obtained using these ensembles are:

$$\theta = 0.1052\, S_a^{0.82} \quad \text{(SAC Boston - natural)} \qquad (4.3.7a)$$

$$\theta = 0.0851\, S_a^{0.82} \quad \text{(Wen/Wu - synthetic)} \qquad (4.3.7b)$$

The median maximum interstory drifts obtained using the natural and synthetic ground motions differ by 24%, the higher drifts being associated with the natural ground motions. Moreover, the variability in the demand indicated by the natural records is substantially larger (0.33 vs 0.13). Accordingly, there appear to be systemic differences in the seismic demands from suites of natural and synthetic ground motions. The Shome/Cornell study (1998), which utilized only natural records, indicated that the relation between deformation and S_a was relatively insensitive to the ensemble selected, provided that accelerograms were selected from events of similar magnitude and distance and no near-field records were included. The reason for the difference here is unclear. A comparison of displacements of elastic and inelastic systems for a frame with ductility 4 (Figure 4.3.6) for Boston Record 30 (natural) and Boston Record 21 (synthetic) indicates no systematic difference across the period range. Research is continuing on this issue, with an aim of identifying systemic differences in structural responses to natural and artificial ground motions. Meanwhile, ensembles of synthetic records should be used with caution in fragility modeling.

Research conducted in the SAC Project indicated that for structural systems designed for high-seismic areas (e.g., Los Angeles, CA), constant b in eq (4.3.6) was approximately equal to 1.0, the implication being that displacements for elastic and yielding systems are approximately equal for first mode-dominant systems with fundamental periods greater than about 0.5 sec. This equivalence was first observed by Newmark, Veletsos, and Chelapati over four decades ago, and has since been confirmed by other investigators (e.g., Gupta and Krawinkler, 2000b). The results in Figure 4.3.6 and the values of b in Figures 4.3.4 and 4.3.5 (b = 0.82) are basically consistent with this observation. Figure 4.3.7 illustrates the coefficient of variation in maximum interstory drift as a function of S_a as it increases from 0.05g to 0.6g, obtained by scaling the Wen/Wu ground motion ensembles upward in order to cover the indicated range in spectral acceleration. Although the coefficient of variation appears to increase with S_a, the ensembles used to develop Figure 4.3.7 are relatively small; if an overall value is required, an appropriate value might be about 0.30; this value is used in the subsequent fragility analysis to model the uncertainty in demand.

The capacity of the steel moment frame is determined from an incremental dynamic analysis (IDA). An IDA involves multiple nonlinear dynamic analyses of a structure subjected to an earthquake record, which is incrementally scaled upward from the elastic range until the structure "fails" according to some definition, described subsequently. The process is repeated using different accelerograms in the ensemble until a plot of S_a vs interstory drift is obtained for the entire ensemble. The results then are post-processed to determine the CDF of the system capacity. An IDA of the frame in Figure 4.3.1using the Wen/Wu 2/50 ensemble for Memphis, TN is provided in Figure 4.3.8. The ground motion scaling cannot be too coarse, lest abrupt changes in structural system behavior not be captured. On the other hand, since an IDA is computationally intensive, a compromise must be struck between these concerns. As a practical matter, step sizes are kept relatively large in linear portions of the analysis, and are refined as the structure begins to deviate from linear behavior. The non-monotonic irregularities in the results of some of the incremental dynamic analyses have been noted by other investigators (e.g., Vamvatsikos and Cornell, 2001).

The structural response quantity selected in this study to represent overall system capacity is maximum inter-story drift. The presumption is that maximum inter-story drifts can be mapped to stipulated building performance or damage levels: Immediate Occupancy, Life Safety and Incipient Collapse. For purposes of illustrating the development of vulnerability curves, we will assume that this mapping can be identified (FEMA 273/356); however, it should be emphasized that this is currently a significant research issue in the earthquake structural engineering community. We assume the following limits:

Immediate occupancy (IO) level deformation demand is limited to the point where non-structural components such as doors, windows and cladding are undamaged or are damaged but can be repaired easily. In this study this level will be represented by the limit of elastic behavior of the structural frame. The nonlinear static pushover analysis of the three-story frame showed that

The slope of the pushover curve drops to 95% of initial slope at a drift angle 0.86%.
The slope of the pushover curve drops to 90% of initial slope at a drift angle 0.95%.
The slope of the pushover curve drops to 85% of linear slope at a drift angle 1 %.

These results are consistent with those found by Song and Ellingwood (1999) in an examination of four steel moment frame buildings damaged during the Northridge Earthquake. In the light of above findings, one can assume that the behavior of many steel moment frames designed by modern codes deviates from nonlinearity at approximately 1% drift. Since nonlinear structural action is likely to be accompanied by limited nonstructural damage, this drift value has been chosen to represent the IO level.

Life Safety (LS) level deformation demand is difficult to determine. It is obvious that it will be somewhere between the Immediate Occupancy and Incipient Collapse levels, as partial collapse of heavy structural elements such as slabs or beams clearly are life-threatening but in a redundant system may not necessarily lead to overall instability or collapse of the structural system. There is no obvious way of determining the interstory drift that threatens life safety. A point where **Structural Damage** (SD) occurs may be easier to identify; this may occur at a drift of approximately 2%.

Incipient collapse(IC) level deformation demands are those at which the frame as a whole is on the verge of reaching the point of overall instability, where small perturbations in force are accompanied by very large increments in lateral deformation. To determine this deformation limit, a series of Incremental Dynamic Pushover Analyses (IDA) (Vamvatsikos and Cornell, 2001) were performed using ensembles of the Wen/Wu ground motions. The incipient collapse levels of the three-story frame were determined by inspection from the IDA curves as the point at which the slope decreased to 20% of initial value or highly irregular behavior was observed. The mean value and standard deviation and coefficient of variation obtained from these results were 8.8%, 2% and 23%, respectively. In effect, then, these statistics define the ultimate capacity of the structural system to withstand earthquake ground motions. [A similar calculation using the 2/50 SAC ground motions for Boston produced a mean capacity of 9.5% using 14 natural records and 9.4% using the entire ensemble of 20 records.]

The seismic fragilities for the three performance levels above (IO, LS and IC) are presented in Figures 4.3.9, 4.3.10 and 4.3.11. Two different demand relations (eqs 4.3.6) were utilized in order to demonstrate the sensitivity of the seismic fragilities to the choice of ground motion ensemble selected to generate these relationships. The fragilities for the immediate occupancy and structural damage performance levels appear to be relatively insensitive to the seismic demand model, as is the 5-percentile of the fragility in all cases. The implications of this insensitivity are discussed in the following section.

4.3.7 Perspectives on risk and loss estimation

The fragilities for IO, SD and IC presented in Figures 4.3.9, 4.3.10 and 4.3.11 can be used as a basis for risk-informed decision-making. For example, the median capacity [using the Wen/Wu ensembles and expressed in units of $Sa(T_1)$] of the frame in Memphis, TN at these three performance levels are, respectively, 0.073g, 0.17g and 1.04g. The corresponding 5-percentile values are, respectively, 0.033g, 0.08g and 0.5g, respectively. In other words, there is a 90% probability that the building could be occupied immediately following an earthquake causing a spectral acceleration of 0.033g, one a mean return period of approximately 500 years for this three-story frame (cf Figure 4.3.3). How best to communicate this risk depends on the preference of the decision-maker.

Additional perspectives on the role of structural response and the relative importance of fragility parameters m_R and β_C on seismic risk can be obtained from an analysis of the limit state probability:

$$P[LS] = \int F_R(x) \, |dH(x)/dx| \, dx \qquad (4.3.8)$$

in which $F_R(x)$ is defined by mean fragility (Eqn 4.3.4) and H(x) is the seismic hazard, defined as the annual probability that earthquake intensities of level x are exceeded. Over the range of significance to structural safety, the seismic hazard curve can be described, to first approximation, by,

$$\ln H(x) = A - k \ln x \qquad (4.3.9)$$

in which slope k of H(x) plotted on log-log paper is related to the COV in annual extreme ground motion (acceleration). With the mean fragility described by the lognormal distribution in Eqn 4.3.4, the limit state probability becomes,

$$P[LS] = H(m_R) \exp[(k\beta_C)^2/2] \qquad (4.3.10)$$

In other words, the limit state probability equals the seismic hazard evaluated at the median capacity, $H(m_R)$, multiplied by a correction factor. In the Eastern US and Mid-America, the hazard curve is very flat (COV in annual extreme in excess of 100%) and k typically is on the order of 1 to 2 (http://eqint.cr.usgs.gov). Such a hazard curve for Memphis, TN is illustrated in Figure 4.3.3. Values of β_c in Figures 4.3.9 – 4.3.11 are approximately 0.45 in all cases. With k = At Memphis, TN, k = 0.98, and the correction factor in Eqn 4.3.8 becomes 1.10. Since the order of magnitude in P[LS] is unchanged, this suggests that the uncertainty in steel frame capacity, measured by β_C, has only a marginal impact on seismic risk. This notion will be tested fully in the next phase of the study using an efficient

sampling plan to propagate the uncertainties in the structural system analysis, as described previously.

Fragility modeling can be used to test the viability of proposed code provisions. It also can be used to assess the need for upgrading an existing facility when new information suggests that the original design conditions may not have been sufficient, or for structural maintenance or rehabilitation and repair following the occurrence of an earthquake. Rehabilitation and repair invariably are costly, can be invasive and disruptive to the function of the facility, may actually cause damage to the structure in some instances (e.g., to weldments), and may not even be feasible in others. Thus, a properly constructed (and peer-reviewed) fragility can provide quantitative evidence that an existing steel structure still can perform its intended function, even though it may not satisfy all requirements of the latest building code.

The starting point for any such evaluation must be a benchmark fragility of the frame in the as-built condition, which should be developed using methods similar to those described in this study. It is recommended that the mean fragility (Eqn 4.3.4) be used for this purpose. All uncertainties should be evaluated carefully; not all uncertainties are equally significant for risk. Subsequent changes in fragility due to in-service modifications, cracking, corrosion or other manifestations of degradation then can be identified clearly, and the fragility may be updated periodically during the service life of the building (or during a period of extended service) following inspection. Since minor changes in β_C may have a negligible impact on limit state probability for seismic events in the Eastern United States, these periodic revisions to structural fragility might be made by performing only one (median-centered) nonlinear structural analysis and assuming that β_C remains unchanged unless there were substantial evidence to the contrary. This would lead to a revised estimate, m_R, which would serve as the anchor point of the revised mean fragility curve and would cause it to shift horizontally. This revised curve could be compared to the current design basis or other review-level event of interest. The rate of change in fragility over an extended service period may be of particular interest, as it would indicate the likelihood of deterioration due to structural aging or damage from some other natural or man-made hazard. Such a finding would warrant a comprehensive investigation and assessment of remaining structural integrity.

NS Moment Resisting Frame

Story #	COLUMNS		GIRDERS
	Line A	Lines B-E	
1	W14X74	W14X99	W21X62
2	W14X74	W14X99	W21X57
3	W14X74	W14X99	W18X35

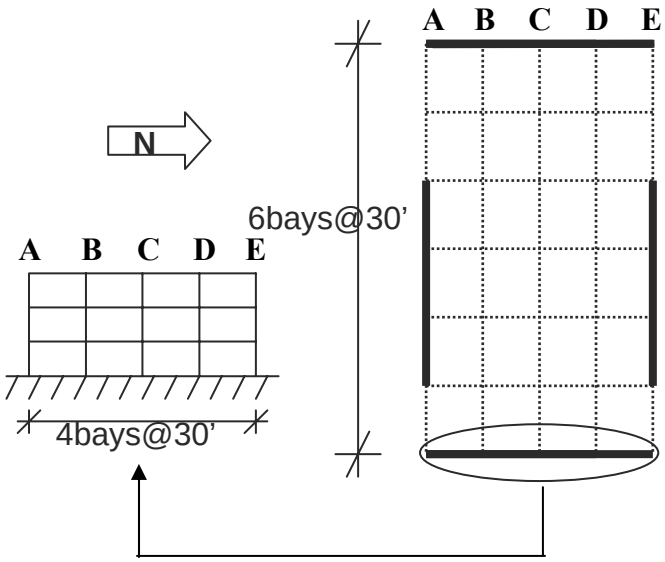

Figure 4.3.1 – Steel moment frame in region of moderate seismicity

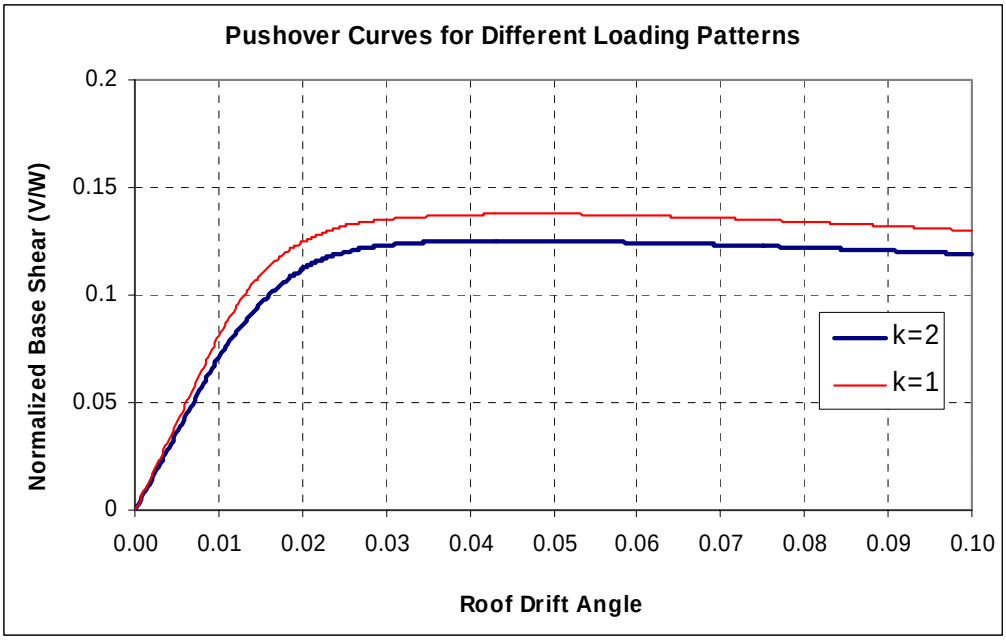

Figure 4.3.2 – Static pushover analysis of steel moment frame

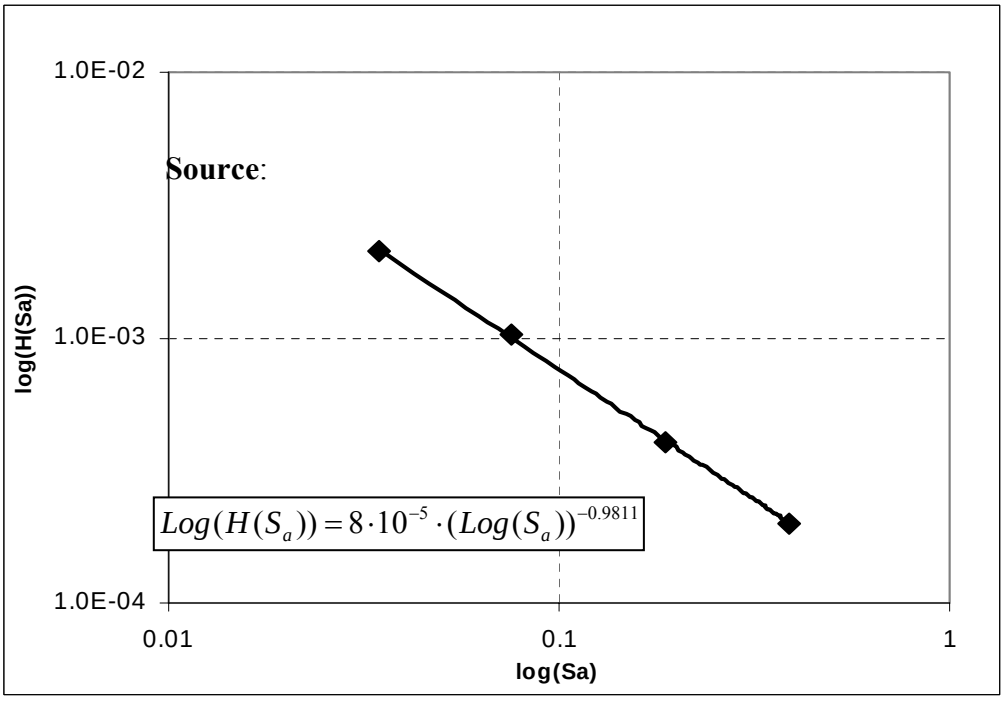

Figure 4.3.3 – Mean seismic hazard for Memphis, TN

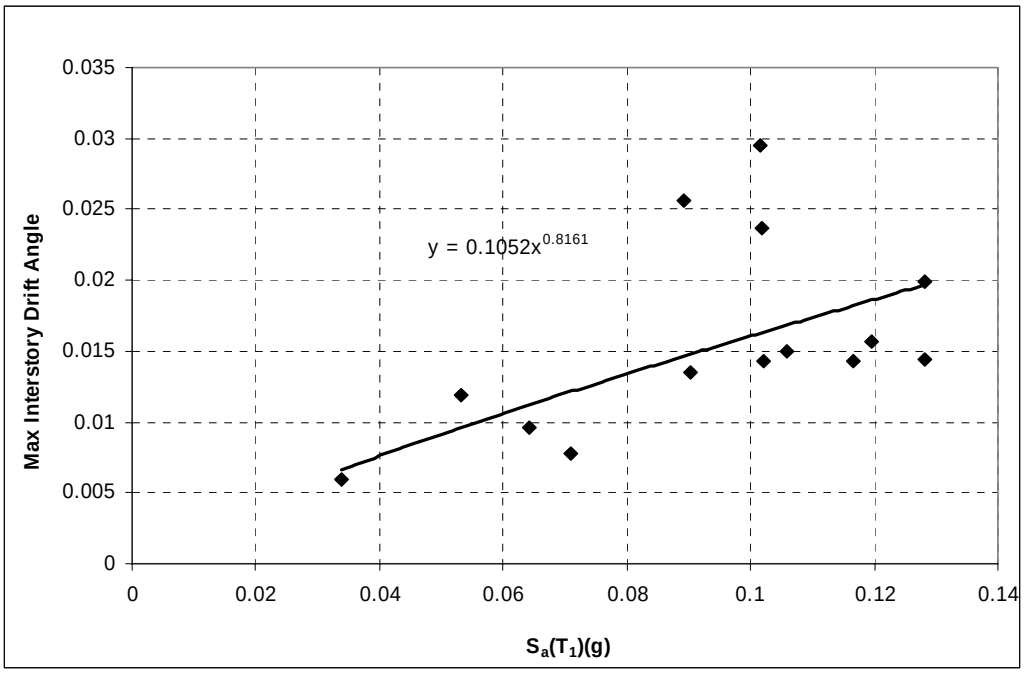

Figure 4.3.4 – Interstory drift (2/50 SAC natural motions for Boston, MA)

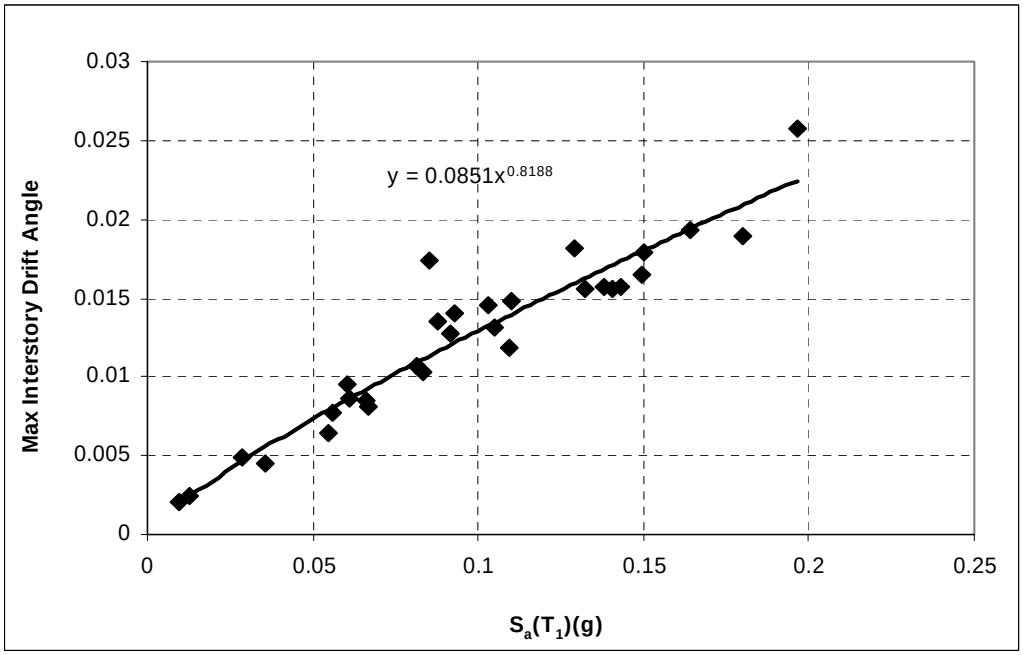

Figure 4.3.5 – Interstory drift (2/50 Wen/Wu synthetic motions for Memphis, TN)

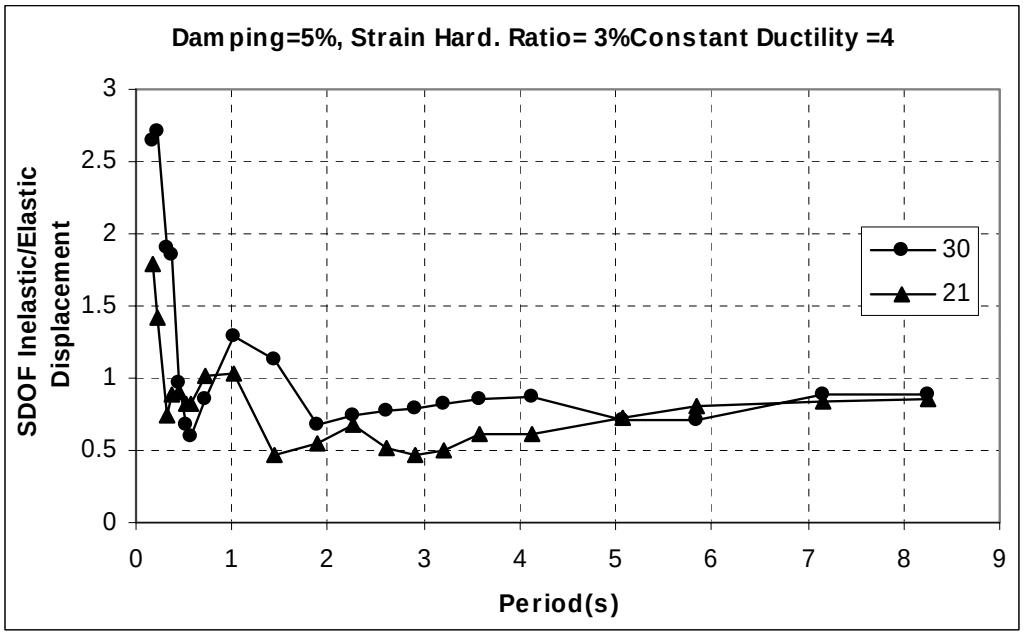

Figure 4.3.6 – Elastic and inelastic displacements for frame with ductility of 4

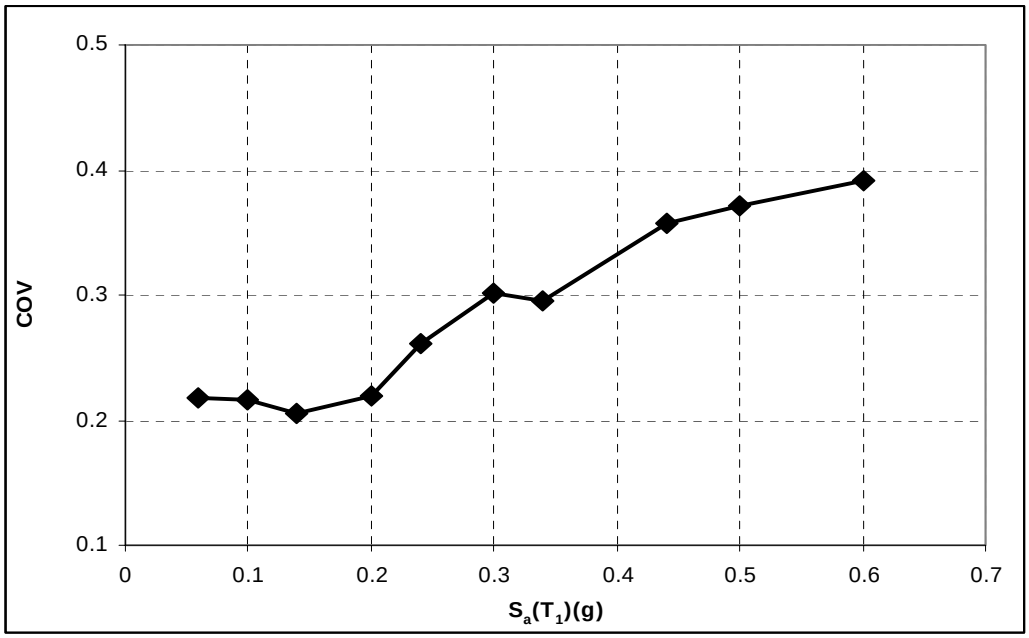

Figure 4.3.7 – Coefficient of variation in maximum interstory drift demand

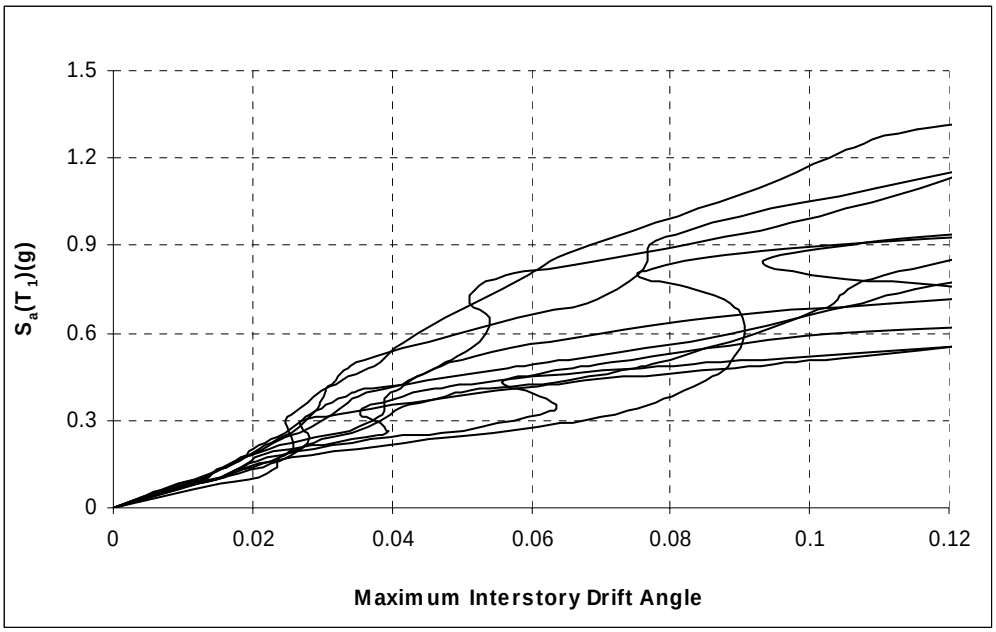

Figure 4.3.8 – Incremental dynamic pushover – 2/50 Wen/Wu ground motions for Memphis, TN

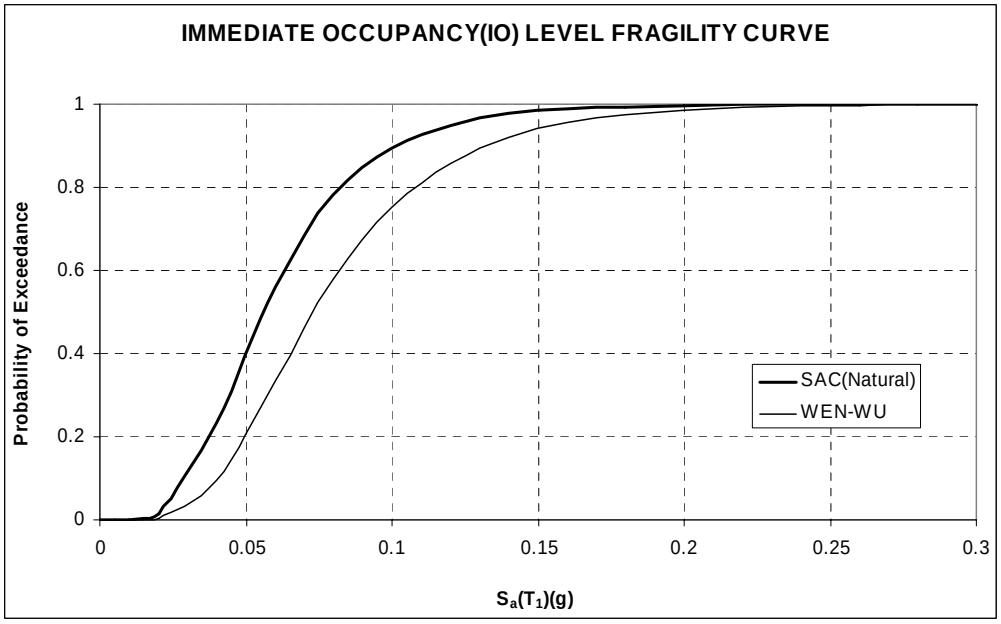

Figure 4.3.9 – Seismic fragility – immediate occupancy

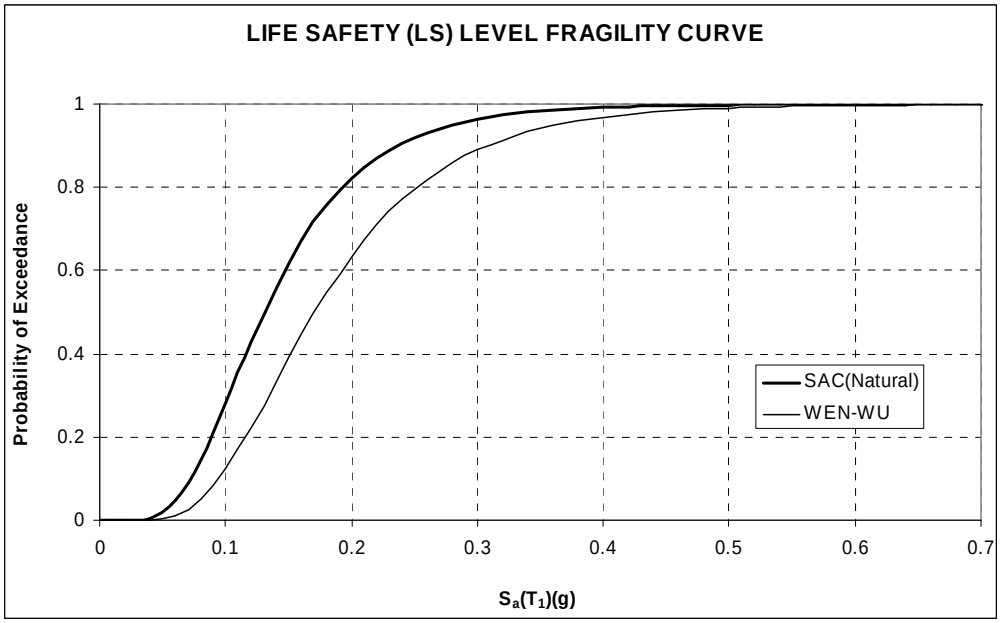

Figure 4.3.10 – Seismic fragility – life safety

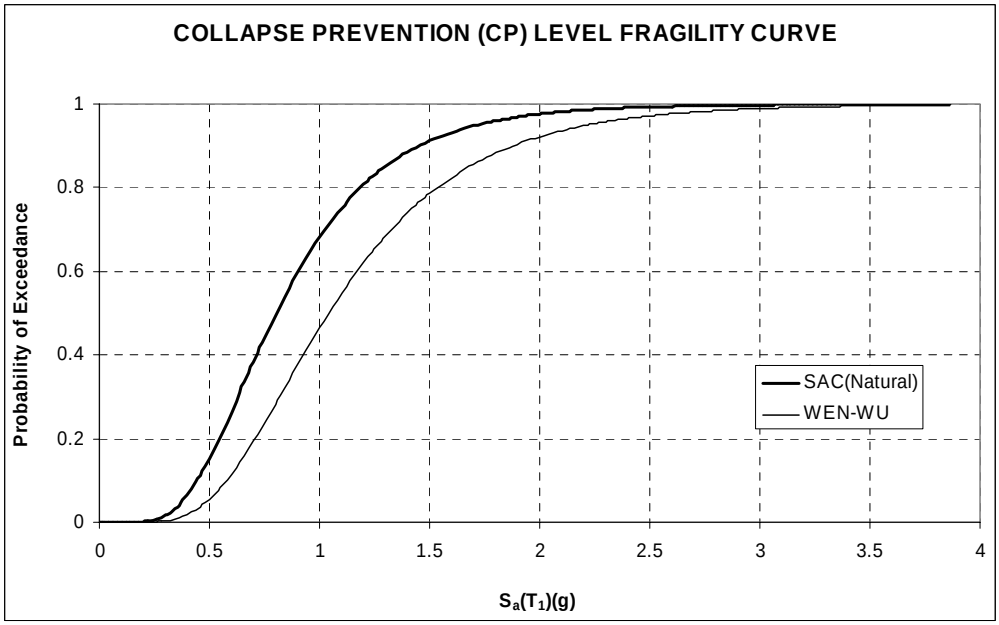

Figure 4.3.11 – Seismic fragility - incipient collapse

5.0 Summary and Conclusions

A framework for vulnerability assessment of building structures for consequence-based engineering under seismic excitation is presented. The method and assessment procedures are demonstrated for a steel building frame, a reinforced concrete building frame, and an un-reinforced masonry building with a lateral force-resisting shear wall system. The methodology is based on a review of current state-of-the-art of methods of uncertainty modeling and treatments in earthquake engineering (Wen et al, 2003). The emphasis is on systematic treatment of uncertainties in seismic excitation, dynamic response demand on the lateral force-resisting structural and capacity of building structures in resisting limit states from immediate occupancy to incipient collapse. The nonlinear inelastic response behaviors of the building after damage occurs until dynamic instability are realistically considered. Both aleatory (randomness) and epistemic (modeling errors) uncertainties in the demand and capacity are considered, with the importance of the latter emphasized since it has not been adequately considered in the past. The proposed methodology is an efficient tool in support of consequence-based engineering, where explicit consideration of uncertainty is an integral part of the engineering risk management and decision process. The methodology also can be applied to other building, bridge or civil infrastructure systems.

6.0 Acknowledgments

This study is a work product of, and is supported by, MAE Center Project DS-4 under the NSF Earthquake Research Centers Program Award Number EEC-9701785.

7.0 References

Abrams, D.P., 2002. “Consequence-based engineering approaches for reducing loss in mid-America,” *Linbeck Distinguished Lecture Series in Earthquake Engineering*, University of Notre Dame.

AISC (1999), *LRFD design specification for structural steel buildings*, American Institute of Steel Construction, Chicago, IL.

American Society of Civil Engineers, *Minimum Design Loads for Buildings and Other Structures*, *ASCE-7-98,* 1999.

Aycardi, L .E., Mander, J. B., and Reinhorn, A. M. (1994). "Seismic Resistance of Reinforced Concrete Frame Structures Designed Only for Gravity Loads: Experimental Performance of Sub Assemblages," *ACI Structural Journal*, ACI, 91(5), 552-563.

Building Code Requirements for Structural Concrete (ACI 318-71) and Commentary (ACI 318R-71), American Concrete Institute, Farmington Hills, MI.

Building Code Requirements for Structural Concrete (ACI 318-83) and Commentary (ACI 318R-83), American Concrete Institute, Farmington Hills, MI.

Building Code Requirements for Structural Concrete (ACI 318-99) and Commentary (ACI 318R-99), American Concrete Institute, Farmington Hills, MI.

Building Code Requirements for Structural Concrete (ACI 318-02) and Commentary (ACI 318R-02), American Concrete Institute, Farmington Hills, MI.

Building Seismic Safety Council (BSSC), (1997), "NEHRP guidelines for the seismic regulation of existing buildings and other structures," *Report No. FEMA 273*, Federal Emergency Management Agency, Washington, DC.

Building Seismic Safety Council (BSSC), (1998), "NEHRP recommended provisions for seismic regulation for new buildings and other structures," *Report No. FEMA 302*, Federal Emergency Management Agency, Washington, DC.

Bracci, J. M., Reinhorn, A. M., and Mander, J.B. (1995a). "Seismic Resistance of Reinforced Concrete Frame Structures Designed for Gravity Loads: Performance of Structural System," *ACI Structural Journal*, ACI, 92(5), 597-609.

Bracci, J.M., Reinhorn, A.M., and Mander, J.B. (1995b). "Seismic Retrofit of Reinforced Concrete Buildings Designed for Gravity Loads: Performance of Structural Model", *ACI Structural Journal*, ACI, 92(6), 711-723.

Collins, K. R., Wen, Y. K., and Foutch, D. A. "Dual-Level Design : A Reliability-Based Methodology", Earthquake Engineering and Structural Dynamics, Vol. 25, No. 12, pp. 1433-1467, 1996.

Cornell C. A, Jalayer F, Hamburger, R. O., and Foutch, D. A. " Probabilistic Basis for 2000 SAC Federal Emergency Management Agency Steel Moment Frame Guidelines", *Journal of Structural Engineering, ASCE,* April 2002, pp.526-533.

Chopra, A. K. and Goel, R. K. (2002). "A modal pushover analysis procedure for estimation of seismic demands for buildings." *Journal of Earthquake Engineering and Structural Dyanmics,* 31(3), 561-582.

Dexter, R. et al (2000), "Structural shape material property survey," Report, Department of Civil Engineering, University of Minnesota, Minneapolis, MN, August.

Dooley, K.L. and J. Bracci. (2001). "Seismic Evaluation of Column-to-Beam Strength Ratios in Reinforced Concrete Frames." ACI Structural Journal, 98 (6), 843-851.

El-Attar, A. G, White, R. N., and Gergely, P. (1997). "Behavior of Gravity Load Designed Reinforced Concrete Buildings Subjected to Earthquakes," *ACI Structural Journal*, ACI, 94(2), 133-145.

Ellingwood, B. R., Galambos T.V., MacGregor J. G., and Cornell C. A. (1980). " Development of a probability based load criteria for American National Institute A58."National Bureau of Standard (NBS) Special Publication 577.

Ellingwood, B. R., Galambos T.V., MacGregor J. G., and Cornell C. A., 1982. "Probability-based load criteria: load factors and load combinations", *Journal of Structural Division*, ASCE, Vol 108, No. 5, pp 978-997.

Ellingwood, B. R., Probability-based Structural Design: Prospects for Acceptable Risk Bases, Keynote lecture, *Proc. 8th International Conference on Applications of Statistics and Probability,* Sydney, Austrailia, 1999.

Ellingwood, B. and T.V. Galambos (1982). "Probability-based criteria for structural design." *Struct. Safety* 1(1):15-26.

Ellingwood, B. and H. Hwang (1985). Probabilistic descriptions of resistance of safety-related structures in nuclear plants." *Nuc. Engrg. and Des*. 88(2):169-178.

Ellingwood, B. (1990). "Validation studies of seismic PRAs." *Nuc. Engrg. and Des*.123(2):189-196.

Ellingwood, B. (1998). "Issues related to structural aging in probabilistic risk analysis of nuclear power plants." *Reliability Engrg. and System Safety* 62(3):171-183.

Ellingwood, B. (2001), "Earthquake risk for building structures," *Reliability Engrg. and System Safety* 7493):251-262.

Federal Emergency Management Agency, NEHRP Guidelines for the Seismic Rehabilitation of Buildings, FEMA-273, October 1997.

Federal Emergency Management Agency, Recommended Seismic Design Criteria for New Steel Moment-Frame Buildings, FEMA 350, July 2000.

Foutch, D. A. "State-of-the art report on performance prediction and evaluation of moment-resisting frame structures", Report No. FEMA-355f, Federal Emergency Management Agency, Washington D. C. 2000.

Frankel, A. D. et al "Documentation for the 2002 Update of the National Seismic Hazard Maps", UGSG Open File Report 02-420. USGS, Denver, Colorado.

Galambos, T.V. and M. K. Ravindra (1978), "Properties of steel for use in LRFD," *J. Struct. Div. ASCE* 104(9):1459-1468.

Galambos, T.V., Ellingwood, B. R., MacGregor J. G., and Cornell C. A., 1982. "Probability-based load criteria: assessment of current design practice", *Journal of Structural Division*, ASCE, Vol 108, No. 5, pp 959-977.

Gardoni, P., A. Der Kiureghian and K.M. Mosalam (2002), "Probabilistic capacity models and fragility estimates for reinforced concrete columns based on experimental observations," *J. Engrg. Mech. ASCE* 128(10):1024-1038

Gupta, A. and H. Krawinkler (2000a). "Behavior of ductile SMRFs at various seismic hazard levels." *J. Struct. Engrg. ASCE* 126(1):98-107.

Gupta, A. and H. Krawinkler (2000b), "Estimation of seismic drift demands for frame structures," *Earthquake Engrg. and Struct. Dyn*. 29:1287-1305.

Imam, R.L. and W.J. Conover (1980). "Small sample sensitivity analysis techniques for computer models with an application to risk assessment." *Comm. in Stat. Part A- Theory and Methods* A9(17):1749-1842.

International Building Code. (2003). International Code Council, Falls Church, Va.

Krawinkler, H. and Seneviratna, G. D. (1998). "Pros and cons of a pushover analysis of seismic performance evaluation." *Engineering Structures* 20(4-6):452-464.

Kunnath,S.K.(2003).*IDASS,* http://cee.engr.urcdavis.edu/faculty/kunnath/kunnath.htm.

Lee, K. and D.A. Foutch (2002), "Seismic performance evaluation of pre-Northridge steel frame buildings with brittle connections," *J. Struct. Engrg*. ASCE 128(4):546-555.

Luco, N. and Cornell, C. A. (2001)"Structure-specific scalar intensity measures for near source and ordinary earthquake ground motions", Proc. 6-th National Conference on Earthquake Engineering..

NEHRP *Guidelines for the Seismic Rehabilitation of Buildings.* (1997). Federal Emergency Management Agency, Washington D.C.

Miranda E. and Bertero V. V., " Evaluation of Strength Reduction Factors for Earthquake-Resistance Design," Earthquake Spectra, EERI, Vol. 10, No.2, 1994.

Nassar, A. A. and Krawinkler H. , 1992, " Seismic Design Based on Ductility and Cumulative Damage Demands and Capacities," Nonlinear Seismic Analysis and Design of Reinforced Concrete Buildings, ed. Fajfar, P. and Krawinkler, H., Elsevier Applied Sciences, 1992.

Nordenson, G. J. P. (1993). "Seismic Codes," *Monograph 2 Mitigation of damage to the Built Environment,* Central United States Earthquake Consortium, 89-114.

Olshansky, R. B. (1993). "Selling Seismic Building Codes in the Central United States," *Proceeding of the 1993 National Earthquake Conference*, 1, 694-658.

Park, Y.J., and Ang, A.H-S. " Mechanistic Seismic Damage for Reinforced Concrete ." *Journal of Structural Engineering*, ASCE, 111, 4 , April, 1985, pp.722-739.

Park, Y.J., and Ang, A.H-S., and Wen, Y. K. "Seismic Damage Analysis of Reinforced Concrete Builidngs" *Journal of Structural Engineering*, ASCE, 111, 4 ,April 1985, pp.740-757.

Pessiki, S.P., Conley, C.H., Gergely, P., White, R.N. (1990). "Seismic Behavior of Lightly Reinforced Concrete Column and Beam-Column Joint Details," *Technical Report NCEER-90-00014,* State University of New York at Buffalo.

Priestley, M.J.N. (1996). "Displacement-based seismic assessment of existing reinforced concrete buildings." *Bull. New Zealand National Soc. Earthquake Engrg*. 29(4):256-272.

Rubenstein, R.Y. and B. Melamed (1998), *Modern simulation and modeling*, John Wiley & Sons, Inc., New York, NY.

Samaras, E., Shinozuka, M., and Tsurui, A. " Time Series Generation Using the Auto-Regressive Moving Average Model", Technical Report, Department of Civil Engineering, Columbia University, New York, May, 1983.

Saikia, C. K. and Somerville, P. G, "Simulated hard-rock motions in Saint Louis, Missouri, from large New Madrid earthquakes (Mw $\geq$6.5)", *Bulletin of Seismological Society of America*, Vol.87, 1997, 123-139.

Sasani, M., Der-Kiureghian, A., and Bertero, V. V." Seismic Fragility of Short Period Reinforced Concrete Structural Walls under Near-Source Ground Motions", *Structural Safety*, Vol. 24, No. 2-4, 2002, pp. 123-138.

Shome, N. and C.A. Cornell (1998), "Normalization and scaling accelerograms for nonlinear structural analysis," *Proc. 6th U.S. National Conf. on Earthquake Engrg*., Earthquake Engineering Research Institute, Oakland, CA.

Somerville, P.G., Smith, N, Punyamurthula, S, and Sun, J., "Development of Ground Motion Time Histories for Phase 2 of the FEMA/SAC Steel Project," Report No. SAC/BD-97/04, SAC Joint Venture, Sacramento, California, 1997.

Song J. and B.R. Ellingwood (1999), "Probabilistic modeling of steel moment frames with welded connections," *Engrg. Journal*, AISC 36(3):129-137.

Structural Engineering Association of California (SEAOC), "Vision 2000, Performance-based Seismic Engineering of Buildings," April 1995.

Vamvatsikos, D. and Cornell, C.A. "Incremental Dynamic Analysis", submitted for publication in *Journal of Earthquake Engineering and Structural Dynamics,*Vol. 31, No.3, 2002. pp. 491-514.

Wen, Y.K., B.R. Ellingwood, D. Veneziano and J. Bracci (2003), "Uncertainty Modeling in Earthquake Engineering," Report FD-2, Mid-America Earthquake Center, University of Illinois at Urbana-Champaign, Urbana, IL (http://mae.ce.uiuc.edu).

Wen, Y. K. and Wu, C. L." Uniform Hazard Ground Motions for Mid-America Cities", *Earthquake Spectra*, Vol. 7, No.2, May 2001, pp. 359-384.

Wen, Y.K. and Foutch, D.A., "Proposed Statistical and Reliability Framework for Comparing and Evaluating Predictive Models for Evaluation and Design and Critical Issues in Developing Such Framework," Report No. SAC/BD-97/03, SAC Joint Venture, Sacramento, California, 1997.

White, D. W. and Kim, S.-C. " Analysis of Gilroy Fire House under Loma Prieta and Carbondale Earthquake Motions", Georgia Institute of Technology, Atlanta, Georgia, April 2001.

Yun, S.-Y., R.O. Hamburger, C.A. Cornell and D.A. Foutch (2002), "Seismic performance evaluation for steel moment frames," *J. Struct. Engrg. ASCE* 128(4):534-545.

Ziemian, R.D., W. McGuire, and G.G. Deierlein (1992), "Inelastic limit states design, part I: Planar frame studies," *J. Struct. Engrg. ASCE* 118(9):2532-2549.